Mirja Palo

Design and development of personalized dosage forms by printing technology

A study in Pharmaceutical Sciences

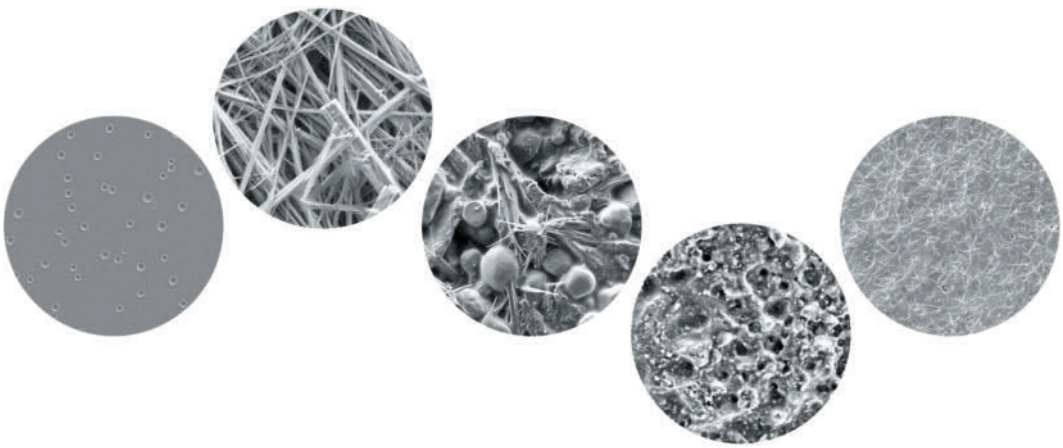

Mirja Palo

Born 1988 in Viljandi, Estonia

Obtained her MSc degree in Pharmacy at the University of Tartu in 2012.

The PhD thesis project in Pharmaceutical Sciences was carried out under a joint supervision (***cotutelle***) agreement between Åbo Akademi University and the University of Tartu during 2012-2017.

Cover figure: Surfaces of different printed dosage forms visualized by scanning electron microscopy.

Design and development of personalized dosage forms by printing technology

A study in Pharmaceutical Sciences

Mirja Palo

Pharmaceutical Sciences Laboratory
Faculty of Science and Engineering
Åbo Akademi University
Åbo, Finland, 2017

Supervisors

Professor Niklas O. Sandler, PhD
Pharmaceutical Sciences Laboratory
Åbo Akademi University
Finland

Assistant Professor Karin Kogermann, PhD
Institute of Pharmacy
University of Tartu
Estonia

Professor Jyrki T. Heinämäki, PhD
Institute of Pharmacy
University of Tartu
Estonia

Reviewers

Professor Julijana Kristl, PhD
Faculty of Pharmacy
University of Ljubljana
Slovenia

Professor Bente Steffansen, PhD
Department of Physics, Chemistry and Pharmacy
University of Southern Denmark
Denmark

Opponent

Professor Julijana Kristl, PhD
Faculty of Pharmacy
University of Ljubljana
Slovenia

ISBN 978-952-12-3557-3 (Print)
ISBN 978-952-12-3558-0 (PDF)
Painosalama Oy – Turku, Finland, 2017

Table of contents

Abstract

The development of tailored dosage forms provides a wide range of possibilities for meeting the needs of individual drug therapy. The personalized dosage forms improve the safety of drug treatment by decreasing the risk of overdosing and adverse reactions. Conventional drug preparations with fixed dose strengths are generally produced in large industrial scale. However, the tailored dosage forms for individual patients could be manufactured in small batches with specific materials, drug content and release profile. Therefore, alternative fabrication methods, such as printing technology, are being investigated for the customization of the dosage forms. Printing technology is a flexible method for the on-demand production of drug preparations with variable doses at the point-of-care.

The thesis was aimed at investigating the feasibility of two-dimensional (2D) printing technology for the fabrication of personalized dosage forms. In the 2D printed dosage forms, a pharmaceutical ink is typically deposited and solidified on a planar carrier substrate according to a predefined pattern. The dosing accuracy and reproducibility of the inkjet-printed formulations could be controlled on the single droplet scale. Furthermore, tailoring the properties and the composition of the formulations allows obtaining drug delivery systems (DDS) with controlled drug release profiles and/or with multiple active pharmaceutical ingredients (APIs).

The versatility of 2D printing technology was demonstrated by preparing printed formulations either by inkjet or flexographic printing on planar edible substrates with different types of pharmaceutical inks. The printed formulations and their components were analyzed to allocate the crucial aspects in the development process and to improve the knowledge about the physicochemical properties, *in vitro* performance and stability of the printed APIs. The printability of the inks and the specific printing parameters were closely related to the rheological properties of the drug solutions. The solid state of the printed APIs was dependent on the ink composition, the ink incorporation capacity of the substrates, and the physicochemical properties of the APIs. Solid state analysis of the final dosage forms showed that the APIs were distributed uniformly in a crystalline or molecularly dispersed state. Furthermore, the flexographically prepared solid nanoparticulate systems exhibited an enhanced *in vitro* drug release due to the spatial distribution of the crystalline nanosuspension inks.

The high dosing precision of the inkjet printing process was ensured by the stable jetting of the drug solutions. However, the dosing of nanosuspensions by flexographic imprinting was less accurate mainly because of the format of the ink transfer system. The dosing flexibility of the inkjet-printed pharmaceuticals could be regulated by adjusting the printing resolution or the physical size of the dosage units. Furthermore, the implementation

of non-destructive attenuated total reflectance Fourier transform infrared spectroscopy with multivariate data analysis showed high applicability for the quantification of printed pharmaceuticals. In addition to edible commercial substrates, the suitability of gelatin-based electrospun fiber matrices as carrier substrates for the fabrication of printed dosage forms was studied. Moreover, drug-loaded electrospun fiber mats were produced by stabilizing the amorphous state of a poorly water-soluble drug within the inner structure of these fibers. The use of drug-loaded fibrous substrates presented a unique approach for the preparation of dual DDS, where an API was inkjet-printed on the drug-loaded matrices that contained another API. The analysis of the designed combination DDS showed that both drugs exhibited an independent release behavior.

The thesis presents an extensive overview on the main aspects of the development of personalized dosage forms by 2D printing technology. The research improves the understanding of the key factors for successful tailoring and manufacturing of the printed dosage forms, elaborates on the quality control aspects of the printing process, and provides an insight into the essential properties and the performance of the printed pharmaceuticals.

List of original publications

The thesis is based on the following publications, which are referred to in the text by Roman numerals (I–IV).

I Genina, N., Fors, D., **Palo, M.**, Peltonen, J. and Sandler, N. (2013). Behavior of printable formulations of loperamide and caffeine on different substrates – Effect of print density in inkjet printing. *International Journal of Pharmaceutics*, *453* (2), 488–497.

II **Palo, M.**, Kogermann, K., Genina, N., Fors, D., Peltonen, J., Heinämäki, J. and Sandler, N. (2016). Quantification of caffeine and loperamide in printed formulations by infrared spectroscopy. *Journal of Drug Delivery Science and Technology*, *34*, 60–70.

III **Palo, M.**, Kolakovic, R., Laaksonen, T., Määttänen, A., Genina, N., Salonen, J., Peltonen, J. and Sandler, N. (2015). Fabrication of drug-loaded edible carrier substrates from nanosuspensions by flexographic printing. *International Journal of Pharmaceutics*, *494* (2), 603–610.

IV **Palo, M.**, Kogermann, K., Laidmäe, I., Meos, A., Preis, M., Heinämäki, J. and Sandler, N. (2017). Development of oromucosal dosage forms by combining electrospinning and inkjet printing. *Molecular Pharmaceutics*, *14* (3), 808–820.

Contribution of **Mirja Palo** to the original publications:

I Participation in the study design; performing part of the experiments and data analysis; reviewing the manuscript.

II Participation in the study design; performing the experiments and data analysis; writing the paper.

III Participation in the study design; performing major part of the experiments and data analysis; writing the paper.

IV Participation in the study design; performing major part of the experiments and data analysis; writing the paper.

Abbreviations

2D	Two-dimensional
3D	Three-dimensional
ACN	Acetonitrile
API	Active pharmaceutical ingredient
ATR	Attenuated total reflectance
BCS	Biopharmaceutics Classification System
CAF	Caffeine
CL	Crosslinked
Cp	Heat capacity
Ctr	Mean centering scaling algorithm
DDD	Drug delivery device
DDS	Drug delivery system
DMF	Dimethylformamide
DoD	Drop-on-demand
dpi	Droplets per inch
DS	Drop spacing
DSC	Differential scanning calorimetry
EDX	Energy-dispersive X-ray spectroscopy
EHD	Electrohydrodynamic
EMA	European Medicines Agency
FDA	United States Food and Drug Administration
FTIR	Fourier transform infrared spectroscopy
GMP	Good Manufacturing Practice
HPC	Hydroxypropyl cellulose
HPLC	High performance liquid chromatography
HPMC	Hydroxypropyl methylcellulose
ICH	International Conference on Harmonisation
IND	Indomethacin
IR	Infrared
ISO	International Organization for Standardization
ITR	Itraconazole
LDT	Liquid Dispensing Technology
LH	Lidocaine hydrochloride
LOP	Loperamide hydrochloride
LV	Latent variable
MT-DSC	Modulated temperature differential scanning calorimetry
NIR	Near-infrared
nonCL	Non-crosslinked
Oh	Ohnesorge number
PAT	Process Analytical Technology
PEG	Polyethylene glycol

PET	Polyethylene terephthalate
PG	Propylene glycol
Ph. Eur.	European Pharmacopoeia
PI	Polydispersity index
PIJ	Piezoelectric inkjet printing
PLS	Partial least squares
PRX	Piroxicam
PTFE	Polytetrafluoroethylene
Q^2	Test validation coefficient
QbD	Quality-by-design
Re	Reynolds number
RH	Relative humidity
R^2	Correlation coefficient
RMSEE	Root mean square error of estimation
RMSEP	Root mean square error of prediction
RSD	Relative standard deviation
SEM	Scanning electron microscopy
SNV	Standard Normal Variate
TF	Transparency film
TIJ	Thermal inkjet printing
UV	Unit variance scaling algorithm
UV-Vis	Ultraviolet-visible
We	Weber number
XRD	X-ray diffraction
Z-value	Inverse of Ohnesorge number

1. Introduction

The significance of personalized medicine has increased tremendously over the last decades. The concept of individualized drug therapy defines that the patient-specific characteristics influencing the performance of pharmaceuticals are considered during the development of treatment. The flexible design of dosage forms could provide valuable advantages for the dosing of therapeutics according to the individual patient profile, reducing drug overdosing and adverse reactions, and increasing patient compliance. On the other hand, the need for such personalized dosage forms sets new requirements for the pharmaceutical manufacturing, since conventional production methods might not provide sufficient flexibility and cost-efficacy for the fabrication.

Alternative methods, such as printing technology, are being investigated to provide precise tailoring of medicines. Due to the flexibility of this on-demand manufacturing method, the daily dose adjustment could be easily accomplished. Furthermore, printing could be feasible for producing drug delivery systems (DDS) for controlled drug release and/or with multiple active pharmaceutical ingredients (APIs) at high accuracy and homogeneity already in low doses. Currently, both two-dimensional (2D) and three-dimensional (3D) printing technologies are being exploited in the pharmaceutics. The accuracy of 2D inkjet printing is provided by the drop-on-demand (DoD) technology that allows controlled deposition of pharmaceutical ink formulations in 2D pattern onto a carrier material. Typically, the solidification of the printed material is required to obtain solid dosage forms from 2D and 3D printing. The properties and therapeutic performance of the printed pharmaceuticals could be adjusted by modifying the individual components of the dosage forms.

Despite its obvious advantages, the manufacturing specifications, requirement guidelines and applicable analytical techniques are needed for ensuring the final quality of the printed drug preparations. Due to the novelty of the production process, the analysis of the physicochemical properties of the formulations and the process-induced solid state transformations is needed. Currently, the pharmaceutical research is concentrating on defining the applicability and limitations of the production methods as well as the techniques for qualitative and quantitative analysis.

The present research work focused on studying the applicability of 2D printing in the design and development of personalized dosage forms. The main objectives were to provide an insight into the tailoring of the printed dosage forms and to gain understanding about the physicochemical properties and behavior of the printed pharmaceuticals.

Different drug formulations were prepared by inkjet printing on planar carrier substrates to define the dosing precision and the flexibility of the

printed pharmaceuticals in the solid dosage forms. The implementation of the attenuated total reflectance Fourier transform infrared (ATR-FTIR) spectroscopy was investigated for the quantitative quality control of printed formulations. Furthermore, solid nanoparticulate systems with poorly water-soluble APIs were prepared by flexographic printing with the aim of improving the drug release behavior of the drugs. Finally, the applicability of drug-loaded electrospun fiber matrices as carrier substrates was studied for the preparation of an inkjet-printed dual drug system. The overall hypothesis was that printing technology could be applied to prepare dosage forms with various APIs in low doses and combinations at high content uniformity, acceptable stability and favorable dissolution profile for individualized drug therapy.

2. Literature overview

2.1. Concept of personalized dosage forms

The concept of personalized medicine is aimed at producing precisely tailored dosage forms for individualized drug therapy. The patient-specific requirements are defined based on various factors, including age, gender, race, weight, body composition, metabolic activity, genetics and lifestyle. This specific approach allows considering the unique factors that influence the pharmacokinetics and -dynamics of drugs, such as differences in drug therapeutic effect and adverse reactions (Cohen, 1999). The diagnostic tests for determining genetic variations and biomolecular pathways that affect the mechanisms of diseases are continuously developing. Therefore, the pharmaceutical manufacturers should provide possibilities for small-scale production for personalized dosage forms to meet the needs of these sub-categories with specific characteristics (Hamburg and Collins, 2010). The flexibility in the manufacturing of personalized dosage forms could allow creating a continuous feedback loop between the clinical diagnostics and the optimization of the drug formulations (Alhnan et al., 2016; Sandler and Preis, 2016).

The preparation of age-appropriate medicines, especially for pediatric and geriatric drug therapy, need to follow some key aspects that help to ensure the suitable bioavailability, safety, dosing uniformity and administration acceptability (Breitkreutz and Boos, 2007; European Medicines Agency, 2013). The route of administration and the suitable dosage forms are often determined by the bioavailability of the active compounds. The metabolic mechanisms of different age groups or concurrent diseases/therapies determine the absorption and the elimination of the drugs. Furthermore, in pediatric formulations, the use of safe excipients and additives is crucial to avoid any additional hypersensitivity reactions (Breitkreutz and Boos, 2007; European Medicines Agency, 2013).

The choice of dosage forms influences the dose uniformity and the dosing scheme. Liquid or solid dosage forms can be acceptable depending on the stability of the formulation and/or accuracy of the dosing devices for multi-dose containers and multiparticulate systems (Wening and Breitkreutz, 2011). Nevertheless, the patient acceptability and compliance is the main factor that ensures the regular intake of the medicines in practice. The palatable properties (size, shape, taste, smell, texture and appearance) of oral dosage forms determine the receptiveness of the formulations in pediatrics, geriatrics and patients with oral hypersensitivity reactions or swallowing problems (Wening and Breitkreutz, 2011). In addition, most of these properties are also crucial for topical dosage forms and affect their acceptability. In a nutshell, single-dose and ready-to-use dosage forms with easy-to-handle packaging

and explicit user instructions are highly preferred.

By considering all the afore-mentioned requirements, the conventional dosage forms with a limited number of fixed drug doses have often shown to be too rigid or imprecise to meet the rapidly increasing needs of individualized drug therapy. When conventional dosage forms fail to provide acceptable flexibility for the personalization of the drug formulations, alternative manufacturing methods should be exploited already at the roots of pharmaceutical dosage form design to fill these requirements.

Recently, a transportable manufacturing platform with a continuous production process from the synthesis to the final formulation was demonstrated (Adamo et al., 2016). The proof-of-concept system was presented to be suitable for the flexible preparation of essential liquid drug formulations in special emergency situations and/or remote locations as well as for the fabrication of rare medications in small quantities. The manufacturing of such a compact production unit shows that the possibility of having simple systems for on-demand fabrication of personalized dosage forms is far from impossible. Computationally controllable systems could be constructed for preparing dosage forms from materials that are already synthesized with a flexible dose adjustment and reliable in-line or on-line quality control.

2.2. Two-dimensional printing technologies in pharmaceutics

Two (2D) and three (3D) dimensional printing techniques provide various possibilities to tackle the increasing demand for tailored drug delivery devices (DDD) and drug delivery systems (DDS), individualized dosing and drug combination therapies. Printing is relatively recent technological approach in pharmaceutics, although different contemporary printing techniques have been used in other fields for many decades. Pharmacoprinting is a manufacturing concept that includes the production of pharmaceutical products by means of printing technology. The research into the applicability of printing to produce DDS has steadily increased over the years (Katstra et al., 2000; Sandler et al., 2011; Alomari et al., 2015). Furthermore, printing of pharmaceuticals has also been exploited in drug discovery (Zhu et al., 2012), biomolecular and cell-based applications (Ihalainen et al., 2015), and the production of DDD (Wu et al., 1996; Tarcha et al., 2007).

The general selection of suitable printing technologies can be made based on the relationship between the printing resolution and throughput. After which the feasibility of different printing methods is often dictated by the requirements for the final product and the properties of the materials. The 2D printing technologies are generally divided into inkjet and roll-to-roll printing methods (**Figure 1**). An overview on the working principles and pharmaceutical applications of inkjet and flexographic printing will be given in more detail.

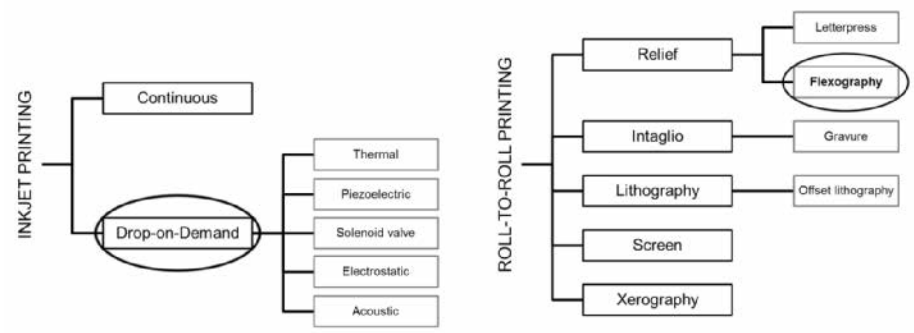

***Figure 1**. Inkjet and roll-to-roll printing technologies.*

2.2.1. Inkjet printing

The development of inkjet printing technology started in the middle of 20th century. In general, inkjet printing is a non-contact method, where an ink is dispensed from an ink container through a printhead nozzle onto a predefined location on a substrate. The inkjet printing types are foremost based on the droplet formation mechanism in the printhead and divide into continuous and drop-on-demand (DoD) jetting technology.

In the continuous inkjet systems, the ink is jetted out of the printhead continuously and single droplets are formed by electrical charge that breaks the jet into droplets that are deposited onto the substrate (charged) or deflected for recirculation (uncharged) (**Figure 2A**). Continuous printing finds use in industrial coding and labeling applications.

In the systems based on the DoD technology, on the other hand, the ink droplets are ejected only when their deposition is needed for creating the printable image; therefore, no recirculation of the ink is necessary. This technique was developed to improve the reliability of the inkjet printing and to reduce problems caused by the ink charging and/or recirculation systems (Le, 1998). The commercially available inkjet printers that came to the market first in 1970s and 1980s are using thermal or piezoelectric DoD jetting (Le, 1998). The 2D printing systems for pharmacoprinting are mainly based on these techniques. However, other DoD methods, like solenoid valve and electrohydrodynamic (EHD) inkjet printing, have also been studied for pharmaceutical applications.

In solenoid valve inkjet printing, the droplet deposition is regulated by an electromagnetically controlled valve (Horsnell et al., 2009). The valve includes a ferromagnetic plunger that opens or closes the ink flow between the printhead ink chamber and nozzle when a magnetic field is generated by a surrounding coil that is activated/deactivated by an electrical current. This non-contact DoD technology allows printing single droplets with various sizes in nanoliter-scale. The printability of the inks and the geometry of the droplets are dependent on the ratio between the length and the orifice

diameter of the nozzle (Horsnell et al., 2009). Therefore, it is suitable for ink solutions and (nano)suspensions with a wide range of viscosity from 1 to 400 mPa·s (Horsnell et al., 2009; Planchette et al., 2015).

The EHD printing is an electrostatic inkjet method, where droplets are pulled out from the nozzle onto/into the substrate when the electrostatic forces of the system overcome the surface tension and the viscosity forces of the liquid (Elele et al., 2012). By tuning the settings of the EHD system, a suitable jetting mode is obtained for uniform droplet formation (Raje and Murmu, 2014). Other jetting modes, such as electro-spraying or -spinning, can be obtained at different configurations (Raje and Murmu, 2014).

Besides the differences in the basic working principles of inkjet printers, the applicability of printing is dependent on the nozzle size and the substrate feeding setup or position. By default, the small size (approximately 30–500 pl) of ink droplets is one of the factors that ensures the high resolution and accuracy suitable for pharmacoprinting.

2.2.1.1. Thermal inkjet printing

The thermal inkjet (TIJ) printing uses an expansion-collapse principle of a vapor bubble for the droplet formation (**Figure 2B**). The vapor bubble forms on the surface of a heater located in the printhead either on the top (roof-shooter) or on the side (side-shooter) of the nozzle. In addition, in 1980s Hewlett-Packard commercialized single-use printheads, allowing the disposal of the empty ink cartridges; thus, increasing the quality and reliability of the inkjet technology.

TIJ printing is suitable for water-based inks that become highly heated (up to 300 °C) for about 2–10 μs during the vapor bubble formation and collapse. The uniformity of the droplet size and the speed of the printing are influenced by the refill of the ink chamber, that takes up to 200 μs depending on the ink properties, and the design of the printhead (Le, 1998).

2.2.1.2. Piezoelectric inkjet printing

In piezoelectric inkjet (PIJ) printing, the droplet formation is caused by the deformation of a piezo-ceramic material (**Figure 2C–D**). The sub-micron scale deformation of the piezo-element changes the volume of the ink in the chamber and produces a pressure wave that forces the ink to be ejected. For the droplet formation and expulsion, the produced acoustic wave needs to be sufficient to overcome the contradictory changes in the viscosity, surface tension and dynamic pressure (Le, 1998). The PIJ printing technologies are subcategorized into four modes – squeeze, bend, push and shear – based on the deformation mode of the piezo-element. Printers with a PIJ printhead are suitable for inks based on aqueous and non-aqueous solvents (de Gans et al., 2004).

In the shear-mode printheads, such as Spectra® PIJ printheads, a perpendicular relationship between the electrical field and the polarization

of the piezo element causes shear deformation of the piezo-ceramic plates for the ejection of the ink droplets (**Figure 2D**). For the droplet formation in the shear-mode printheads, the ink and the piezo-element are in direct contact.

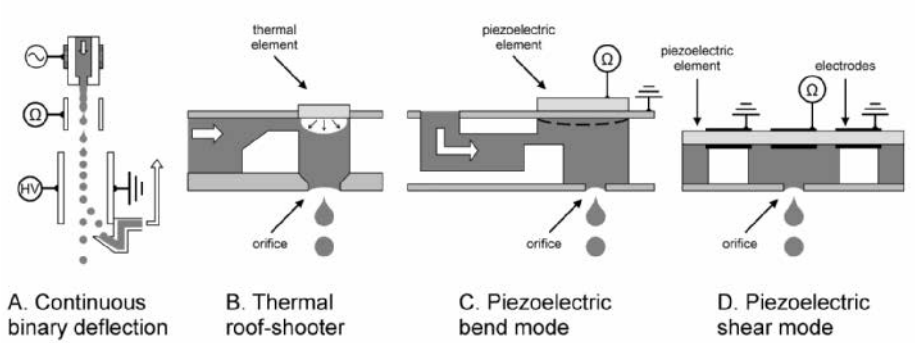

***Figure 2**. **A**: Continuous inkjet system with a binary deflection mode. **B**: Thermal inkjet system with a roof-shooter heating mode. **C**: Piezoelectric inkjet system with a bending deformation mode. **D**: Piezoelectric inkjet system with a shear deformation mode.*

2.2.2. Roll-to-roll printing

Roll-to-roll methods are mainly non-digital contact techniques that require physical transfer of the printing pattern onto the substrates. Typical roll-to-roll methods, including relief, gravure, (offset) lithography and xerography printing, have multiple industrial applications due to their high throughput capacity. However, the lower resolution of these methods is one of the limiting factors in the method selection for biomedical and pharmaceutical applications. Nevertheless, screen and (roto)gravure printing technologies have been successfully used for the fast deposition of biomolecules (Ihalainen et al., 2015). In pharmaceutics, the flexographic printing has shown limited applicability for the preparation of oral DDS (Genina et al., 2012; Janßen et al., 2013).

2.2.2.1. Flexographic printing

Flexography is an imprinting method that is based on the concepts of relief printing, where ink transfer occurs by pressing or rubbing the substrate against a printing plate that has ink-covered relief surface (raised areas) with ink-free recessed areas.

The flexographic printing is typically a three-step process, where the system is built up from an anilox roll, doctor blade, patterned printing plate and an impression roll (**Figure 3**). The ink transfer from the anilox roll to the printing cylinder is controlled by the doctor blade. The small engraved cells on the surface of the anilox roll dictate the amount of the transferred ink. The printed area is formed by the relief pattern on the polymeric plate that covers the printing cylinder. Finally, the ink pattern is carried on to an

impression roll that is surfaced with the substrate. The printing quality is dependent on the individual properties of the ink and the substrates, the uniformity of the transferred ink layer and the connectivity between the printing plate and the substrate/impression roll (Kolakovic et al., 2013). Flexography is suitable for various ink formulations with non-volatile solvents that are stable at room temperature during the printing process. The printing speed and the robustness of flexography makes it a fruitful option for the on-demand manufacturing of DDS; however, its lack of dosing precision has been recognized as one of the major challenges in the fabrication of solid dosage forms (Genina et al., 2012; Kolakovic et al., 2013).

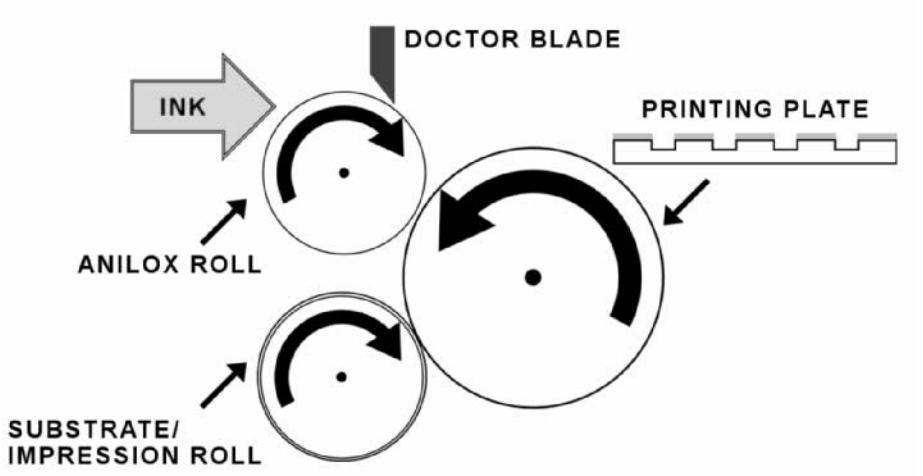

***Figure 3**. Flexographic printing system.*

2.3. Biomedical and pharmaceutical applications of printing

Inkjet printing is typically used for home/office printing, graphic art or industrial/postal marking applications. However, the feasibility of 2D and 3D printing technologies in polymer light-emitting diode displays, electronics, ceramics, textiles, imaging and several biomedical applications is trending continuously (Le, 1998; de Gans, 2004).

The quality and automated high throughput characteristics of inkjet printing have shown to be attractive for cost-effective biomedical and pharmaceutical applications. Besides 3D printing of DDD (Wu et al., 1998; Katstra et al., 2000; Shafiee and Atala, 2016), carrier-free 3D microstructures with predefined shapes can also be fabricated by inkjet printing (Yun et al., 2009; Lee et al., 2012).

Several reviews have been published on the inkjet and 3D printing of functional liquids or bioinks that contain biological materials, such as cells, extracellular matrices and bioactive macromolecules for tissue engineering

(Calvert, 2001; Zhu et al., 2012, Shafiee and Atala, 2016; Neves et al., 2016). The main practical challenges in the printing of proteins and cells are the biocompatibility between the materials and the printing system, and the suitable rheological properties of the liquids (Wilson and Boland, 2003; Derby, 2008). Due to the high shear rates in the printing systems, the optimization of bioinks is crucial to avoid the loss of biomaterial functionality (Di Risio and Yan, 2007; Derby, 2008).

The precision, simplicity, robustness and rapid working speed of inkjet technologies provide cost-effective solutions in drug discovery (Lemmo et al., 1998; Zhu et al., 2012; Scoutaris et al., 2016). In high throughput screening and microarrays, the inkjet deposition of reagents and assay compounds improves the screening processes for identifying new lead compounds or for discovering functional pathways and interactions in biological systems, respectively (Arrabito and Pignataro, 2000; Okamoto et al., 2000). Furthermore, inkjet printing is advantageous in the fabrication of simple and disposable biodevices (e.g., biosensors, biochips) for the detection of clinical analytes and biological samples (Zhu et al., 2012; Ihalainen et al., 2013, 2015). Due to the rapid development of inkjet-printed biomaterials, the lack of universal protocols and the intrinsic limitations of the inkjet principle have been identified as the main issues for its practical applications.

2.3.1. Pharmaceutical applications of two-dimensional printing

The applicability of inkjet printing in the production of solid DDS has been studied mainly for oral drug administration (Kolakovic et al., 2013; Alomari et al., 2015; Preis et al., 2015; Scoutaris et al., 2016). Besides that, 2D printing technologies have the potential to be exploited for preparing drug-loaded microparticulate systems (Lee et al., 2012) or functional drug-loaded coatings for medical devices (Tarcha et al., 2007), transdermal microneedles (Boehm et al., 2014; Ross et al., 2015; Uddin et al., 2015) and implants (Nganga et al., 2014). The dose adjustment by pharmacoprinting has been noted to be a good alternative for liquid dosage forms or splitting of tablets (Alomari et al., 2015).

The preparation of oral dosage forms by inkjet printing is beneficial for formulations containing APIs with low dose, narrow therapeutic index, rare therapeutic use and/or short-term stability. Due to the computationally controlled design and the simplicity of the production process, non-complex solid formulations can be prepared for personalized drug therapy. One of the proposed on-site manufacturing concepts includes providing the pharmacies or hospitals with pre-prepared inert substrates and drug-loaded ink containers that can be used for fabricating solid dosage forms in five steps: printing, drying, controlling, rolling and inserting into capsule (Voura et al., 2011). However, the capsulation of the printed materials is barely optional, since printed APIs on biocompatible carrier matrices can be directly administrated for enteral and/or transmucosal drug delivery.

The applications of inkjet printing/jetting have also been investigated and described for the preparation of oral or dermal DDS in pharmaceutical industry (Pickup et al., 2003; Figueroa and Ruiz, 2005). In addition, an industrial scale liquid dispensing technology (LDT) has been designed by GlaxoSmithKline (GlaxoSmithKline, n.d.). The LDT is a continuous manufacturing process, where water-soluble APIs in small doses (1–5 μg) are deposited on inert tablets with a subsequent drying, on-line near-infrared (NIR) imaging and coating process.

In pharmacoprinting, flexography has been shown to be applicable for the deposition and solidification of (nano)suspensions that are problematic for inkjet printing due to nozzle clogging (Janßen et al., 2013; Raijada et al., 2013; Malamatari et al., 2016). Compared to TIJ or PIJ printing, flexography allows depositing inks with higher viscosity (Genina et al., 2012; Raijada et al., 2013). Flexography with verified dosing can provide possibilities for printing suspension inks with poorly water-soluble APIs and applying coating/barrier layers in advanced DDS.

The oral DDS that have been prepared by 2D printing technologies on various biocompatible carrier matrices are presented in **Table 1**.

Table 1. *Examples of oral dosage forms prepared by two-dimensional (2D) printing technologies.*

Technology	Ink type	Inkbase	Active ingredient	Substrate	Reference
TIJ	Solution	10:90 (v/v) of glycerol and water	Salbutamol sulfate	Easybake® edible rice paper	Buanz et al., 2011
	Solution	30:70 (v/v) of PG and water	Rasagiline mesylate	HPMC film	Genina et al., 2013
	Solution	10:20:70 (v/v/v) of glycerol, methanol and water	Clonidine	Polyvinyl alcohol-carboxymethylcellulose sodium salt film	Buanz et al., 2015
	Solution	DecoColour® yellow edible ink	Combination of B vitamins – B_1, B_2, B_3 and B_6	Icing sheet Easybake® edible rice paper	Wickström et al., 2016
	Solution	10% (v/v) edible red ink in a 10:90 (v/v) mixture of glycerol and water	Propranolol hydrochloride	Icing sheet Easybake® edible rice paper HPC-coated Easybake® edible rice paper	Vakili et al., 2016
PIJ	Solution	40:60 (v/v) of PEG 400 and ethanol	Piroxicam	Icing sheet	Raijada et al., 2013
	Solution	water	Sodium picosufate	Rapidfilm® CureFilm™ hydrophilic film CureFilm™ hydrophobic film	Planchette et al., 2015
	Nanosuspension	5% (w/v) PEG 8000 in water	Ciprofloxacin in a drug-polysaccharide complex	HPMC film	Cheow et al., 2015
Dropwise printing (pump)	Solution	Ethanol	Naproxen-polyvinylpyrrolidone complex	HPMC film Chitosan film	Hsu et al., 2012
	Solution	Ethanol	Naproxen-polyvinylpyrrolidone complex	HPMC film	Hirshfield et al., 2014
EHD	Solution	PEG 400	Ibuprofen	HPMC film	Elele et al., 2012
	Solution	2% (w/v) sodium lauryl sulfate in PEG 400	Griseofluvin	HPMC film	Elele et al., 2012
Flexography	Solution	PEG 400	Piroxicam	Icing sheet	Raijada et al, 2013
	Solution	5:95 (w/w) of HPC and ethanol	Rasagiline mesylate	HPMC film	Janßen et al., 2013
	Suspension	5:95 (w/w) of HPC and water	Tadalafil	HPMC film	Janßen et al., 2013

TIJ – thermal inkjet printing; PIJ – piezoelectric inkjet printing; EHD – electrohydrodynamic printing; HPC – hydroxypropyl cellulose; HPMC – hydroxypropyl methylcellulose; PEG – polyethylene glycol; PG – propylene glycol

2.3.2. Regulatory aspects of printed dosage forms

The importance of personalized therapy has been recognized in terms of drug selection and dosing for the advanced prevention and treatment strategies based on the individual variability (Reidenberg, 2003; Woodcock, 2007; Collins and Varmus, 2015). The precision medicine can be successfully implemented by combining therapeutics with diagnostic tests for the analysis of relevant biomarkers (Beaver et al., 2016). Therefore, the benefits of individualization depend greatly on the valuable information received from the diagnostic data that can be used to optimize the patient's treatment. With the analytical advancements and the huge quantity of data, the focus lies in the quality and the interpretation of the received information (Woodcock, 2007; Anaya et al., 2016).

With the shift towards personalized medicine involving adjustable dosing and patient-specific drug combinations, the regulatory requirements are necessary to provide guidelines for the safety and quality control of the tailored dosage forms, as well as for the innovative manufacturing processes and devices. Thus, the development of printed DDS will be confronted with many challenges while future regulations on the evolving technologies for the fabrication of personalized dosage forms are worked out (Kolakovic et al., 2013).

The quantitative quality control and the sterility procedures of inkjet printing have been noted to be the key points for successful and safe drug dispensing at the point-of-care (Alomari et al., 2015). However, simple and applicable solutions for in-line monitoring of dosing are not yet developed. Currently available industrial methods are foremost for off-production testing and require regular cleaning (Daly et al., 2015). In addition, the occurrence of solid state transformations in pharmacoprinting must be addressed and controlled within the regulatory acceptance criteria (Daly et al., 2015).

The advancements in the 3D printing technologies have led to an intense discussion by the regulatory parties on its applicability in practice (Di Prima et al., 2016). A clear differentiation between the industrially manufactured pharmaceutical preparations and magistral formulas could help to formulate the regulations around the printed medicines (Alhnan et al., 2016). In general, the production of drug preparations for individual patients and/or smaller patient groups is not beneficial for pharmaceutical companies. In that case, the importance of compounding facilities, e.g., pharmacies that prepare ex tempore preparations for patients, increases tremendously. However, currently these facilities are not regulated by the same laws as pharmaceutical manufacturing companies; thus, the safety guidelines for the compounding facilities should be revised with the increase of on-demand preparation of personalized medicines (Drues, 2013).

The present regulatory requirements provided by the U.S. Food and Drug Administration (FDA) and the European Medicines Agency (EMA) are

not adjusted for the manufacturing flexibility that is offered by the printing technologies (Alhnan et al., 2016). The un-resolved issues related to the process units, including the pharmaceutical ink formulation, the printer, the printing design and the printed drug preparations, have led to the need to modify the traditional regulations on pharmaceutics (Davies et al., 2015). However, despite the unconventional preparation approach, the solid dosage forms prepared by printing technologies must be manufactured according to the chemistry, manufacturing and control standards, including the International Conference on Harmonisation (ICH) Q10 Pharmaceutical Quality System guidelines, the International Organization for Standardization (ISO) quality standards and the good manufacturing practice (GMP) principles (International Conference on Harmonisation, 2008; Di Prima et al., 2016; Goole and Amighi, 2016).

The identification of critical process parameters by implementing Quality by Design (QbD) and Process Analytical Technology (PAT) tools could increase the conformity between new manufacturing methods and traditional regulatory evaluation systems (Goole and Amighi, 2016). The safety and efficacy issues for printed DDS raised by the authorities include mainly (1) the geometric features, porosity, mechanical properties and function of different materials; (2) the validation of manufacturing processes of individual production lines and quality assurance; (3) the evaluation and validation of parameters related to the patient matching and identification procedures; and (4) the cleanness of the instruments and the validation of the sterilization process (Food and Drug Administration, 2014; Di Prima, 2016). Furthermore, the applicability of these requirements and standards should be evaluated for non-traditional manufacturing sites (i.e., hospitals, clinics, pharmacies and academic centers) to avoid any unlawful adulteration to the printed DDS at the point-of-care (Davies et al., 2015; Sandler and Preis, 2016). Despite the recognition of the issues around pharmacoprinting, the evaluation of the critical aspects of printing technologies and the preparation of manufacturing guidelines will take time (Sparrow, 2014; Pollack and Coburn, 2015).

So far, several 3D printed medical devices and implants without APIs have been approved through emergency use or expanded access pathways (i.e., as an investigational medical product that is accepted without prior clinical trials) (Davies et al., 2015; Alhnan et al., 2016). In addition, in 2015 FDA approved the production of 3D printed Spritam® (levetiracetam) tablets for oral suspension in fixed formulations of four dose strengths (Aprecia, 2015; Spritam, 2016). These 3D printed products have been cleared for use by providing at least an equivalent therapeutic performance compared to already marketed devices/products (Jacobson, 2015). All these achievements have been considered as significant steps towards the marketing of printed dosage forms with bioequivalent performance and further towards even more complex personalization of drug therapies.

Besides 3D printed tablets, the applicability of printing technology in the manufacturing of oral film formulations has been recognized (Preis et al., 2015). Recently, the European Pharmacopoeia's (Ph. Eur.) monograph on oromucosal preparations was expanded by two formulation types – mucoadhesive preparations and orodispersible films (European Pharmacopoeia, 2016a). However, the method specifications for the production guidelines and the analysis methods for the formulations, and the global harmonization of these regulations are still developing (Slavkova and Breitkreutz, 2014; European Pharmacopoeia, 2016a).

The legal support of manufacturers, formulation designers and patients should be ensured by the clearly defined intellectual property rights, the tort liability issues, the reimbursement policies on the value of personalized medicines, and the authorization of shared design files (Davies et al., 2015; Alhnan et al., 2016; Beaver et al., 2016). Furthermore, the ethical, legal and regulatory basis for handling inter-subject pharmacokinetic differences (genetic factors and metabolic polymorphism) in clinical trials and the treatment prescriptions are not coherently defined yet (March et al., 2001; Lesko and Woodcock, 2002; Woodcock, 2007).

2.4. Design of printed dosage forms

Developing therapeutically effective DDS with suitable performance profile (drug release and absorption) and verified quality is the foundation of any dosage form design. The structure of printed dosage forms is dependent on their administration route. Moreover, the patient compliance should be ensured by meeting the general requirements for size and shape of the dosage forms as well as for the organoleptic properties. Hereafter, the tailoring aspects of the printed dosage forms for oral (enteral, buccal, sublabial or sublingual) administration are described.

The properties of the two main components of a typical printed system – ink and substrate – strongly influence the printing outcome. An optimized balance between the printability of the ink formulation, the physical properties of the substrate and the ink-substrate compatibility needs to be established to achieve final preparations with high quality.

2.4.1. Ink formulations

An optimized ink formulation is one of the key components of a successfully printed DDS. The inks can be divided generally into drug solutions (the most common type for inkjet printing), (nano)suspensions (Pardeike et al. 2011; Janßen et al., 2013; Cheow et al., 2014; Essel et al., 2014) and bio-functional inks (Di Risio and Yan, 2007; Derby, 2008; Borchers et al., 2011; Montenegro-Nicolini et al., 2016a, 2016b). Furthermore, inkjet printing can be applied for in situ formation of solid dispersions (Hsu et al., 2012; Hirshfield et al., 2014), microcapsules (Yeo et al., 2003), co-crystals (Buanz et al., 2013) or co-amorphous systems (Wickström et al., 2015).

The properties of the solvent and the dissolved APIs, excipients and other additives determine the viscosity and surface tension of the ink, which are critical attributes for the ink printability.

The dose of the printed API is directly influenced by its concentration in the inkbase solution. Water-based inks are preferred due to their non-toxic nature and suitability for TIJ and PIJ printing (Goodall et al., 2002; Buanz et al., 2011, 2015; Pardeike et al., 2011; Sandler et al., 2011; Genina et al., 2012, 2013; Janßen et al., 2013; Cheow et al., 2015; Planchette et al., 2015; Vakili et al., 2016). In aqueous solutions, the concentration of water-soluble APIs can be easily modified to adjust the printed drug amount (Buanz et al., 2011). However, many APIs possess certain limitations in solubility. Unlike TIJ printing, the PIJ printing is also applicable for inks with non-aqueous solvents, such as ethanol (Melendez et al., 2008; Scoutaris et al., 2011; Hsu et al., 2012; Janßen et al., 2013; Raijada et al., 2013; Hirshfield et al., 2014) or dimethyl sulfoxide (Wickström et al., 2015). However, the use of organic solvents should be limited, since it requires the removal of residual solvents after printing to avoid any toxic effects. In addition, solvents with low evaporation point might cause nozzle clogging and affect the printing quality. Hence, the ink concentration is highly dependent on the used solvent and/or the addition of solubilizing co-solvents (Di Risio and Yan, 2007; Kolakovic et al., 2013; Daly et al., 2015). The effect of various viscosity modifying agents, e.g., glycols, on the printability of enzymatic inks was tested by Di Risio and Yan (2007). Since then, humectants, such as glycerol (Melendez et al., 2008; Buanz et al., 2011; Genina et al., 2012, Buanz et al., 2015; Vakili et al., 2016), propylene glycol (PG) (Sandler et al., 2011; Genina et al., 2012, 2013; Wickström et al., 2016), polyethylene glycols (PEG) (Goodall et al., 2002; Elele et al., 2012; Raijada et al., 2013; Cheow et al., 2015) and hydroxypropyl cellulose (HPC) (Janßen et al., 2013) have been successfully added to various pharmaceutical ink formulations. Other ink components, including coloring and taste-masking agents, could be added to the formulation to obtain certain characteristics (Vakili et al., 2016; Wickström et al., 2016).

On the other hand, the applied system defines the suitable properties of the ink solutions for the printing. Therefore, the final ink formulation is established based on the properties of the API and the requirements of the printing system.

2.4.2. Substrates

The manufacturing methods of carrier matrices that can be used as substrates for inkjet printing are very versatile. Polymer films that are typically used in orodispersible or mucoadhesive preparations are prepared by solvent casting or hot-melt extrusion. Edible porous icing sheets or starch-based papers that are widely used in the food industry could also be feasible alternatives in the printed dosage forms. Ideally, generic substrates that are inert and compatible with a wide range of ink formulations and APIs are

preferred. On the other hand, the functionalization of the substrates provides additional properties, such as mucoadhesion, rapid disintegration or taste masking.

The dosing capacity of the printed dosage forms is defined by the size and the fluid uptake capacity of the substrates. The administrable dimensions of oral films are 1–20 cm^2 with an average size of 4–6 cm^2 that is suitable for all age groups (Dixit and Puthli, 2009; Krampe et al., 2015). The dimensions of buccal DDS are generally smaller due to the limited application area (Krampe et al., 2015).

Considering the afore-mentioned limitations, the printing systems are generally suitable for APIs with low therapeutic dose (in a µg–mg range). The combination DDS with multiple potent APIs can be designed on a small printing area with defined drug deposition in separate compartments and/or by applying barrier coating layers (Scoutaris et al., 2011; Preis et al., 2015).

2.4.2.1. Solvent casting of polymer films

In solvent casting, thin films are produced by casting/spreading a homogeneous layer of a polymer solution on an inert surface. These polymer films are used in rapidly disintegrating orodispersible or prolonged-release buccal drug formulations (Dixit and Puthli, 2009; Hoffmann et al., 2011; Morales and McConville, 2011).

The solution preparation, de-aeration, casting/molding, drying, cutting and packaging of the final dosage forms are the main six steps in the preparation of drug-containing films by solvent casting process (Hoffmann et al., 2011; Morales and McConville, 2011). Soluble additives and active compounds can be added to the film formulation in the solution preparation phase (Siemann, 2005). Whereas, the fabrication of polymer films with poorly soluble drugs in a suspension or emulsion has been known to cause precipitation or phase separation during drying. The solvent selection and the rheological properties of the solution determine the range of applicable APIs, toxicity (e.g., the presence of residual organic solvents), drying time, mechanical strength and stability of the films (Hoffmann et al., 2011). As an alternative to film casting, a solvent-free hot-melt extrusion method could be used to produce polymer films with thermostable materials under a heat-controlled process (Hoffmann et al., 2011; Morales and McConville, 2011).

The basic concepts on producing advanced DDS on oral films by inkjet printing for personalized drug therapy have been discussed by Preis et al. (2015). Inkjet printing of pharmaceuticals on quickly disintegrating, slowly eroding or permanent film substrates allows designing multi-component systems as mucoadhesive or orodispersible preparations for local or systemic drug delivery. Moreover, previous studies have demonstrated that flexography (Janßen et al., 2013) and inkjet printing (Buanz et al., 2015) showed no significant effect on the mechanical properties of the formulations printed on unloaded polymer films, whereas the incorporation of the API during

film preparation decreased the strength of the drug-loaded solvent-cast films compared to the unloaded films.

2.4.2.2. Fibrous substrates by electrospinning

During the electrospinning process, high an unidirectional electrical field is applied to the droplet of a polymer solution/melt to produce fine fibers / fibrous mats (Greiner and Wendorff, 2007; Agarwal et al., 2008; Bhardwaj and Kundu, 2010) (**Figure 4**). When the electrical forces overcome the forces of surface tension and charge, the fluid/melt forms a Taylor cone (i.e., a cone that forms at the tip of the capillary/needle where the liquid polymer jet is ejected during electrospinning or spraying) (Taylor, 1964). This causes the deformation of the droplet and the ejection of a charged jet towards a grounded counter electrode (drum/plate collector). The solvent evaporates during the transfer of the solution from the ejector to the collector, and finally continuous solid fibers are collected on the grounded metal drum/plate. Generally, non-woven fibrous scaffolds with random fiber alignment are produced due to the rapid whipping during the fiber formation. However, non woven mats with parallelly aligned fibers can be produced by applying suitable fiber collection methods (Liang et al., 2009).

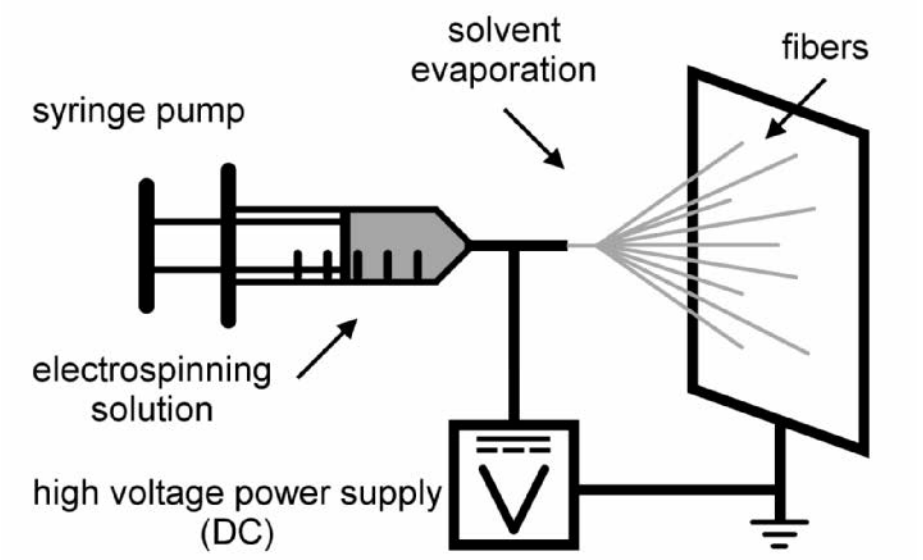

Figure 4*. Electrospinning system.*

Electrospinning is an easy-to-use but complex method, where the formation of fibers is highly dependent on the properties of the polymer(s) solution/melt and the parameters and conditions of the electrospinning process (Greiner and Wendorff, 2007; Bhardwaj and Kundu, 2010). Due to the adjustability of these attributes, it concurrently allows modifying and optimizing the properties of the fibers for versatile applications. For

example, the diameter, shape, surface topography and inner structure of the electrospun fibers are significantly influenced by the properties of the materials and the electrospinning solution/melt (e.g., molecular weight of the polymer, concentration, additives, viscosity, surface tension, conductivity), the process parameters (e.g., applied voltage, feed rate of the solution, the distance between the ejector tip and the collector), and the environmental conditions (humidity, temperature). Furthermore, the fiber morphology is dependent on the solvent properties, such as vapor pressure and boiling point, that determine the evaporation rate of the solvent(s) and the drying time. By optimizing the composition of the solution/melt and the electrospinning conditions, fibrous matrices with modified morphology and structure can be obtained.

The electrospun fibrous mats provide high biocompatibility in tissue engineering and local drug delivery due to their porous 3D structure that mimics the structure of the extracellular matrix (Agarwal et al., 2008). The fibrous matrices have large surface area to volume ratio and drug-loading capacity that is advantageous for developing DDS (Greiner and Wendorff, 2007; Agarwal et al., 2008; Bhardwaj and Kundu, 2010; Hu et al., 2015). The electrospun fiber mats can be functionalized during the spinning process or via post-treatment (Liang et al., 2009). Furthermore, electrospinning is an attractive method from the industrial viewpoint due to the simplicity of the process and the possibility for large scale production. Nevertheless, the use of non-toxic solvents and ensuring the uniformity of the electrospun fibers remains challenging, and thus contributes to the limitations in the production (Agarwal et al., 2008; Schiffmann and Schauer, 2008; Bhardwaj and Kundu, 2010; Hu et al., 2015).

Electrospun products are commercially available for various applications, such as filtration and textiles (Greiner and Wendorff, 2007; Bhardwaj and Kundu, 2010). Typical biomedical applications of electrospun fiber scaffolds are tissue engineering and drug delivery (Greiner and Wendorff, 2007; Agarwal et al., 2008; Bharwaj and Kundu 2010; Sridhar et al., 2011; Hu et al., 2015). The adhesion/adsorption and proliferation of cells on the electrospun fibrous mats have led to their increased use in regenerative medicine. Electrospun fibrous systems provide advantageous possibilities for local drug delivery and controlled drug release. Fiber scaffolds containing APIs, such as antibacterial agents, anticancer drugs, growth factors and other bioactive molecules, for wound healing, chemotherapy or implants have been extensively investigated in the recent years (Agarwal et al., 2008; Sridhar et al., 2011; Hu et al., 2015).

Electrospinning enables producing fibers with diameters in nano- to micrometer scale from natural (e.g., cellulose derivatives, chitosan, collagen, gelatin, elastin, silk protein) and synthetic (e.g., poly(lactic acid), polycaprolactone, copolymer poly (lactide-co-glycolide)) polymers, polymer

mixtures, non-polymeric materials and multi-component systems (Greiner and Wendorff, 2007; Schiffmann and Schauer, 2008; Liang et al., 2009; Bhardwaj and Kundu 2010). Furthermore, the post-treatment of electrospun fibers has shown to improve their mechanical strength and elasticity (Greiner and Wendorff, 2007).

The porous matrices provide increased stability of metastable forms of drug molecules within the substrate structure and reduce the surface roughness of printed dosage forms (Sandler et al., 2011; Raijada et al., 2014). Therefore, the loosely fibrous structure of electrospun scaffolds shows high suitability for their use as substrates in inkjet printing.

2.5. Quality of printed dosage forms

The quality of the printed dosage forms is derived from three major aspects: ink printability, ink-substrate interactions and printing parameters. The optimization of the printing parameters allows fine-tuning of the printed DDS within the defined limits of the printing system.

In PIJ printing, the droplet geometry and behavior can be optimized by adjusting the applied voltage, waveform (Liu et al., 2013), printing frequency and/or temperature. However, the effect of these parameters on the performance of pharmaceutical inks has not been systematically studied yet. The volume, velocity and trajectory angle of jetted droplets are directly influenced by the diameter of the nozzle (typically 30–60 μm). Generally, the ejection of smaller droplets enables to produce printable products at higher resolution. The definition of inkjet printing is limited by the diameter of the deposited droplet with a 1 pL droplet having a diameter of approximately 12 μm (Derby, 2010). In that context, the main problem related to the inconsistency of the printing quality is nozzle clogging (Le, 1998; Calvert, 2001). In comparison, the printing resolution of flexography is approximately 30–75 μm (Kolakovic et al., 2013). The accuracy of the ink deposition is also determined by the substrate feeding system and the overall formulation design (e.g., printing pattern, resolution, layering).

2.5.1. Printability of ink formulations

The evaluation of the printability of an ink is based on its physical properties: viscosity, surface tension and density. These properties influence the droplet formation and the jetting stability (Le, 1998; Calvert, 2001).

Viscosity is a dynamic parameter of a material that is defined as its resistance to flow and expressed as the rate of deformation (shear rate) against the applied stress (shear stress) at a constant temperature. Due to the small structures and applied forces, the shear rates involved in inkjet printing are about 10^5 s^{-1} (de Gans et al., 2004). This can lead to a non-linear flow behavior (i.e., shear thinning or thickening); hence, the viscosity of the ink solutions must be controlled (Barnes et al., 1989).

A phenomenon that describes the intermolecular forces between the liquid

molecules is called surface tension. Its value is defined by the force that is needed to increase the surface of a liquid by a unit area. For example, at room temperature the surface tension of water and ethanol is 73 and 23 mN/m, respectively. The optimal viscosity and surface tension for inkjet printing are in the range of 2–30 mPa·s and 25–50 mN/m, respectively (Calvert, 2001; de Gans et al., 2004; Park and Moon, 2006; Di Risio and Yan, 2007; Jang et al., 2009; Daly et al., 2015).

Printability can be estimated by determining the Z-value of the fluid. The dimensionless Z-value (**Equation 1**) is an inverse of the Ohnesorge number (*Oh*), which is derived from the Reynolds (*Re*) and Weber (*We*) numbers (Fromm, 1984; McKinley and Renardy, 2011), where the v, ρ, η, γ and a are defined as the average velocity, density, viscosity of the fluid and the radius of the printing nozzle.

$$Z = \frac{1}{Oh} = \frac{Re}{\sqrt{We}} = \frac{\sqrt{\gamma \rho a}}{\eta} \qquad \textit{(Equation 1)}$$

$$Re = \frac{v \rho a}{\eta}$$

$$We = \frac{v^2 \rho a}{\gamma}$$

The *Re* and *We* numbers characterizes the fluid flow properties under viscous and capillary forces, respectively. Then again, the Z-value is independent of the fluid velocity or flow rate (Jang et al., 2009; McKinley and Renardy, 2011). The Z-value in a range from 1 to 14 has been described for printable inks (Jang et al., 2009; Derby, 2010). The schematic of the printability range is presented on **Figure 5**.

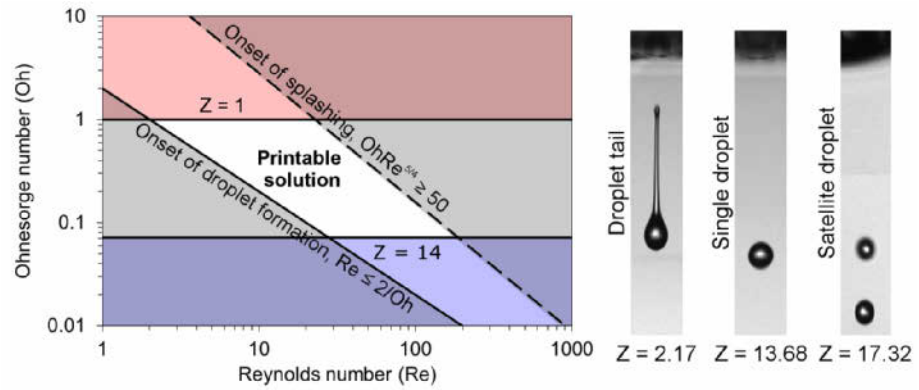

***Figure 5**. Operational range of printable fluids for drop-on-demand inkjet printing, and photographic images of different ink droplets 140 ms after ejection from a single nozzle (Ø 50 μm) at a voltage of 25 V (Jang et al., 2009; McKinley and Renardy, 2011). Onset criterions for droplet formation and splashing have been given by Derby (2010).*

In inkjet printing, the optimal viscosity and surface tension ensure the uniform formation of spherical droplets and the ink deposition by avoiding nozzle clogging or unwanted dripping of the ink (Calvert, 2001; de Gans et al., 2004). By adjusting these parameters, the jetting of ink droplets without tails ($Z > 1$) and without satellite droplets ($Z < 14$) can be obtained. In aqueous inks, the printability is achieved by incorporating water-soluble/miscible solvent(s) as viscosity modifying agent(s) and/or surfactants.

In the flexographic printing, the printability is foremost dependent on the viscosity of the ink. A uniform ink transfer onto a substrate can be achieved with viscous solutions or suspensions with values between 50–500 mPa·s (Genina et al., 2012; Janßen et al., 2013; Kolakovic et al., 2013).

2.5.2. Ink-substrate interactions

In the printed DDS, where the ink is deposited on a carrier matrix, the ink-substrate physical interactions affect the drying mechanism of the ink. These interactions can be categorized as the droplet spreading upon impact, the patterning on non-porous and porous substrates, and the droplet solidification (Derby, 2010).

After a droplet is ejected from the printhead, the contact with the substrate is driven by the inertial impact and capillary forces (Derby, 2010). The contact angle of the droplets determines the droplet shape and the printed pattern caused by the merging of the droplets. Thus, the pattern of the solidified particles differs depending on the surface wettability and the hydrodynamic flows. Within the droplet these hydrodynamic flows, including the convective flow and the surface tension-based Maragoni flow, try to compensate for the solvent evaporation during drying (Park and Moon, 2006). A comprehensive overview by Park and Moon (2006) defined some of the underlying reasons for the differences in the inkjet-printed patterns on hydrophilic and hydrophobic surfaces by the deposition of ink formulations with silica microspheres in varied compositions and concentrations.

The wettability of the substrate is affected by its roughness, surface energy and porosity (pore size, volume and geometry). A reduced ink spreading has been seen on porous substrates (Määttänen et al., 2010). However, on homogeneous non-porous materials the ink droplets tend to merge and form larger beads rather than to form a uniform layer (Calvert, 2001; Derby, 2010).

On porous substrates, e.g., copy paper, the drying of water-based inks is dependent on the wettability of substrate surface (adsorption/spreading) and the ink penetration into the substrate (absorption/infiltration) with a concurrent evaporation of the solvent (Le, 1998; Määttänen et al., 2010). In the printed systems on impermeable substrates, the drying rate is determined mainly by the evaporation of the solvent (Le, 1998). The solidification process strongly dictates the ink distribution, and thus the shape and the pattern of the printed formulation.

A homogeneous printing pattern is obtained by the sufficient solute

distribution during drying. The printing quality is diminished by the excessive and/or irregular spreading of ink droplets on the substrates (Le, 1998). Based on the adsorptive infiltration theory by Holman et al. (2002), the droplet localization can be controlled by increasing the ink affinity towards the substrate that causes the adsorptive confinement of the droplets to the surface.

Layered systems are produced by printing several ink layers on top of each other with an intermediate drying step. The problems with smearing and erosion can be avoided by applying printing systems with stationary substrate holders, by separate solidification of the layers (e.g., by UV curing or thermal treatment) and/or by using porous substrates to increase the absorption capacity (Calvert, 2001). In DDS, the ink penetration into the porous substrates contributes to the high dosing precision (Genina et al., 2013). When a solution is deposited on impermeable surfaces, the ink layers are merged due to the redissolution, resuspension or re-melting of the dried layers after depositing an additional layer (Calvert, 2001).

Coated substrates provide additional flexibility for adjusting the characteristics of printing surfaces (Määtänen et al., 2010; Planchette et al., 2016; Vakili et al., 2016). Vakili et al. (2016) noted that a hydrophilic coating on porous rice paper made the surface smoother, but also disintegrated/ dissolved after printing due to the ink incorporation into the surface layer. In addition, by adding backing and/or coating layers the drug release behavior can be modified (Voura et al., 2011; Genina et al., 2012; Preis et al., 2015). However, planar carrier substrates are not an obligatory part of DDS, since it is possible to use printing to produce drug-loaded coatings for DDD (Tarcha et al., 2007; Boehm et al., 2014; Nganga et al., 2014; Ross et al., 2015; Uddin et al., 2015) or to prepare independent drug-loaded microstructures (Lee et al., 2012).

Controlling the solid state characteristics of the printed solids is crucial in pharmaceutical formulations (Kolakovic et al., 2013; Daly et al., 2015). In the preparation of solid dosage forms, the properties of the substrates and the ink-substrate interactions influence the solidification and the crystallization of the printed APIs after solvent evaporation (Sandler et al., 2011; Hsu et al., 2012; Raijada et al., 2013; Buanz et al., 2013).

2.6. Solid state properties of printed pharmaceuticals

The identification of solid state forms of drugs and their stability within the dosage forms as well as the rate of the solid state transformations is a crucial part of the pharmaceutical product development. The ICH guidelines for new drug substances and drug products stipulate that the solid state (i.e., polymorphic, solvate/ hydrate or amorphous state) of APIs needs to be specified and controlled, when it is known to affect the biopharmaceutical performance of the drug product (International Conference on Harmonisation 1999a, 1999b). The pharmacoprinting process involves the

phase transformation of the API from a solution, suspension or emulsion into a solid state. For that reason, the crystallization behavior and the solid state properties of the printed pharmaceuticals need to be studied to control the performance of the DDS.

2.6.1. Solid state forms

Pharmaceutical materials that exhibit different solid state forms can exist as crystalline polymorphs, solvates/hydrates or in an amorphous state. Polymorphism is the ability of solid compounds to exist in more than one different crystalline phases (Haleblian and McCrone, 1969). The polymorphic materials have the same molecular composition, but a distinct structure due to the differences in the molecular arrangement in the crystalline lattice (Haleblian and McCrone, 1969; Byrn et al., 1994). The crystals of pharmaceutical compounds are connected with each other by physical non-bonded interactions and/or by non-covalent hydrogen bonding (Byrn et al., 1994). The physicochemical and thermodynamic properties and the stability vary between the solid state forms of APIs, and thus lead to modifications in their therapeutic performance (Haleblian and McCrone, 1969; Byrn et al., 1994). The presence of thermodynamically stable and/or metastable forms affects mainly the solubility, dissolution rate and consequently the bioavailability of the active compounds (Haleblian and McCrone, 1969). The stability of solutions or dispersions (suspensions, emulsions) is generally highly dependent on the initial polymorphic form of an API used for the preparation and on the solid state transformations occurring during storage (Haleblian and McCrone, 1969). In addition, it has been noted that the solid state form affects the chemical stability and the degradation rate of the drugs (Haleblian and McCrone, 1969; Hancock and Zografi, 1997).

Solvates or hydrates are crystalline solids that contain solvent or water molecules within their crystal structure, respectively (Byrn et al., 1994; Vippagunta et al., 2001). Their properties, such as solubility, response to humid conditions and loss of solvent, vary from to their anhydrous counterparts as a consequent of different hydrogen bond patterns and crystal packing (Byrn et al., 1994; Vippagunta et al., 2001). The solvation/desolvation (or hydration/dehydration) phase transformations can cause instabilities in pharmaceutical systems and affect the bioavailability of drugs. For example, during drug release testing the formation of a hydrate within the solid dosage form can significantly affect the dissolution rate of an API (Aaltonen et al., 2006). The solubility and dissolution rate of zwitter-ionic piroxicam (PRX) anhydrous and monohydrate forms were shown to have different aqueous solubility and dissolution behavior due to their distinct molecular structure (packing density, conformation, intra- and intermolecular bonding) and the degree of ionization in solutions with different pH values (Paaver et al., 2012).

Amorphous state is a unique non-crystalline state of solids, which has no 3D molecular order in long-range and the randomly arranged molecules

possess ordered structures only in short-range (Hancock and Zografi, 1997; Yu, 2001). The solids in an amorphous state are thermodynamically and chemically less stable, prone to moisture uptake and usually more soluble in water than in a crystalline state (Byrn et al., 1994; Hancock and Parks, 2000). Furthermore, small differences in the amorphous state can occur depending on the hydrogen bonding properties of the solid state form of the starting material (Savolainen et al., 2006). The formation and presence of amorphous solids influences its manufacturability, stability and biopharmaceutical performance (Hancock and Zografi, 1997). The amorphous state of materials can be obtained during vapor condensation, wet granulation, quench cooling of a melt, milling and compaction of crystals or precipitation from solutions by freeze- or spray-drying (Hancock and Zografi, 1997; Yu, 2001). However, amorphous solids can undergo crystallization at sufficient molecular mobility, upon exposure to heat and/or humidity (Yu, 2001).

Solids in different polymorphic forms, amorphous state or as their mixture can be obtained intentionally or appear unintentionally during pharmaceutical processes. In the preparations containing drugs in amorphous or metastable forms, the systems need stabilizing in order to hinder the solid state transformations into thermodynamically most stable crystalline form (Haleblian and McCrone, 1969; International Conference on Harmonisation, 1999a). The concentration of different polymorphs has a significant effect on the physiological availability of APIs mainly because of the variation in their absorption characteristics (Aguiar at al., 1967; Haleblian and McCrone, 1969).

2.6.2. Factors affecting solid state of printed pharmaceuticals

Pharmaceutical materials, such as proteins, polymers and some sugars are commonly present in a fully or partially amorphous state (Yu, 2001). On the other hand, most APIs in amorphous state have higher energy levels compared to a thermodynamically stable crystalline (polymorphic) form and are inherently unstable. The bioavailability of APIs in Class I and III of Biopharmaceutics Classification System (BCS) is less likely to be impacted by the occurrence of polymorphism (Amidon et al., 1995). However, the solid state form of APIs belonging to the Class II (and Class IV) of BCS can affect their in vivo behavior due to the solubility-limited absorption (Amidon et al., 1995).

The preparation of multicomponent systems with stabilizing additives is one of the most common ways for stabilizing the amorphous state of drugs. The physical interactions between the components are mainly based on non-covalent hydrogen bonding, van der Waals forces (atomic repulsion/attraction), electrostatic polar forces (dipole–dipole attraction), π–π or ionic interactions. In addition, the solid state form and water sorption properties of excipients affect the stability of pharmaceutical formulations. For example, Airaksinen et al. (2005) demonstrated that amorphous excipients hindered the hydrate formation from nitrofurantoin anhydrate during wet granulation,

whereas the crystalline excipients were unable to control the phase transformation.

Phase transformations based on solution mechanism occur upon solvent removal/evaporation from solutions with entirely or partially dissolved drugs, for example, during wet granulation or spray-drying. Polymorphic transition, desolvation/dehydration, amorphous crystallization and vitrification are the main possible phase transitions during rapid solvent removal (Zhang et al., 2004). The solidification of drugs can result in a stable or unstable single phase or consist of a mixture of amorphous or crystalline solid state forms depending on the extent and rate of solvent removal and crystallization. The loss of crystallinity during printing process is influenced by the rapid evaporation of the solvent and the reduction of particle size (Vippagunta et al., 2001).

The printed layer(s) on substrate can exhibit similarities with solid solutions or dispersions. Solid solutions are single phase systems consisting of multiple components. The dissolution rate of molecularly dispersed or dissolved drug(s) in these systems is determined by the carrier. Thus, the formation of solid solutions of poorly water-soluble drugs in aqueously soluble carriers is one way of increasing oral bioavailability. On the other hand, when the API is partially dispersed in the carrier material without any detectable crystallinity, multi-phase solid dispersions are obtained (Leuner and Dressman, 2000).

The solidification of inkjet-printed pharmaceuticals is affected by the ink formulations, the substrate properties (roughness, porosity) and the ink-substrate interactions. In exceptional cases, printing can be used to produce co-crystals (Buanz et al., 2013) or uniform nanoparticulate layers (Ihalainen et al., 2013), whereas DDS are generally obtained with well-distributed APIs in (micro)crystalline, molecularly dispersed and/or amorphous state. The type and the composition of the ink formulations affect the solid state of the API in the final preparations. For example, solubilizing agents, such as PG, are known to inhibit the crystallization of the dissolved API(s) and ease the dosing process (Scoutaris et al., 2011; Voura et al., 2011; Kolakovic et al. 2013). However, the solid state transformations with crystalline nanosuspension inks are unlikely, and their release behavior is mainly influenced by the particle size reduction and the extent of redispersion.

2.7. Analytical methods for quality control of printed dosage forms

In pharmaceutical manufacturing, the analysis of qualitative and quantitative attributes of the dosage forms can be conducted with several techniques in off-line, on-line or in-line measurement setups. Fast and non-destructive methods that could be used for on-line or in-line quantification of active compounds, detecting and/or quantifying solid state transformations

are preferred. As part of the QbD approach, the implementation of PAT tools with multivariate data analysis allows achieving a continuous control and optimization of the manufacturing process. Besides the availability of instrumentation, acceptable detection and quantification limits must be assured for dose verification.

Onsite fabrication of printed dosage forms can reduce the occurrence of solid state transformations and time-dependent physical or chemical degradation prior to drug administration (Raijada et al., 2013). However, the physical stabilization of amorphous APIs, e.g., by preparing hydrogen-bonded solid dispersions with polymers, might still be necessary (Serajuddin, 1999; Tantishaiyakul et al., 1999; Weuts et al., 2005, Lust et al., 2015). Nevertheless, monitoring the manufacturing process is crucial for controlling and detecting stability issues that can arise during the preparation of drug formulations.

The solid state characterization methods and their feasibility in qualitative and quantitative analysis of pharmaceutical solids have been investigated extensively over the last 50 years (Haleblian and McCrone, 1969; Hancock and Zografi, 1997; Newman and Byrn, 2003; Rodríguez-Spong et al., 2004; Zhang et al., 2004; Aaltonen et al., 2008, 2009; Chieng et al., 2011). For the quantification of active ingredients, conventional methods like high performance liquid chromatography (HPLC), ultraviolet-visible (UV-Vis) spectrophotometry and mass spectrometry are still the mainly used techniques. However, non-destructive spectroscopic and diffraction methods that provide molecular information about the APIs have also been applied in the quantitative analysis. Many of these instrumentations can be integrated into the production line or used as handheld devices for fast quality control. Furthermore, continuously collected data can effectively be interpreted by multivariate data analysis.

The X-ray diffraction (XRD) technique provides information in a particulate level about the crystallographic properties of materials and enables to differentiate between the polymorphic forms and the amorphous state of solids (Haleblian and McCrone, 1969; Hancock and Zografi, 1997, Chen et al., 2001; Vippagunta et al., 2001; Aaltonen et al., 2009; Chieng et al., 2011). For example, XRD together with chemometrics could detect solid-state transformations and the formation of amorphous PRX during ball-milling process (Kogermann et al., 2011).

The vibrational spectroscopic methods – infrared (IR), NIR, Raman – have developed immensely over time and are used alone or in combination with other techniques and multivariate data analysis to detect and quantify solid state forms of pharmaceuticals (Savolainen et al., 2006; Aaltonen et al., 2008). Moreover, vibrational spectroscopy in combination with multivariate data analysis could be used for advanced qualitative and quantitative analysis of complex systems and/or controlling pharmaceutical processes (Auer et al., 2003; Helmy et al., 2003; Boyer et al., 2006; Silva et al., 2009; Rajalahti and

Kvalheim, 2011; Mazurek and Szostak, 2012).

The intramolecular vibrations in the structure of chemicals can be analyzed by IR spectroscopy. The IR spectroscopy allows detecting the absorption of the IR radiation caused by the changes in the dipole moment of the molecules. Thus, the obtained IR spectra allow identifying specific functional groups, presence of water and hydrogen bonding in pharmaceutical and other chemical compounds (Kalinkova, 1999; Auer et al., 2003). IR spectroscopy provides also valuable information on the intermolecular interactions, such as hydrogen bonding, between the drugs and the excipients (Kalinkova, 1999). Furthermore, the principle of attenuated total reflection (ATR) enables obtaining spectral information from the surface of the materials without any sample pretreatment (**Figure 6**) (Fahrenfort, 1961; Offermann et al., 1995).

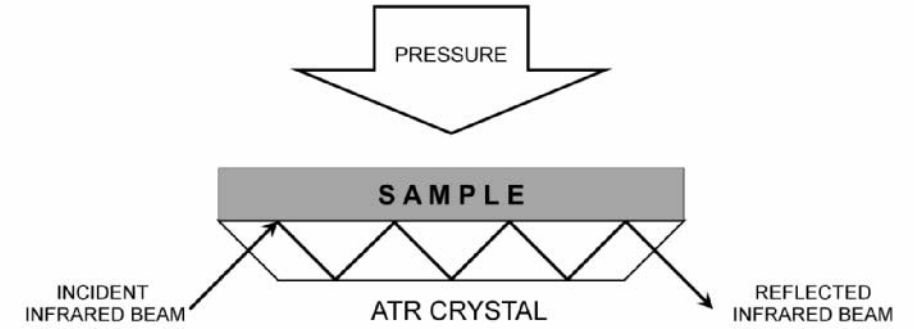

***Figure 6**. Attenuated total reflectance (ATR) infrared spectroscopy.*

IR and Raman spectroscopy are generally complementary techniques for identifying the molecular structure and conformation of chemical entities (Halebian and McCrone, 1969; Byrn et al., 1994; Hancock and Zografi, 1997; Vippagunta et al., 2001; Christy and Egeberg, 2006; Aaltonen et al., 2009; Chieng et al., 2011). For example, Raman spectroscopy with chemometrics has been successfully used for the quantification of polymorphic mixtures of indomethacin (Heinz et al., 2007) and to observe amorphization of PRX during ball-milling (Kogermann et al., 2011).

NIR spectroscopy, on the other hand, is less API-specific and provides valuable information on solid-water interactions (Aaltonen et al., 2009; Chieng et al., 2011). The in-line implementation of NIR or Raman spectroscopy with multivariate data analysis has allowed monitoring the hydrate formation from anhydrates (Jørgensen et al., 2002) or dehydration of APIs during drying process (Kogermann et al., 2008). Depending on the vibrational spectroscopy technique, the detection of compounds in low content has been shown to be limited by the method sensitivity towards the particle size of the solids and the homogeneity of the sample mixtures (Campbell Roberts et al., 2002; Heinz et al., 2007; Mazurek and Szostak,

2012).

So far, IR (Hammes et al., 2014; Offermann et al., 1995), NIR (Tumuluri et al., 2004) or Raman (Tumuluri et al., 2008; Zhang et al., 2014) spectroscopy in an off-line or in-line setup have been successfully used for drug content analysis of pharmaceutical film formulations. Research conducted by Melendez et al. (2008) was the first to apply Raman spectroscopy and XRD in the solid state characterization of printed pharmaceuticals. Later, Buanz et al. (2013) applied IR spectroscopy for detecting co-crystal formation during inkjet printing.

Furthermore, hyperspectral imaging techniques that could be integrated into the manufacturing line are highly valuable for providing information about the drug distribution, surface chemistry and API content in the printed dosage forms. Recently, Vakili et al. (2014) showed that non-destructive NIR hyperspectral imaging combined with partial least squares (PLS) regression modelling was applicable for the API quantification in layered formulations (1–32 printed layers) prepared with a desktop inkjet printer. Furthermore, other high throughput imaging tools that have been applied for analyzing printed pharmaceuticals are time-of-flight secondary ion mass spectrometry (Scoutaris et al., 2012) and IR imaging (Chan and Kazarian, 2005).

Another promising approach for quality control of printed pharmaceuticals is the use of handheld devices. In a combination with spectral libraries and multivariate data analysis, the handheld spectroscopic (Raman, mid-IR, NIR) devices show good acceptability for quality control applications (Sorak et al., 2012). To date, the use of Raman spectroscopy has shown to be limited by the excitation wavelength and the strength of Raman scattering and fluorescence (Sorak et al., 2012; Hajjou et al., 2013). Additionally, a handheld colorimetry device was introduced for the quantification of printed pharmaceuticals. The incorporation of an edible color into the ink solutions allowed obtaining a correlation between the propranolol hydrochloride content and the color intensity in the printed layered formulations on three different edible substrates (up to 16 layers) (Vakili et al., 2015). On the other hand, it was shown that in a combination formulation when naturally colored active ingredients are added to the solution containing an edible color, the colorimetric analysis is limited by the color saturation at much lower number of printed layers (Wickström et al., 2015).

The hyperspectral imaging methods and the handheld devices are promising approaches for the quality control of dosage forms that are manufactured on-demand at the point-of-care. These techniques could be integrated into the printing device or used separately after the printing process, respectively. The main challenges that have arose are the detection and quantification limitations, the resolution of the measurements and their reliability in the analysis of drug combinations. The qualitative validation of

such devices for each DDS is necessary to avoid false results.

Besides the quantitative analysis and the solid state characterization, tests that are related to the acceptability by the patient (mouth feel, taste and appearance), the stability and the mechanical strength during production, storage and handling are of importance in the development of oromucosal and/or topical dosage forms (Krampe et al., 2015). The structure of the manufacturing and quality control apparatuses must ensure minimal microbiological contamination and cross-contamination, for example by exploiting disposable ink cartridges and by using easily cleaned parts (tubing, printhead, probes etc.) that come into contact with the drug formulation.

3. Aims of the study

The main goal of this research study was to investigate and gain understanding of the applicability of printing technology for the preparation of personalized dosage forms. The presented work aimed to design and characterize the printed dosage forms for patient-tailored drug therapy, and to establish the crucial attributes in the development process.

The specific objectives were to:

- Formulate the pharmaceutical inks, substrates and the dosage forms for inkjet and flexographic printing (I, III, IV)
- Characterize the physicochemical properties of the printed dosage forms (I-IV)
- Evaluate the dose accuracy and dosing flexibility of inkjet printing (I)
- Investigate the use of infrared (IR) spectroscopy in the quantification of printed dosage forms (II)
- Analyze the drug release behavior of solid nanoparticulate systems prepared by flexographic printing (III)
- Design and study the properties of a combination drug delivery system (DDS) with two active compounds (IV)

4. Materials and methods

The detailed descriptions of the materials and methods used for each research work are presented in the original publications (I–IV).

4.1. Materials

4.1.1. Active pharmaceutical ingredients

The active pharmaceutical ingredients (APIs) used in the printed dosage forms are presented in **Figure 7**. The solutions for the inkjet printing contained caffeine (CAF) (Ph. Eur., Sigma-Aldrich, Germany) (I, II), loperamide hydrochloride (LOP) (Sigma-Aldrich, Italy) (I, II) and lidocaine hydrochloride (LH) monohydrate (≥99%, Sigma-Aldrich, India) (IV).

Nanosuspensions with itraconazole (ITR) (Orion Pharma, Finland) and indomethacin (IND) (≥99%, Sigma–Aldrich, China) were prepared for flexographic printing (III). Piroxicam (PRX) in anhydrous form II (Letco Medical Inc., USA) was used as a poorly water-soluble model compound in the electrospun fiber substrates (IV).

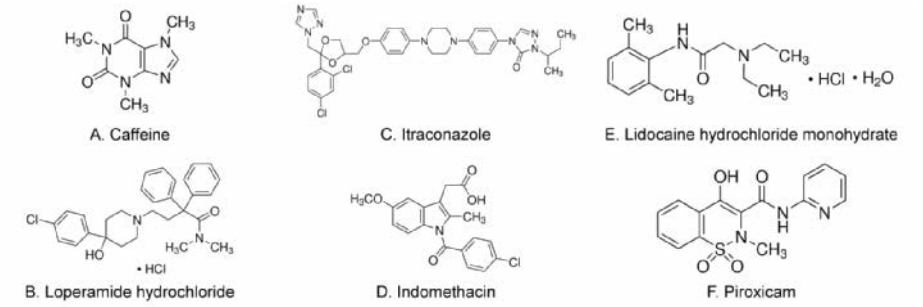

Figure 7. *Chemical structures of caffeine (***A***), loperamide hydrochloride (***B***), itraconazole (***C***), indomethacin (***D***), lidocaine hydrochloride (***E***) monohydrate and piroxicam (***F***).*

4.1.2. Substrates

Polyethylene terephthalate (PET) films (Mylar® A, Dupont Teijin Films Europe, Luxembourg) (I, II) and transparency films (TF) (DatalineTM, Esselte Office Products Oy, Finland) (III) were used as non-biocompatible reference substrates. Icing sheets (Sutton Valence, UK) (I), rice sheets (Easybake® edible rice paper, N.J. Products Ltd., UK) (III) and rice papers (Blue Dragon® Spring Roll Wrappers, UK) (III) were exploited as commercially available edible substrates. Solvent-cast hydroxyl propyl cellulose (HPC) (Klucel LF PHARM, Ashland, USA) films (I) and electrospun gelatin (Type A from porcine skin, Sigma-Aldrich, USA) substrates (IV) were prepared on a laboratory scale.

4.2. Methods

4.2.1. Preparation of pharmaceutical inks

Different inks were used for inkjet (I, II, IV) and flexographic (III) printing (**Table 2**). Propylene glycol (PG) (≥99.5%, Sigma-Aldrich, USA) acted as a viscosity modifying agent in the ink solutions (I, II, IV). A wet ball milling technique (Pulverisette 7 Premium, FritschCo., Germany) was used for the preparation of aqueous ITR and IND nanosuspensions (III). In the nanosuspensions a non-ionic surfactant Poloxamer 407 (Pluronic® F-127, BASF Co., Ludwigshafen, Germany) was exploited as a stabilizer. The solvents were purified water (Milli-Q) and ethanol (≥99.7%, Etax Aa, Altia OYj, Finland).

***Table 2**. Composition of the pharmaceutical inks.*

	API	Concentration	Ink type	Inkbase
I, II	Caffeine (CAF)	20 mg/ml	Solution	PG and water in 30:70 (v/v) ratio
I, II	Loperamide hydrochloride (LOP)	50 mg/ml	Solution	PG and ethanol in 40:60 (v/v) ratio
IV	Lidocaine hydrochloride (LH)	330 mg/ml	Solution	PG and water in 40:60 (v/v) ratio
III	Itraconazole (ITR)	112 mg/ml	Nanosuspension	Poloxamer 407 (60% (w/w) of the drug amount) and water
III	Indomethacin (IND)	145 mg/ml	Nanosuspension	Poloxamer 407 (60% (w/w) of the drug amount) and water

API – active pharmaceutical ingredient; PG – propylene glycol

4.2.2. Preparation of solvent-cast substrates (I)

The HPC films were prepared by solvent casting. A 5% (w/w) HPC aqueous solution was uniformly distributed onto a TF with 0.15 ml/cm^2. The HPC films were dried at a temperature of 22 ± 2 °C and relative humidity (RH) of 45 ± 5% for 12 h.

4.2.3. Preparation of electrospun substrates (IV)

Electrospinning (ESR-200Rseries, eS-robot®, NanoNC, South Korea) was used to prepare fibrous gelatin substrates. Three different solutions for electrospinning were obtained by mixing the components at elevated temperatures (40–50 °C) (**Table 3**). An automatic syringe pump equipped with a syringe and a metallic syringe needle was used for continuous jetting of the solutions. For maintaining a steady solution temperature at 50 °C for G20 and G20-PRX formulations, a melt electrospinning setup equipped with an oil circulator (NNC-OCB200, NanoNC, South Korea) was exploited. The specific parameters of the electrospinning for the preparation of different gelatin fibers are presented in **Table 3**. The fibrous gelatin substrates were crosslinked

through heat treatment after electrospinning. The theoretical concentration of PRX in the final drug-loaded gelatin substrate (G20-PRX) was 6.5% (w/w).

***Table 3**. Composition of the electrospinning solutions and the parameters of electrospinning and crosslinking for the preparation of fibrous gelatin substrates.*

	G25[a]	G20	G20-PRX
Electrospinning solution			
Gelatin concentration	25% (w/v)	20% (w/v)	
Glucose concentration	3.75% (w/v)	3% (w/v)	
PRX concentration	-	-	16 mg/mL
Solvent(s)	10 M acetic acid aqueous solution	10 M acetic acid aqueous solution and DMF in 1:4 (v/v) ratio	
Electrospinning parameters			
Pumping rate	8 µl/min	25–30 µl/min	
Voltage	17–18 kV	14 kV	
Distance between spinneret and collector	~14 cm	~18 cm	
Solution temperature	25 ± 1 °C	50 °C	
Crosslinking			
Heat treatment conditions	3 h at 170–175 °C	3 h at 130 °C	

[a]Formulation by Siimon et al. (2014); PRX – piroxicam; DMF – dimethylformamide

4.2.4. Printing technology

4.2.4.1. Piezoelectric inkjet printing (I, II, IV)

A Dimatix DMP-2800 piezoelectric inkjet (PIJ) printer (Fujifilm Dimatix Inc., USA) with a typical droplet volume of approximately 10 pL was used for the printing of CAF and LOP inks (I, II). The printed dose of CAF and LOP on the substrates was varied by changing the printed area (cm^2) or the drop spacing (DS) of the jetted droplets. Firstly, the effect of the printed area from 0.4 to 4 cm^2 on the dosing was studied with a step of 0.4 cm^2 at a fixed DS of 10 µm corresponding to a resolution of 2540 droplets per inch (dpi). Secondly, the flexibility of the dosing was investigated with increasing the printed dose by decreasing the DS of the printed ink from 50 µm (508 dpi) to 10 µm (2540 dpi) with a step size of 5 µm. The prepared samples were stored in a desiccator over silica granules (RH of 0–10%) at a temperature of 21 ± 1 °C.

The printing of the LH ink solution was conducted with a PixDro LP50 PIJ printer (Roth&Rau, The Netherlands) equipped with a Spectra® SL-128AA printhead (Fujifilm Dimatix Inc., USA) (IV). The formulations were printed with a resolution of 500 dpi on an area of 2 cm^2 in two layers. A single nozzle at a voltage of 110 V was exploited to obtain droplets with an approximate size of 45–55 pL. The samples were dried for 2 h at 25 ± 1 °C before adding the second printed layer. All the printed dosage forms containing LH were stored at ambient conditions (temperature of 25 ± 1 °C and RH of 20 ± 2%) for a short-term stability study of 4 and/or 8 months.

The theoretical dose of APIs in the inkjet-printed formulations was calculated based on the droplet volume (pL), printing resolution (dpi), printed area (cm^2), number of printed layers and ink concentration (mg/mL).

4.2.4.2. Flexographic printing (III)

The flexographically printed formulations were prepared by using a laboratory scale printability tester (IGT Global Standard Tester 2, IGT Testing system, The Netherlands). The ITR and IND inks were mixed for 15 min before the printing to ensure the homogeneity of the nanosuspensions. All the printed formulations consisted of 10 layers of the nanosuspension ink printed onto a sample area of 0.5 cm^2. The dose of the deposited drug was determined only experimentally.

4.2.5. Characterization of pharmaceutical inks (I, III)

The viscosity of the CAF and LOP inkbase solutions was measured with a Physica MCR 300 rheometer (Anton Paar, Germany) in triplicate (I). A CAM 200 contact angle goniometer (KSV Instruments Ltd., Finland) was used for measuring the surface tension of the inkbases by a pendant drop method in six parallel measurements and the contact angle of the CAF and LOP inks on the substrates by a sessile drop method in triplicate (I).

The ITR and IND inks (III) for the flexographic printing were characterized with regards to the mean particle size and polydispersity index (PI) of the nanosuspensions by dynamic light scattering (Malvern Zetasizer Nano ZS, Malvern Instrument, Malvern, UK) in triplicate.

4.2.6. Thickness of substrates (I, IV)

Absolute™ Digimatic (Mitutoya Corporation, Japan) and Ironside® (France) digital calibers were used for measuring the thickness of edible (I) and electrospun (IV) substrates, respectively. For the mechanical testing, the dimensions of the electrospun samples were determined with the Absolute™ Digmatic digital caliper (Mitutoyo Corporation, Japan).

4.6.7. Physical characterization of electrospun substrates (IV)

The non-crosslinked (nonCL) and crosslinked (CL) electrospun gelatin substrates were characterized in terms of moisture uptake and mechanical properties (IV). The moisture uptake after exposing the substrates to high humidity (RH of 70%) was analyzed by a weighing method (APX-200 balance, Denver Instrument, USA). The mechanical properties of the electrospun gelatin substrates before and after printing were studied by TA.XT*plus* Texture Analyzer (Stable Micro Systems Ltd., UK) equipped with a 10 kg load cell (sensitivity of 0.001 N). All the measurements were carried out at ambient conditions (temperature of 25 ± 1 °C and RH of 20 ± 2%).

In the puncture test, fixed samples with a circular sample area (Ø 10 mm) were punctured by a flat cylinder probe (Ø 5 mm) at a speed of 0.1 mm/s. The applied force (N) and displacement (mm) of the sample was used for the measurements of puncture strength (mN/mm^2) and elongation (%) at

break. A tensile test with a speed of 0.1 mm/s was conducted to determine the tensile strength (N/mm^2), elongation (%) at break and elastic modulus (kPa). Reference materials were copy paper (80 g/cm^2, Staples Europe B.V., Finland) and 3-ply tissue paper (Kleenex®, Kimberly-Clark Worldwide Inc., UK).

4.2.8. Scanning electron microscopy

The surface morphology of the substrates and the printed formulations was visualized with LEO Gemini 1530 (Zeiss®, Germany) (I, III) and EVO MA 15 (Zeiss®, Germany) (IV) scanning electron microscopes (SEM). In addition to surface visualization by SEM, an energy-dispersive X-ray spectroscopy (EDX) (Thermo Scientific, USA) extension was applied to detect the chemical elements of printed LOP (I). Furthermore, the diameter of the electrospun fibers was measured from the SEM images with ImageJ 1.49V software (National Institute of Health, USA) (IV).

4.2.9. Thermal analysis

The thermal properties of the printed CAF and LOP were studied by differential scanning calorimetry (DSC) (PYRIS Diamond, PerkinElmer Instruments, USA) (I). The printed CAF and LOP were detached from the PET substrate prior to the analysis, while the samples printed on HPC film and icing sheet remained attached to the substrates.

A DSC (Q2000, TA Instruments, USA) with a conventional heating method and in a modulated temperature mode (MT-DSC) was used for the thermal analysis of the fibrous gelatin substrates and the printed formulations with LH (IV). All the measurements were conducted with intact samples (the printed LH remained attached to the substrate).

In both studies a heating rate of 10 °C/min was applied in the conventional DSC mode, whereas in the MT-DSC measurements an average heating rate of 3 °C/min with modulation amplitude of ± 1 °C over a period of 60 s was used. The DSC systems were calibrated with indium (156.60 °C).

4.2.10. Solid state characterization

4.2.10.1. X-ray diffraction

The solid state characterization of the printed formulations was conducted by X-ray diffractometry (XRD) (Philips, X'Pert PRO MPD, The Netherlands) (I, II, III). The measurements were carried out in θ/2θ Bragg-Bretano geometry with Cu Kα radiation (l = 1.54 Å) at a voltage of 40 kV and a current of 50 mA in the measuring range of 3–40° 2θ with the rate of 0.04°/2 s. The solid state of the formulation compounds was evaluated based on the XRD diffractograms of the raw materials (I, III).

A XRD (D8 Advance, Bruker AXS GmbH, Germany) equipped with a LynxEye one-dimensional detector (Bruker, Germany) was used for the analysis of the formulations printed on fibrous gelatin substrates (IV). A diffraction range from 3 to 55° 2θ with a step size of 0.02° 2θ and a total measuring time of 166 s/step at 40 kV and 40 mA was applied for measuring

the properties of the fibrous formulations. The International Centre for Diffraction Data PDF-2 database (2013 edition, USA) was used for the verification of the raw materials of LH monohydrate, PRX anhydrous form II and D-(+)-glucose. Experimental results from the samples containing PRX were compared with the theoretical patterns of PRX anhydrous form I (BIYSEH), anhydrous form II (BIYSEH02) and monohydrate (CIDYAP01) from the Cambridge Structural Database (UK), and PRX anhydrous form III (Naelapää et al., 2012) (IV).

4.2.10.2. Attenuated total reflectance Fourier transform infrared spectroscopy (II, IV)

An attenuated total reflectance Fourier transform infrared (ATR-FTIR) spectroscope (PerkinElmer, UK) equipped with a DiComp™ crystal was used for the spectroscopic analysis. The measurements were conducted in a spectral range from 400 to 4000 cm^{-1} with 4 accumulations and a resolution of 4 cm^{-1}. A force of 150 N was applied during the analysis of the substrates and the printed formulations, whereas a force of 90–100 N was applied for the reference materials. Spectrum 10.03 software (PerkinElmer, UK) was used for the data collection and the pre-treatment of IR spectra with baseline correction and normalization.

4.2.11. Quantitative analysis

The method selection for the content analysis of the drug-loaded samples was dependent on the API. The details of the analyses are described below. All the measurements were conducted at least in triplicate.

4.2.11.1. Ultraviolet-visible spectrophotometry (I–III)

The printed formulations of CAF (I, II) were measured at 206 and 273 nm by ultraviolet-visible (UV-Vis) spectrophotometry (Lambda 25, PerkinElmer, USA) after 12 h of incubation in water.

The determination of IND (III) content in the nanosuspensions was performed by UV-Vis spectrophotometry (Ultrospec 2100 pro, Biochrom Ltd., UK) at 265 nm after 24 h of incubation in phosphate buffer (pH 5.0).

4.2.11.2. High performance liquid chromatography (I–IV)

The printed formulations of LOP (I, II) were measured by high performance liquid chromatography (HPLC) with a modified method previously presented by Weuts et al. (2004). The LOP formulations were incubated in water for 12 h prior to analysis. A HPLC (Hewlett Packard Series II 1090 LC instrument) with Inertsil® ODS 3 column (4.0 × 150 mm, 5 µm) and a Security Guard Cartridge Kit (C18) (4.0 × 2.0 mm, 5 µm) was exploited to carry out an isocratic method at 40 °C with a 70:30 (v/v) mixture of 1 mM tetrabutylammonium hydrogensulfate aqueous solution and acetonitrile (ACN) as mobile phase. The flow rate of the mobile phase was 1.0 mL/min and the injection volume of the samples was 10 µL. LOP was detected at a retention time of 10 min at a wavelength of 220 nm.

The formulations with flexographically printed ITR nanosuspensions (III) were analyzed by HPLC (Agilent 1100 Series, Agilent Technologies, USA) equipped with a UV diode array detector and a Gemini-NX-C18 column (100 × 4.6 mm, 3 μm) with a Security Guard Cartridge Kit (4.0 × 3.0 mm, 3 μm) (Phenomenex Inc., USA). An isocratic method at 25 °C was utilized with a 50:50 (v/v) mixture of 0.1% trifluoroacetic acid aqueous solution and ACN as mobile phase. The flow rate was 1.0 mL/min and the injection volume was 20 μL. The concentration of ITR was determined at a retention time of 3.2 min at a detection wavelength of 261 nm.

For the content analysis of the printed formulations with LH on unloaded or PRX loaded gelatin substrates (IV), a HPLC (Shimadzu Prominence LC20, Japan) equipped with a photodiode array detector and a Phenomenex Luna® C18(2) column (250 × 4.6 mm) with base-deactivated end-capped octadecylsilyl gel for chromatography R (5 μm) as stationary phase was used. A HPLC method at 40 °C from the European Pharmacopoeia piroxicam monograph for the test for related substances was applied with minor modifications (European Pharmacopoeia, 2016e). The mobile phase was a 30:70 (v/v) mixture of ACN R1 and 6.81 g/L solution of potassium dihydrogen phosphate R previously adjusted to pH 3.0 with phosphoric acid R. The flow rate was 1.0 mL/min and the injection volume was 10 μl. The APIs were detected spectrophotometrically at a wavelength of 230 nm with an approximate retention time of 3.9 min and 22.0 min for LH and PRX, respectively. The LH formulations were analyzed after 6 h-incubation in water. The PRX content in the drug-loaded electrospun fibers was measured in 10 M acetic acid solution. The formulations with LH printed on CL PRX-loaded substrates (G20-PRX) were measured after *in vitro* enzymatic degradation by collagenase (235.00 units/mg, Glibco® Collagenase Type I isolated from Clostridium histolyicum, Life Technologies Corporation, USA) (Park et al., 2002).

4.2.11.3. Spectral quantification (II)

The IR spectra of the CAF and LOP formulations printed on PET reference substrate were subject to quantitative analysis. The original spectra were collected and pretreated with baseline correction, normalization and data tune-up processing in Spectrum 10.03 software (PerkinElmer, UK). Univariate and multivariate data analysis was conducted by preparing calibration models from two-thirds of the data and using one-third of the data to test the models.

The univariate data analysis was conducted by plotting the height and area of API-specific absorbance bands against the resolution (expressed as DS) or the measured drug content. The models were evaluated based on their correlation coefficient (R^2) and the root mean square error of prediction (RMSEP).

The multivariate data analysis was conducted with SIMCA-P+ 12.0.0.0

software (Umetrics AB, Sweden). Partial Least Squares (PLS) regression models (Wold et al., 2001) for quantification were prepared from the pretreated spectroscopic data. The API content was used in logarithmic scale for linear PLS regression models and recalculated for further analysis. Unit variance (UV) and mean centering (Ctr) scaling algorithms and Standard Normal Variate (SNV) pre-processing were applied to improve the quality of the data. Furthermore, the impact of the selected spectral regions, 400–4000 cm^{-1} and 400–1750 cm^{-1}, on the model performance was tested. The number of PLS latent variables (LVs) was set according to the cross-validation for auto-fitting (Eriksson et al., 2001) and verified by visual inspection. The quality of the PLS regression models was evaluated based on the correlation coefficients (R^2X, R^2Y), test set validation coefficient (Q^2), root mean square error of estimation (RMSEE) and RMSEP.

4.2.12. *In vitro* drug release studies (III, IV)

The drug release from the flexographically printed nanosuspensions of IND and ITR was studied by a modified dissolution testing method (III). A water bath was used to hold the temperature of the dissolution media at 37 ± 0.5 °C. The printed samples in spiral capsule sinkers were immersed in 50 mL of dissolution media and a continuous mixing at 100 rpm was ensured by a magnetic stirrer. The samples were taken manually and analyzed by HPLC. Prior to the analysis, the samples were filtered through 0.2 µm polytetrafluoroethylene (PTFE) membrane syringe filters. The drug release from the printed IND formulations was determined in phosphate buffer (pH 5.0), whereas the dissolution rate of ITR formulations was studied in 0.1 M hydrochloric acid solution (pH 1.2).

A simulated saliva solution (pH 6.8) (Marques et al., 2011) was used to determine the drug release of PRX from nonCL and CL gelatin fibers and the dosage forms with printed LH on unloaded (G25) and PRX-loaded (G20-PRX) substrates (IV). The dissolution studies were conducted in Falcon tubes containing 10 mL of dissolution media. The Falcon tubes were inserted into water-filled paddle apparatus vessels for obtaining appropriate dissolution conditions (temperature of 37 ± 0.5 °C and a mixing speed of 50 rpm). Separate samples were prepared for each time point and measured after manual sampling and filtering (0.45 µm PTFE membrane syringe filters) by HPLC. The dissolution studies were conducted under sink conditions in duplicate.

5. Results and discussion

5.1. Preparation and characterization of pharmaceutical inks and substrates for inkjet and flexographic printing (I, III, IV)

5.1.1. Preparation and characterization of ink solutions (I, IV)

The viscosity and surface tension are the most important physicochemical properties that affect the printability of an ink solution. The droplet formation and volume at a specific jetting voltage are directly influenced by these parameters (Jang et al., 2009). The ink performance quality outside the recommended viscosity and surface tension values is limited, and can lead to nozzle clogging, formation of satellite droplets and/or incomplete droplet ejection (Calvert, 2001; Jang et al., 2009).

In the preparation of drug-loaded inks, the solubility of the API in the solvent system (inkbase) and the evaporation rate of the solvent(s) must be considered. According to the solubility properties of APIs, an ethanol-based ink formulation was prepared with slightly water-soluble LOP and aqueous ink systems were obtained for CAF (sparingly soluble in water) and LH (very soluble in water) (European Pharmacopoeia, 2016b, 2016c, 2016d).

The use of water or less toxic solvents, such as ethanol, acetone or dimethyl sulfoxide, is encouraged in pharmaceutical manufacturing (European Medicines Agency, 2016). However, these solvents are usually not appropriate for inkjet printing alone; thus, the addition of humectants, viscosity and/or surface tension modifying agents is needed to ensure the printability of the ink formulations. Here, PG with a high boiling point (188 °C) was added to drug-loaded ink formulations to hinder the nozzle clogging and the crystallization of the solute by decreasing the evaporation rate of the inkbase. Despite of its benefits in the formulation, the administration of PG in high doses (above 25 mg/kg/day) and/or long-term should be monitored to avoid toxic effects especially in pediatrics and patients with renal or hepatic insufficiency (Lim et al., 2014). The PG content in all the printed formulations was well below the suggested limits.

The printability of CAF and LOP inks was estimated based on the measured viscosity and surface tension (**Table 4**) (I). The calculated Z-value supported these findings. A stable jetting of both inks was obtained without any evident clogging. However, the differences in the surface tension influenced the droplet ejection resulting in the formation of satellite droplets or elongated droplet tails with CAF and LOP inks, respectively.

The LH ink was prepared in a mixture of PG and water in 40:60 (v/v) ratio based on the preliminary analysis of the inkbase solutions (IV). The concentration of PG correlated linearly with the physicochemical properties of the inkbase solutions and the Z-value. A stable droplet formation was

maintained throughout the printing process of the LH ink. It was noted that the range of printable inks depends on the printhead configuration (nozzle diameter), and the droplet formation process could be adjusted by the settings of the printing process.

***Table 4**. Physicochemical properties and calculated Z-value for the ink formulations with caffeine (CAF) and loperamide hydrochloride (LOP).*

	Viscosity[a] (mPa·s)	Surface tension[b] (mN/m)	Average Z-value (nozzle Ø 21.5 µm)
CAF ink	2.6 ± 0.1	50.7 ± 1.0	12.8
LOP ink	3.6 ± 0.2	25.7 ± 0.7	6.9

[a]mean ± standard deviation, n = 3; [b]mean ± standard deviation, n = 6.

5.1.2. Preparation and characterization of nanosuspensions (III)

The preparation of nanosuspensions is a common method to enhance the dissolution rate and absorption of solubility-limited APIs. The nanosuspensions with particles in sub-micron size range were prepared with BCS Class II model compounds, IND and ITR (Amidon et al., 1995).

In the wet ball-milling process, the particle size of the solids was decreased by mechanical grinding with milling pearls in an aqueous environment in the presence of a stabilizing polymer. Maintaining the particle size of nanosuspensions in long-term is the main challenge, because of the higher surface energy of the nanoparticles that promotes their aggregation into thermodynamically stable state (Merisko-Liversidge and Liversidge, 2008). Typically freeze- or spray-drying of nanosuspensions has been exploited to stabilize these systems (Lee, 2003; Van Eerdenbrugh et al., 2008a; Chung et al., 2012; Figueroa and Bose, 2013). Moreover, the preparation of solid redispersible nanoparticulate systems by inkjet micro-dose dispensing (Pardeike et al., 2011) and flexographic printing (Janßen et al., 2013) has been shown to be a fitting alternative. The even spatial distribution of particles by printing could enhance the redispersion of the particles in the dissolution medium.

The ITR and IND inks were prepared with typical particle size and distribution for ball-milled nanocrystalline suspensions (**Table 5**). The differences in the average particle size were attributed to the stabilizing efficiency of non-ionic Poloxamer 407, since the drug-polymer interactions are affected by the hydrophobicity and ionization degree of the API molecules (Liu et al., 2011).

***Table 5**. Mean particle size and polydispersity index (PI) of itraconazole (ITR) and indomethacin (IND) nanosuspension inks.*

	Particle size[a] (nm)	PI[a]
ITR ink	698.1 ± 14.0	0.37 ± 0.03
IND ink	422.6 ± 7.7	0.31 ± 0.01

[a]mean ± standard deviation, n = 3.

5.1.3. Characterization of electrospun substrates (IV)

5.1.3.1. Fiber diameter

The G25 and G20 gelatin fibers with different fiber diameters were produced by electrospinning (**Table 6**). The higher viscosity of the G20 electrospinning solutions contributed to the increased diameter of the fibers. The G25 and G20 fibrous substrates were prepared with a thickness of 0.05 ± 0.02 and 0.06 ± 0.02 mm, respectively.

The thermal post-treatment did not affect the average diameter of G25 fibers, whereas the diameter of G20 decreased by 8.6%. This phenomenon was attributed to the higher solvent residue in the G20 fibers that evaporated during crosslinking at elevated temperature (Bhardwaj and Kundu, 2010).

5.1.3.2. Mechanical properties

Various crosslinking methods have been reported to improve the mechanical strength of electrospun gelatin fibers and films (Zhang et al., 2006; Nguyen and Lee, 2010; Zha et al., 2012; Siimon et al., 2015). The physical properties of the electrospun gelatin substrates showed up to 5-fold enhancement after thermal crosslinking and the calculated elastic modulus demonstrated that the flexibility of the substrates was significantly increased after the heat treatment (**Table 6**). The higher mechanical strength of the CL G25 gelatin substrate formulation led to its use in the preparation of the inkjet-printed dosage forms.

***Table 6**. Average fiber diameter and physical properties of non-crosslinked (nonCL) and crosslinked (CL) G25 and G20 gelatin substrates, and reference materials.*

	Fiber diameter[a] (nm)	Puncture test[b]		Tensile test[b]		
		Burst strength (mN/mm²)	Elongation at break (%)	Tensile strength (N/mm²)	Elongation at break (%)	Elastic modulus (kPa)
G25 substrate						
nonCL G25	589.3 ± 70.1	32.3 ± 3.6	1.1 ± 0.1	4.4 ± 0.4	1.2 ± 0.4	48.6 ± 7.7
CL G25	607.8 ± 79.2	203.7 ± 6.4	6.6 ± 0.8	6.1 ± 0.7	8.1 ± 2.3	9.8 ± 0.7
G20 substrate						
nonCL G20	1292.9 ± 231.2	79.0 ± 16.2	1.4 ± 0.2	2.3 ± 0.7	1.1 ± 0.4	24.7 ± 3.1
CL 20	1186.3 ± 225.7	95.8 ± 22.2	2.3 ± 0.5	2.8 ± 0.6	2.7 ± 0.3	6.5 ± 1.1
Reference materials						
Copy paper	-	1685.8 ± 75.0	6.3 ± 0.4	50.0 ± 5.4	5.6 ± 0.8	86.5 ± 6.6
3-ply tissue	-	137.5 ± 11.2	23.4 ± 6.9	2.5 ± 0.1	1.2 ± 0.1	1.1 ± 0.1

[a]mean ± standard deviation, n = 100. [b]mean ± standard deviation, n = 3–5.

5.1.3.3. Solid state properties

The effect of the electrospinning and subsequent crosslinking on the solid state properties of gelatin was evaluated by thermal and IR spectral analysis. The physical properties of the substrates were influenced by the changes in the gelatin structure that occurred during the preparation process.

The characteristic endotherm that was attributed to the water evaporation with an overlapping denaturation of gelatin (107 °C) decreased approximately 30 °C after electrospinning (**Figure 8A**). However, the stability of gelatin fibers was not affected by thermal crosslinking. Contradictory results have been obtained by the post-treatment with glutaraldehyde, showing an increased thermal stability of fibers (Zhang et al., 2006; Nguyen and Lee, 2010). After crosslinking the melting endotherm (at 149–160 °C) of glucose disappeared (**Figure 8A**), suggesting that the thermal properties of gelatin fibers were stabilized by a reaction between glucose and gelatin at high temperature.

The electrospinning and crosslinking processes affected the intramolecular vibrations of the fiber components. The absorbance bands of gelatin amide groups at 1234, 1524 and 1634 cm^{-1} were shifted to higher wavenumbers after electrospinning. This indicated a formation of a less-ordered amorphous structure because of the acidic gelatin solution (Mindru et al., 2007; Elliot et al., 2009; Siimon et al., 2014; Etxabide et al., 2015). The presence of an ordered helical structure was also hindered in the G20 fibers. That has been reported to be caused by elevated temperatures and by using solvent mixtures containing acetic acid and dimethylformamide (DMF) (Kozlov and Burdygina, 1983). The spectral analysis did not reveal any additional changes to the secondary structure of gelatin after thermal crosslinking.

The glycation process is known to be promoted by high temperature and the increased amount of the crosslinking agent (Siimon et al., 2014, 2015; Etxabide et al., 2015). Permanent changes to the fibrous structure of gelatin substrates were detected by the changes to the CO vibrations at 1029 and 1080 cm^{-1} (**Figure 8B**). These changes were attributed to the non-enzymatic Maillard reaction between the carbonyl group of glucose and amino group of gelatin (Siimon et al., 2014, 2015; Etxabide et al., 2015).

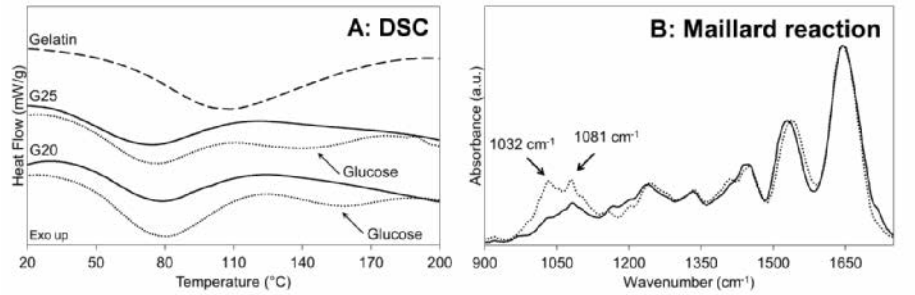

***Figure 8**. **A**: Conventional DSC thermograms of untreated gelatin (---), noncrosslinked (nonCL) (···) and crosslinked (CL) (—) G25 and G20 gelatin substrates. **B**: Pretreated ATR-FTIR spectra of nonCL (···) and CL (—) G25 gelatin substrates in the spectral range from 900 to 1750 cm^{-1}.*

5.1.4. Ink-substrate interactions in printed dosage forms (I, IV)

The wettability and absorption properties of the substrates allow estimating the drug-loading capacity and the drying conditions for obtaining solid dosage forms by printing. The drying process of the printed dosage forms has similarities with the production of solvent-cast films (Boateng et al., 2009). In the optimization of the drying process, it is crucial to avoid the sedimentation of the solid particles and the solidification of the film surface to ensure the physical stability of the solvent-cast films (Siemann, 2005). Hence, the dried equilibrium state of the printed dosage forms is dependent on the drying environment and the properties of the substrate and ink components, such as the absorption capacity, the droplet volume and the solvent evaporation rate (Sandler et al., 2011; Genina et al., 2013; Wickström et al., 2015). Due to the porous structure of copy paper, printing up to 9 layers of water-based inks was shown to be feasible without any intermediate drying steps, whereas the ink solidification on the substrates with lower absorbability required a drying time of 1 h at ambient conditions (Genina et al., 2013). However, for the removal of residual organic solvents drying at elevated temperature with or without a vacuum oven should be considered (Wickström et al., 2015).

In the first study (I), the physical interactions between the ink solutions and the different substrates were investigated by contact angle measurements during the liquid absorption process. The extensive spreading of the CAF ink on the carriers was prevented by the higher surface tension of the solution compared to the LOP ink (**Figure 9**). The formation of cavities was visually observed on the thin (0.10 ± 0.01 mm, n = 10) HPC films leading to the interaction with the impermeable sub-liner for both ink solutions. The decreased size of the ink droplets on the PET and HPC films was mainly attributed to the solvent evaporation. On the icing sheet, the ink absorption was noticeably faster without any evident cavities due to the higher thickness (0.45 ± 0.06 mm, n = 10) of the substrate compared to the HPC film.

The physical stability of electrospun fibrous substrates was evaluated at high humidity (RH of 70%) conditions (IV). The moisture uptake was shown to be affected by the diameter and the packing density of the fibers, giving noticeable differences between nano-fibrous G25 and micro-fibrous G20 substrates (**Figure 10**). The moisture uptake analysis allowed predicting their behavior during storage and printing. At high humidity, the nonCL fiber substrates turned into unfavorably hard and brittle film-like structures. However, the CL fiber mats maintained their initial appearance with a slight contraction of the edges of the micro-fibrous G20 scaffolds.

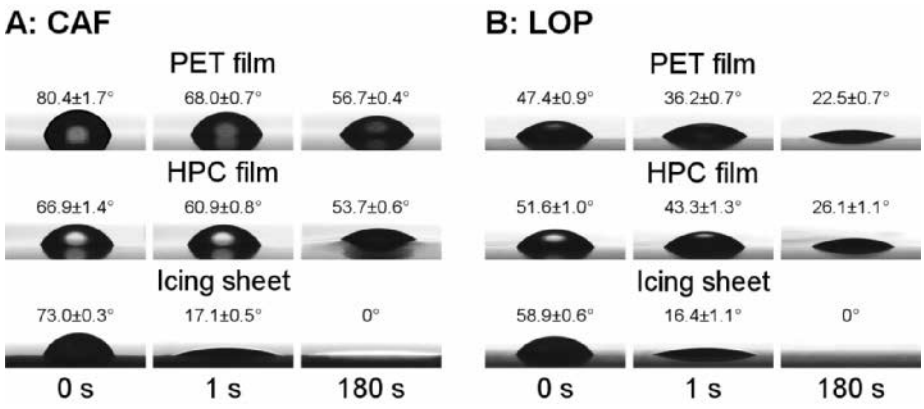

***Figure 9**. Wettability of caffeine (CAF) (**A**) and loperamide hydrochloride (LOP) (**B**) inks on polyethylene terephthalate (PET) film, hydroxypropyl cellulose (HPC) film and icing sheet with values for contact angle (°) as mean ± standard deviation, n = 3.*

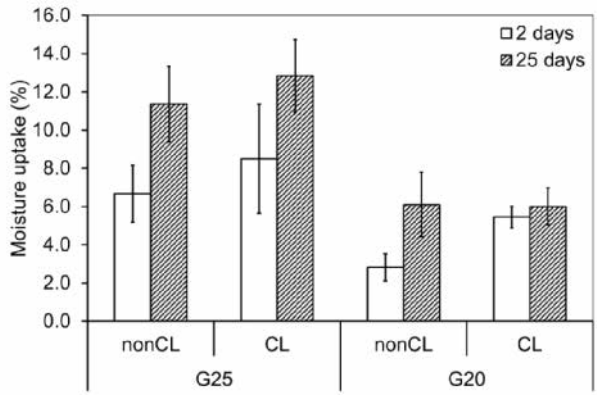

***Figure 10**. Moisture uptake (%) of non-crosslinked (nonCL) and crosslinked (CL) G25 and G20 gelatin substrates after 2 or 25 days presented as mean with standard deviation bars, n = 3.*

5.2. Preparation and characterization of printed dosage forms

The printed dosage forms were prepared according to process scheme presented in **Table 7**. In the inkjet-printed systems, the fixed spatial resolution defined the deposition of the picoliter-size droplets. The printed area on the substrates was visible with clear borders on all substrates except for the icing sheet, where a single layer of a colorless ink solution could not be detected due to the extensive absorption of the ink into the substrate.

In the flexographically printed formulations, the nanosuspension inks were deposited in 10 consecutive layers on the substrates. The printed formulations were obtained with distinct micro-scale pattern from the

anilox roll structure. In addition, the manual adjustment of the printing rolls during the process caused the occurrence of smeared edges from the slight displacement of the printed layers.

***Table 7**. Experimental setup and design of the printed drug formulations.*

	I, II studies			III study			IV study
Substrate	HPC film	Icing sheet[a]	PET	Rice paper[a]	Rice sheet[a]	TF	Electrospun gelatin fibers
API	Caffeine		Loperamide HCl	Itraconazole		Indomethacin	Lidocaine HCl
Printing method	PIJ			Flexography			PIJ
	1 printed layer			10 printed layers			2 printed layers
Printed formulation	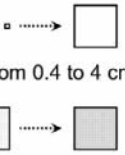 Size from 0.4 to 4 cm^2 Drop spacing from 50 to 10 µm			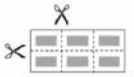 Printed area 0.5 cm^2			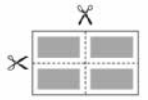 Printed area 2 cm^2

[a]commercial edible substrates; HPC – hydroxypropyl cellulose, PET – polyethylene terephthalate film, TF – transparency film, PIJ – piezoelectric inkjet printing

5.2.1. Morphology of printed dosage forms (I, III, IV)

The surface of the printed formulations with CAF and LOP was visualized by SEM (**Figure 11**) (I). The CAF ink crystallized on all the substrates with a dose-dependent amount and size of the needle-shaped crystals. The uniform distribution of the crystalline CAF was seen in low-dose formulations on PET film, whereas in the high-dose formulations inhomogeneous coverage was caused by the merging of the ink droplets prior to crystallization. On the surface of the HPC film, the crystallization of the CAF ink was less pronounced due to the partial penetration of the ink into the substrate. The amount of the crystallized CAF on the surface of the icing sheet was lower compared to PET and HPC substrates. Overall, the results correlated with the contact angle measurements indicating that the ink behavior on the surface was dependent on the absorptivity of the substrates.

The LOP ink solidified on the impermeable PET film in single (at low resolution) or merged (at high resolution) droplets. On the smooth HPC film, the water-based LOP ink merged into the substrate with small visible droplets on the surface of the high-dose formulations. The LOP ink was not detectable on the icing sheet, because of the extensive absorption of the ink into the substrate matrix. Nevertheless, the SEM-EDX could detect the chloride element of LOP salt at low levels on the surface of the icing sheet in the high-dose formulations.

The ITR and IND nanosuspensions were distributed uniformly on the substrates by flexographic printing without any evident agglomeration (**Figure 12**) (III). However, the close contact between the patterned printing

rolls and the substrates attributed to the uneven topography of the printed formulations. The partial penetration of the ink into the matrix of the rice sheet was contributed to the higher porosity of the edible substrate.

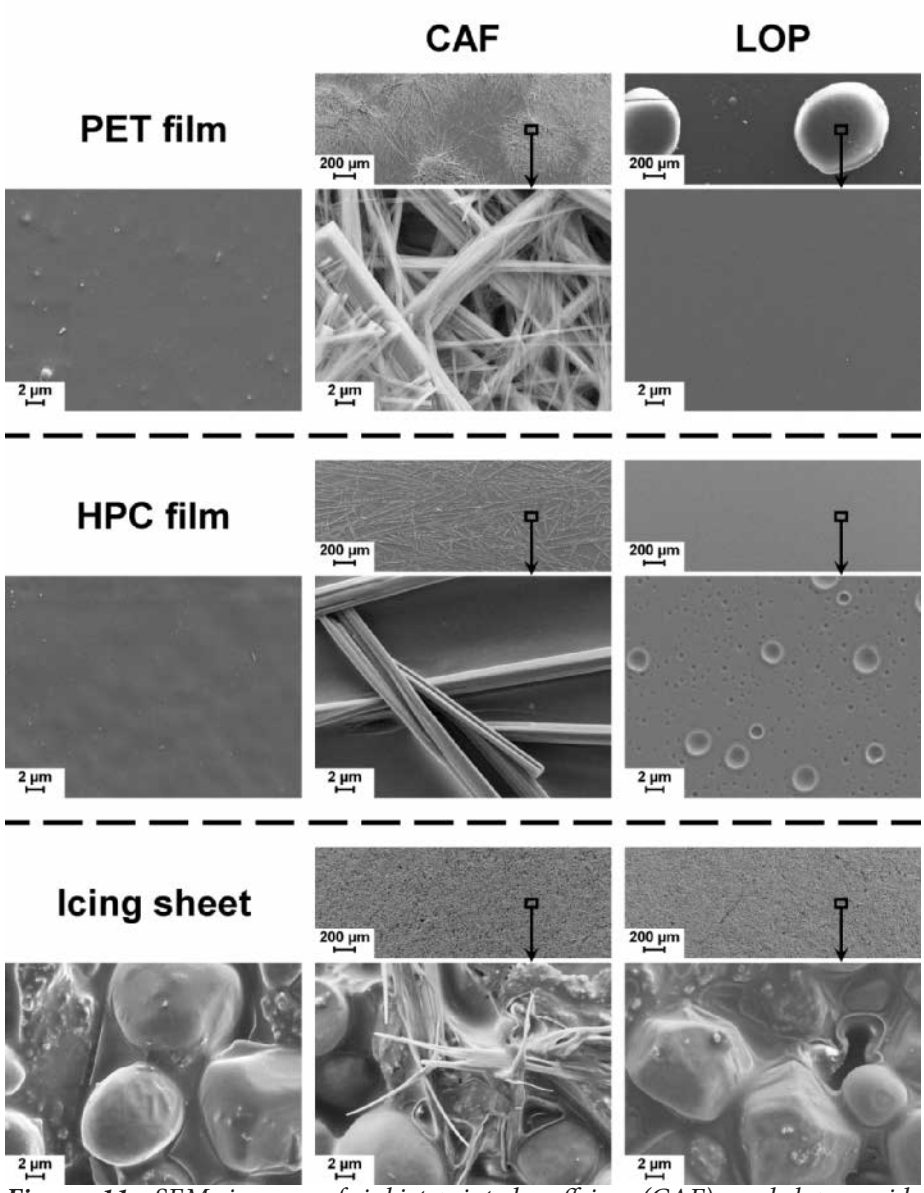

***Figure 11**. SEM images of inkjet-printed caffeine (CAF) and loperamide hydrochloride (LOP) on polyethylene terephthalate (PET) film, hydroxypropyl cellulose (HPC) film and icing sheet at drop spacing of 10 µm; 30× (scale bar of 200 µm) and 2500× (scale bar of 2 µm) magnifications.*

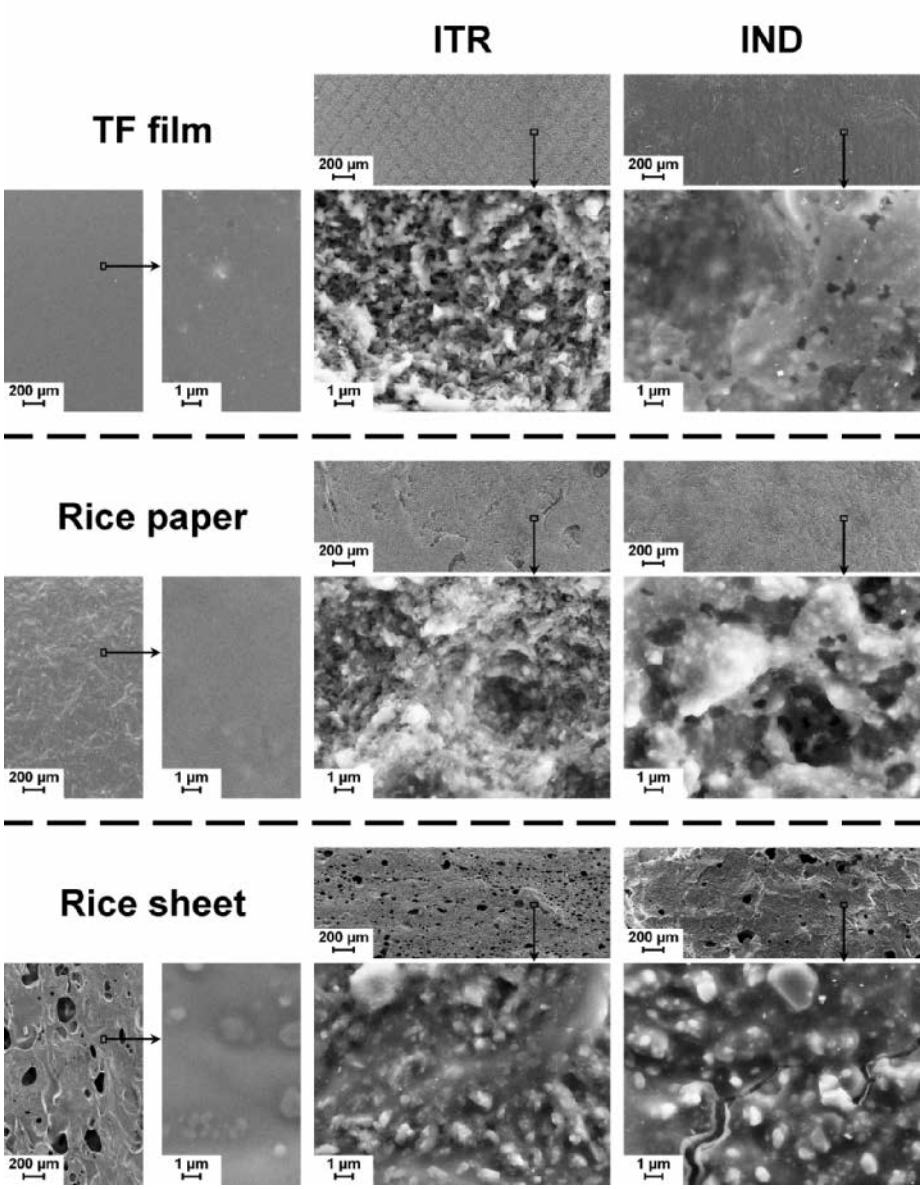

***Figure 12**. SEM images of flexographically printed itraconazole (ITR) and indomethacin (IND) on transparency film (TF), rice paper and rice sheet; 30× (scale bar of 200 µm) and 5000× (scale bar of 1 µm) magnifications.*

The electrospun gelatin substrates consisted of individually detectable fibers even after crosslinking (**Figure 13A**) (IV). The surface of the printed dosage forms was smoother compared to the unprinted substrates due to the swelling and adhesion of the gelatin fibers (**Figure 13B**). Furthermore, the mechanical testing indicated that the deposition of the ink solution had no significant effect on the puncture strength of the dosage forms with LH printed on CL gelatin substrates compared to unprinted fiber mats. The elasticity (expressed as the elongation at break) of the final preparations was enhanced by approximately 2-fold. Recently, Preis et al. (2014) studied the mechanical strength of several orodispersible and buccal film formulations that are commercially available. The mechanical properties of the printed dosage forms on the CL fiber matrices in the current study (IV) were comparable with the marketed film products analyzed by Preis et al. (2014), indicating that these printed dosage forms could be suitable for oromucosal drug delivery.

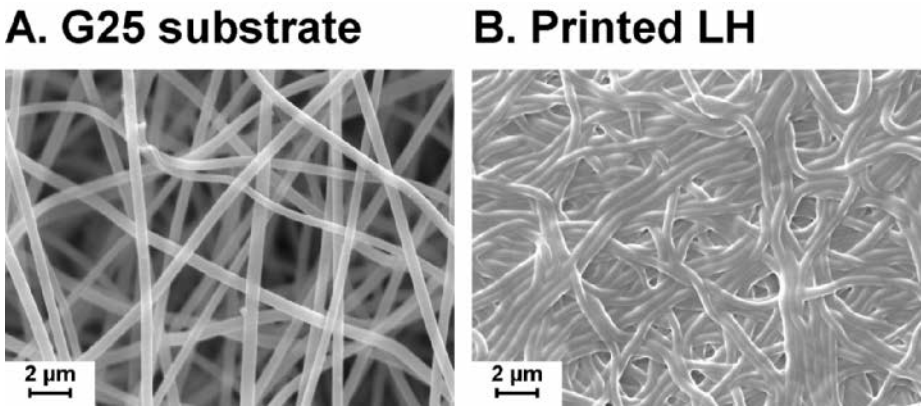

Figure 13*. SEM images of the crosslinked (CL) G25 gelatin substrate (**A**) and lidocaine hydrochloride printed on CL G25 substrate (**B**); 10000× (scale bar of 2 µm) magnification.*

5.2.2. Solid state characterization of printed pharmaceuticals

5.2.2.1. Caffeine (I, II)

The raw material used for the ink preparation was confirmed as CAF anhydrous form II based on the comparison with the previously reported data (Jørgensen et al., 2002; Wyttenbach et al., 2007). At least a partial crystallization of CAF into its stable anhydrous form II was detected in the printed formulations by XRD with a characteristic 2θ angle at approximately 12° (**Figure 14A**).

The thermal analysis of the raw material and the CAF that was detached from the PET film demonstrated a polymorphic transformation of an anhydrous form II into form I at 142 °C (onset) with a melting endotherm

at 236 °C (**Figure 14B**). In addition, a low intensity endotherm at 30–140 °C suggested the moisture elimination from the crystalline material or a dehydration process of a non-stoichiometric CAF hydrate (Wyttenbach et al., 2007). CAF was not detectable on edible substrates by DSC.

CAF anhydrous form II exhibits several characteristic absorbance bands in the "fingerprint" region of the IR spectra from 400 to 1700 cm^{-1} (Kesimli et al., 2003; Nolasco et al., 2006; Srivastava and Singh, 2013). The spectral characteristics of CAF anhydrous form II were detected on the ATR-FTIR spectra of the printed formulations. The absorbance bands at 444, 481, 610, 1025, 1358 and 1403 cm^{-1} showed high specificity towards the quantitative content of crystalline CAF without any overlapping from the residual PG and the PET film.

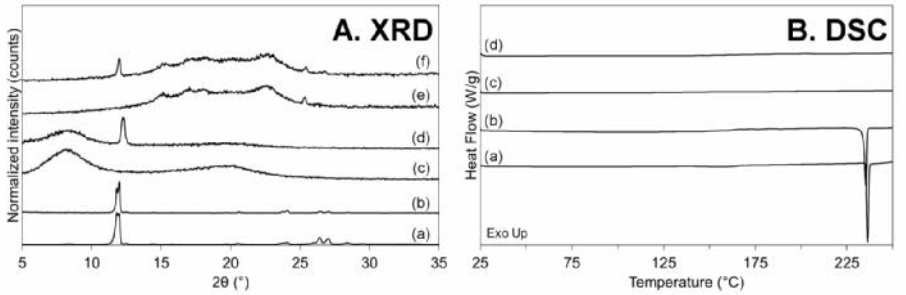

***Figure 14**. **A**: X-ray diffractograms of caffeine (CAF) anhydrous form II (a), printed CAF detached from polyethylene terephthalate (PET) film (b), hydroxypropyl cellulose (HPC) film (c), CAF printed on HPC film (d), icing sheet (e) and CAF printed on icing sheet (f). Diffractograms are offset in intensity for clarity. **B**: DSC thermograms of CAF anhydrous form II (a), printed CAF detached from PET film (b), CAF printed on HPC film (c) and CAF printed on icing sheet (d). Thermograms are offset in y-axis for clarity. The CAF formulations were printed at a drop spacing of 10 μm.*

5.2.2.2. Loperamide hydrochloride (I, II)

The data from the XRD and DSC analysis of LOP was compared to the previously reported solid state forms of LOP (Van Rompay and Carter, 1990). The results showed that LOP anhydrous form I was used for the preparation of the printed dosage forms (**Figure 15A**).

The X-ray diffractograms of the printed dosage forms reflected mainly the crystalline components of the substrate materials without any observed crystalline reflections for the printed LOP on all three substrates. The printed LOP that was detached from the PET film exhibited a low degree of crystallinity without any evident proof about its polymorphic form (**Figure 15A**).

The thermal analysis of the LOP that was removed from the PET film exhibited an exothermal event at 106 °C (onset) with a subsequent melting of

an anhydrous form II at 218 °C (**Figure 15B**). The low drug amount in the intact printed formulations hindered the thermal analysis of the printed LOP on edible substrates.

In addition, the IR spectra of the printed LOP formulations was matched with the previously reported data on the solid state forms of LOP (Weuts et al., 2004; Bagmar Ujwala et al., 2013; Bruni et al., 2013). The printed drug showed some characteristic features for LOP anhydrous form I on the ATR-FTIR spectra in the spectral range from 500 to 1650 cm^{-1}. The absorbance bands at 541, 641, 1385, 1449 and 1625 cm^{-1} were characteristic for crystalline LOP. However, the presence of an amorphous LOP was suggested by the small changes in the intensity and shape of the absorbance bands. The absorbance bands for –OH vibrations of LOP at 3560 and 3390 cm^{-1} have been reported to be absent in the IR spectrum of LOP in an amorphous state (Weuts et al., 2004). The presence of an amorphous LOP could not be verified by the spectral analysis of the printed formulations due to a clear overlapping with the PG spectrum in the spectral range from 2800 to 3500 cm^{-1}.

The results from the solid state analysis indicated that the solidified LOP in the printed formulations was in a molecularly dispersed or amorphous state. This was obviously due to the high content of the non-volatile PG in the printed formulations that is known to hinder the crystallization of active compounds (Cilurzo et al., 2005).

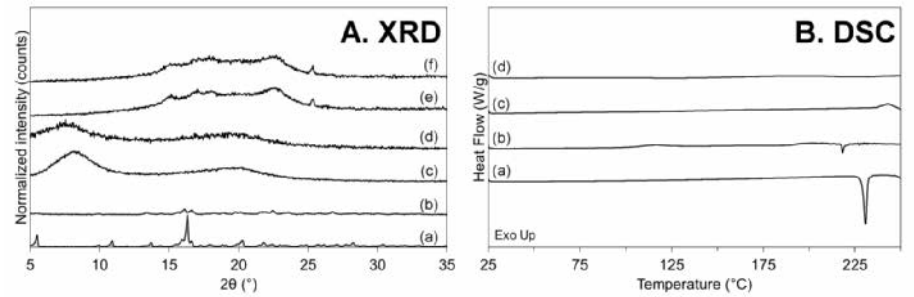

***Figure 15**. **A**: X-ray diffractograms of loperamide hydrochloride (LOP) anhydrous form I (a), printed LOP detached from polyethylene terephthalate (PET) film (b), hydroxypropyl cellulose (HPC) film (c), LOP printed on HPC film (d), icing sheet (e) and LOP printed on icing sheet (f). Diffractograms are offset in intensity for clarity. **B**: DSC thermograms of LOP anhydrous form I (a), printed LOP detached from PET film (b), LOP printed on HPC film (c) and LOP printed on icing sheet (d). Thermograms are offset in y-axis for clarity. The LOP formulations were printed at a drop spacing of 10 µm.*

5.2.2.3. Itraconazole (III)

The solid state analysis of the nanosuspensions is crucial, since active compounds in an amorphous state could also be obtained by milling due to the mechanical disruption of the crystalline structure and/or by the strong

interactions between the drug and the stabilizing agents (Müller and Peters, 2001; Kayaert and Van den Mooter, 2012).

Due to the low weight fraction of the active compound in the final formulations and the nano-size range of the printed particles, the solid state analysis of the printed formulations was limited (Phadnis et al., 1997; Jenkins and Snyder, 1996). Nevertheless, the printed ITR on the surface of the TF film was detectable by XRD at low levels of intensity (**Figure 16A**). The obtained X-ray diffractograms were compared with the ITR-specific X-ray reflections reported earlier by Van Eerdenbrugh et al. (2008b). On the diffractograms, the reflections at 14.5°, 17.6° and 20.4° 2θ angles indicated the presence of ITR in a stable crystalline form (**Figure 16A**). The results were in compliance with a previous study by Liu et al. (2011), where it was presented that the crystalline state of the API in aqueous nanosuspensions was not altered by the milling process and the subsequent solidification by freeze-drying.

5.2.2.4. Indomethacin (III)

The results from the XRD analysis of the printed formulations indicated that IND was at least partially present in a crystalline state on the TF film. Similarly to the ITR formulations, the reflections from the substrate material contributed most to the X-ray diffractograms (**Figure 16B**). The polymorphic α, β and γ forms have been previously differentiated by XRD with some possible overlapping of the diffraction peaks in polymorphic mixtures (Kaneniwa et al., 1985). A single reflection at 11.7° was attributed to the stable γ form of IND in the printed formulations. The presence of IND in an amorphous state was unlikely due to the production of an aqueous nanosuspension (Ali et al., 2011; Liu et al., 2011).

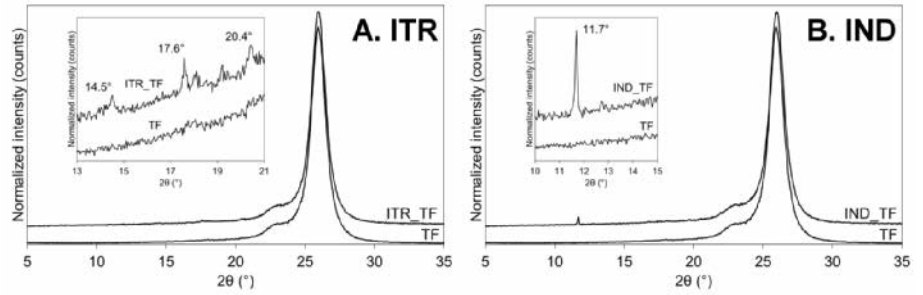

Figure 16*. X-ray diffractograms of itraconazole (ITR) (**A**) and indomethacin (IND) (**B**) printed on the transparency film (TF). Diffractograms are offset in intensity for clarity.*

5.2.2.5. Lidocaine hydrochloride (IV)

The LH monohydrate was used as the raw material in the ink formulations. The LH monohydrate exhibited a melting endotherm at 79 °C (data not shown). On the DSC thermograms of the printed dosage forms, the

characteristic endotherm of LH monohydrate was superposed by the thermal events of water evaporation and the denaturation of gelatin fibers. LH anhydrous form has a melting point at approximately 130 °C (Koehler and Hefferren, 1964). This was not observed on any of the obtained DSC thermograms. However, further MT-DSC analysis allowed detecting the increase of heat capacity (Cp) in the printed dosage forms with LH compared to the unprinted substrates (**Figure 17A**). No crystallinity of the drug was detected in the dosage forms by XRD (**Figure 17B**).

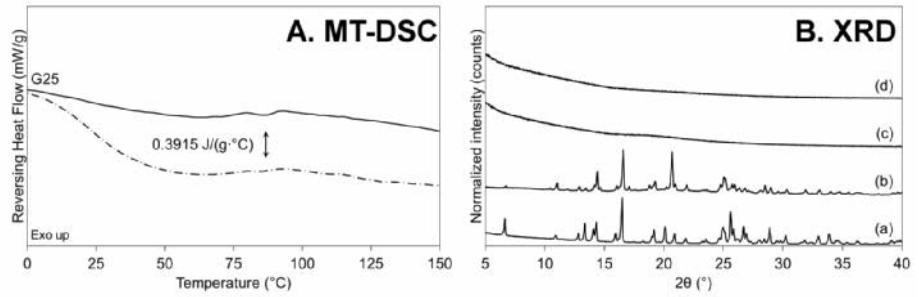

***Figure 17**. **A**: Modulated DSC (MT-DSC) thermograms (reversing heat flow signal) of crosslinked (CL) G25 gelatin substrate (—) and lidocaine hydrochloride (LH) printed on CL G25 substrate (–·–). **B**: X-ray diffractograms of LH monohydrate (a), physical mixture corresponding to the dosage form with LH printed on CL G25 substrate (b), CL G25 substrate (c) and LH printed on CL G25 substrate (d). Diffractograms are offset in intensity for clarity.*

The ATR-FTIR spectral analysis indicated the formation of a solidified ink layer on the electrospun substrates. Small spectral changes (e.g., peak broadening, shifting, merging and/or change of intensity) to the absorbance bands of LH monohydrate at 1477, 984, 952, 773, 716 and 691 cm^{-1} were detected in the printed dosage forms. In addition, LH monohydrate exhibits characteristic NH stretching vibrations at 2200–3000 cm^{-1} (Neville and Regnier, 1969). However, these absorbance bands were not detectable on the spectra of the printed dosage forms, suggesting that LH monohydrate was not crystallized after printing.

Thus, based on the solid state analysis, LH was present most likely in a molecularly dispersed state after inkjet printing. The non-crystalline state of the drug was stabilized by the homogeneous distribution of the printing. Furthermore, the solubilizing effect of PG contributed to the inhibition of the crystallization of the printed API (Cilurzo et al., 2005).

5.3. Dosing accuracy and flexibility of printing

5.3.1. Content analysis of printed dosage forms

The theoretical dose of LOP (ink concentration of 50 mg/ml) in the printed dosage forms ranged from 0.08 to 2.0 mg (I, II). The obtained drug

content was therapeutically relevant for pediatric administration with the single dose of 0.1 mg/kg and for adults with a single dose of 2–4 mg. The CAF (ink concentration of 20 mg/ml) was printed in the range from 0.03 to 0.8 mg (I, II). The content analysis of the printed formulations revealed that the actual amount of the deposited drugs was slightly higher compared to the theoretical dose. Dong et al. (2006) reported that the droplet size of the inks was increased due to the differences in the physicochemical properties of the inks. Thus, the droplet size and dose validation is needed for each ink formulation separately.

The drug content in the dosage forms with LH printed on an area of 2 cm^2 was obtained in a low therapeutically relevant dose (IV). The measured content (2.85 ± 0.06 mg, n = 6) showed no significant deviation from the theoretically expected amount (2.84 mg). However, degradation up to 18% from the initial content of LH derived from the hydrolysis of the amide group was observed over a short-time storage period of 8 months at room temperature.

The drug content of ITR and IND in the flexographically printed formulations with 10 layers of ink on 0.5 cm^2 was well below therapeutic levels ranging from 40 to 380 μg and from 110 to 270 μg, respectively (III). The results indicated that the printing process was not optimal for the precise dosing of the nanosuspension inks. Furthermore, an insufficient homogeneity of the nanosuspensions and possible sedimentation of the particles could explain the fluctuation in the deposited drug amount.

The dosing accuracy of the inkjet printing was significantly superior to the flexographic printing. The relative standard deviation (RSD) values below 4% were obtained for all inkjet-printed formulations, whereas in the flexographically printed formulations the RSD values for drug content varied from 8 to 39%.

5.3.2. Dosing flexibility of inkjet-printed dosage forms (I)

The drug content in the printed formulations can be adjusted by various methods, such as changing the size of the printed area, the number of printed layers and/or optimizing the concentration of the inks (Buanz et al., 2011; Janßen et al., 2013; Raijada et al., 2013; Wickström et al., 2015). On the other hand, the porosity, absorbability and thickness of the substrates also affect the loading capacity of the printed formulations (Sandler et al., 2011).

The drug content in the inkjet-printed dosage forms was adjusted by varying the printing resolution or the size of the printed area. Expectedly, adjusting the size of the dosage forms correlated linearly with the printed drug amount (**Figure 18A–B**). Whereas the drug content in the dosage forms printed on 4 cm^2 increased with the increasing resolution as a power function (**Figure 18C–D**). The behavior of the printed inks on the PET substrate correlated with the obtained drug content. The size of the solidified droplets in the LOP formulations as well as the crystallization of CAF was noticeably

increased above the resolution of 846 dpi (DS of 30 μm) as the distance between the jetted droplets decreased.

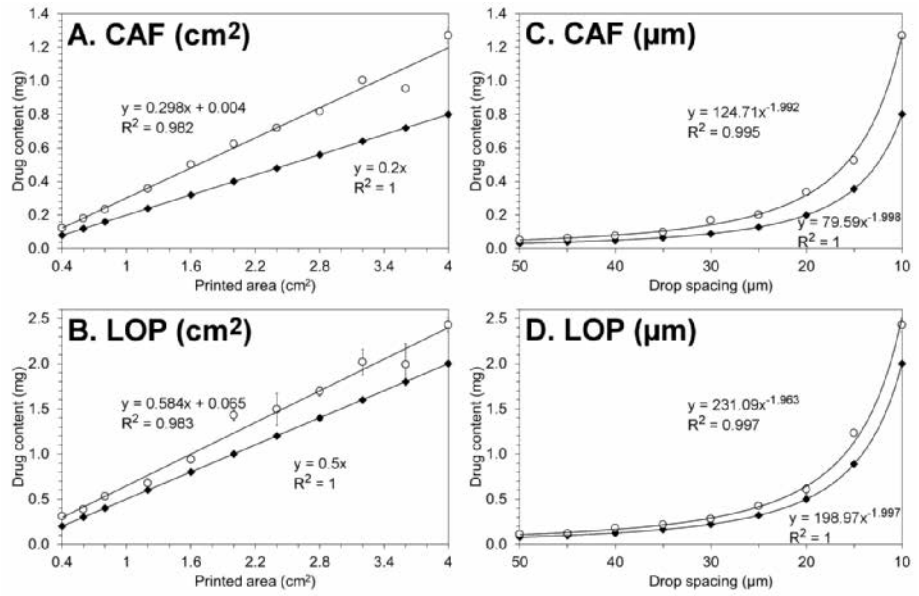

***Figure 18**. **Left**: Dosing flexibility of caffeine (CAF) (**A**) and loperamide hydrochloride (LOP) (**B**) by varying the size of the printed patterns, while the resolution remained constant (drop spacing of 10 μm). **Right**: Dosing flexibility of CAF (**C**) and LOP (**D**) by varying the resolution of the printed patterns, while the size of the dosage form remained constant (4 cm^2). Drug content is presented in theoretical (♦) and measured content (○) as mean with standard deviation bars, n = 3. R^2 – correlation coefficient.*

5.4. Spectral quantification of printed dosage forms (II)

A quantitative analysis was conducted on the ATR-FTIR spectra of the formulations with printed CAF and LOP on impermeable PET substrate. The use of an ATR setup allowed obtaining API-specific spectral information directly from the surface of the planar printed formulations (Fahrenfort, 1961; Offermann et al., 1995). The collected spectra of the CAF and LOP printed formulations were subject to univariate and multivariate data analysis.

5.4.1. Univariate data analysis of infrared spectra

In the univariate data analysis, the peak area and height of qualitatively relevant absorbance bands were correlated with the printing resolution that was expressed as DS values and the drug content (**Figure 19**).

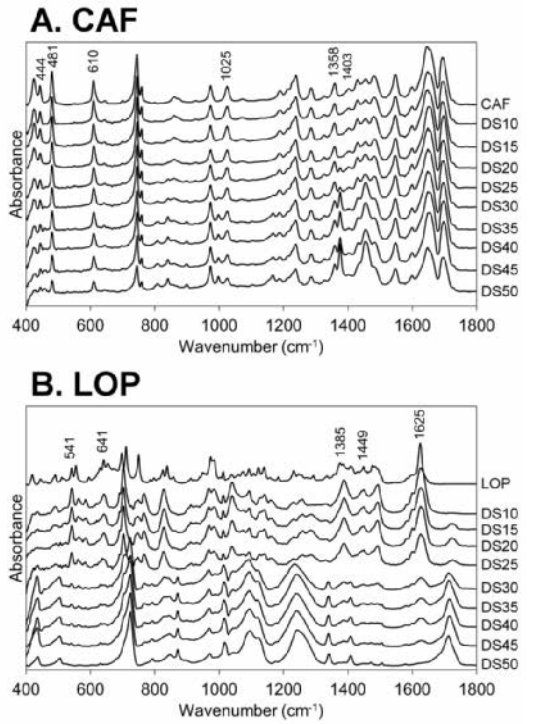

***Figure 19**. Pretreated ATR-FTIR spectra of caffeine (CAF) anhydrous form II (**A**), loperamide hydrochloride (LOP) anhydrous form I (**B**) and the printed formulations of both drugs with the increasing resolution – drop spacing (DS) from 50 μm (DS50) to 10 μm (DS10). Spectra are offset in absorbance for clarity.*

In drug formulations with printed CAF or LOP, the height and/or area of the selected individual absorbance bands was found to have a linear relationship with the DS and a logarithmic correlation with the actual drug amount. Specific examples with the highest correlation coefficients are shown in **Figure 20**. It was noted, that the formulations with CAF allowed obtaining a better quantitative relationship due to a uniform distribution of the crystalline drug on the printed surface compared to the unevenly spread LOP ink. The analysis of the printed LOP was dependent on the size of the solidified droplets that increased with the resolution (decreased DS). The interference from the underlying PET substrate decreased due to the coalescence of the droplets and provided a more uniform coverage of the analysis area of the ATR FTIR spectroscope. The effect of the ink distribution on the drug quantification can be clearly detected between the LOP formulations printed with DS of 25 or 30 μm (**Figure 20**). The narrower selection of the analyzed samples improved the correlation coefficient (R^2) between the peak height and the drug content or DS, but not the predictive properties of the correlation models (**Figure 20**).

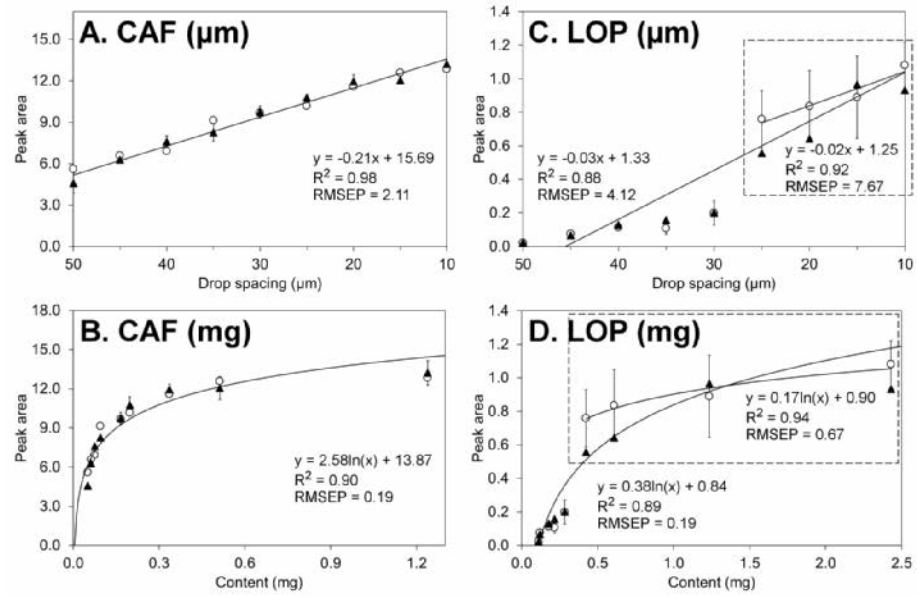

Figure 20. ***Left***: *Drop spacing (**A**) and caffeine (CAF) measured content (**B**) correlation plots with peak area at 610 cm^{-1} in the calibration (○) and test (▲) sets.* ***Right***: *Drop spacing (**C**) and loperamide hydrochloride (LOP) measured content (**D**) correlation plots with peak height at 1385 cm^{-1} in the calibration (○) and test (▲) sets. R^2 – correlation coefficient; RMSEP – Root Mean Square Error of Prediction.*

5.4.2. Multivariate data analysis of infrared spectra

In-line and on-line methods, such as Raman and NIR spectroscopy, are applicable for monitoring the qualitative and quantitative properties of drug preparations during the manufacturing process (Auer et al., 2003; Helmy et al., 2003; Rajalahti and Kvalheim, 2011; Mazurek and Szostak, 2012). Besides that, IR-based analysis tools coupled with chemometrics provide a fast and non-destructive alternative for at-line quality control compared to conventional and time-consuming off-line quantification methods (Pöllänen et al., 2005; Boyer et al., 2006).

The correlation models between the spectral data and the DS of printing could predict and verify the printing parameter value for the CAF and LOP formulations. More interestingly, the correlations between the spectral data and the printed drug content were evaluated for the quantitative quality control of the printed formulations. Based on the observations from the univariate analysis, the drug content was used in logarithmic values to establish linear models in the PLS regression analysis. The evaluation of the statistical parameters showed that by adjusting the model attributes, such as specifying the spectral range and applying different scaling algorithms and/or pre-processing filters, the performance of the PLS regression models

increased.

The significant changes in the spectral data (independent X-variables) for the prediction of drug content (dependent Y-variables) are demonstrated in the PLS weights plots (**Figure 21**). In the PLS regression model for CAF quantification, the first latent variable (LV) explained over 70% of the data by differentiating between the CAF and PG content. The relevant absorbance bands from the univariate analysis contributed also to the PLS regression models without any significant disturbance from the PET substrate. However, the first LV in the PLS regression model for LOP quantification explained approximately 86% of the spectral variation derived from the differences between the deposited ink components and the PET substrate. As expected from the univariate analysis, the division of the data into two clusters was also observed in the PLS regression analysis. The LOP and PG content within the sub-clusters of the data was in correlation with the second LV. Smaller spectral changes that were not apparent from the univariate analysis were incorporated into the PLS regression models by the additional LVs.

Interestingly, the multivariate data analysis could obtain good quantitative correlations between the LOP formulations with inhomogeneous drug distribution. The obtained PLS regression models showed good predictability and high correlations between the measured and predicted drug content (**Figure 22**). The quantitative analysis of the printed formulations was shown to be influenced by the performance range of the analysis method and the printing quality.

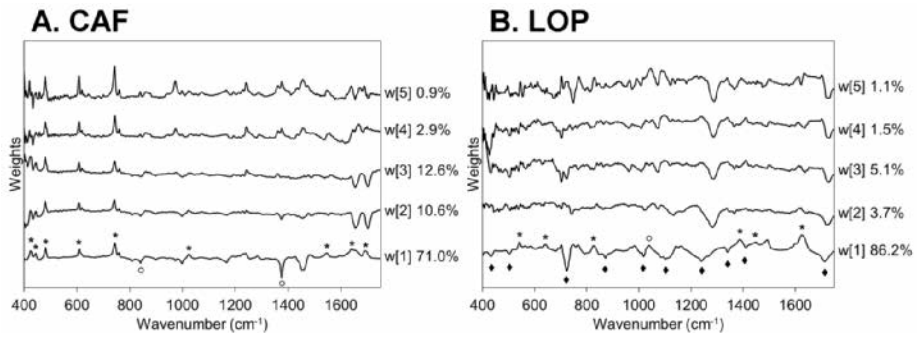

***Figure 21**. Weights of partial least squares (PLS) latent variables (LVs) for the quantification of caffeine (CAF) (**A**) and loperamide hydrochloride (LOP) (**B**) in the printed formulations. Model parameters: spectral range of 400–1750 cm^{-1}, Standard Normal Variate (SNV) pre-processing, mean centering (Ctr). The main absorbance bands for the corresponding drug (*), PET substrate (♦) and PG (○) that contributed to the first LV are marked. Weights are offset for clarity.*

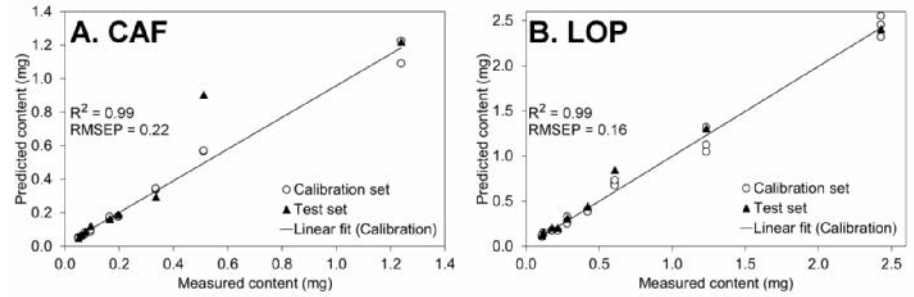

***Figure 22**. Prediction of caffeine (CAF) (**A**) and loperamide hydrochloride (LOP) (**B**) content in the printed formulations. Model parameters: spectral range of 400–1750 cm^{-1}, Standard Normal Variate (SNV) pre-processing, mean centering (Ctr). R^2 – correlation coefficient; RMSEP – Root Mean Square Error of Prediction.*

5.4.3. Evaluation of spectral quantification for quality control of printed dosage forms

The ATR-FTIR spectroscopy together with the multivariate data analysis could be applied to distinguish between the different components in complex formulations (e.g., printed dosage forms) and to provide a feasible non-destructive quantification method for the quality control of printed dosage forms.

The univariate data analysis determined the relationship between the spectra and the drug content in the printed formulations. Unlike PLS regression, where linear correlation between the variables is expected, the univariate method allowed applying various types of correlation models. Furthermore, some quantitative correlations were obtained with separated and high intensity absorbance bands.

The uniform distribution of the drug in the formulations has shown to be crucial in obtaining reliable spectroscopic quantification models (Mazurek and Szostak, 2011, 2012). The variations caused by the uneven coverage of the substrate were seen in the univariate spectral analysis of the printed LOP formulations. These differences were not apparent in the multivariate analysis that enabled the quantification of the printed pharmaceuticals in the systems with heterogeneous distribution of ingredients and/or spectral overlapping.

5.5. *In vitro* drug release from solid nanoparticulate systems prepared by flexographic printing (III)

The dissolution rate of an active compound is directly affected by the available surface area of particles that is increased non-linearly with the reduction of particle size (Noyes and Whitney, 1897; Merisko-Liversidge and Liversidge, 2008). The Noyes-Whitney equation (**Equation 2**) determines that the dissolution rate (*dC/dt*) of the solute is proportional to the available

surface area of the solute particle (*A*), diffusion coefficient (*D*), concentration difference between the saturation solubility (*Cs*) in the diffusion layer and the solute concentration (*C*) in the bulk solution, and inversely proportional to the thickness of the diffusion layer (*h*).

$$\frac{dC}{dt} = \frac{DA}{h}(C_s - C) \qquad \textit{(Equation 2)}$$

The preparation of nanosuspensions increases the effective surface area of the particles. Thus, this could subsequently improve the dissolution rate of drug substances. In addition, the increased dissolution rate is presumed to promote bioavailability of solubility-limited APIs (Müller and Peters, 1998).

The dissolution profiles of the nanoparticulate formulations were obtained with high deviations from the estimated drug content and notable intersample variations (**Figure 23**). The *in vitro* drug release from the impermeable TF substrate was comparable to the enhanced performance of the plain nanosuspensions. This was explained primarily by the even ink distribution that hinder the agglomeration of the particles upon solidification. The release of ITR and IND from the solid dosage forms printed on edible substrates was prolonged due to the incorporation of the drug particles into the porous substrate. However, these apparent advantages might not be expressed in the physiological conditions for nanocrystalline DDS containing APIs with pH-dependent solubility (Sarnes et al., 2014).

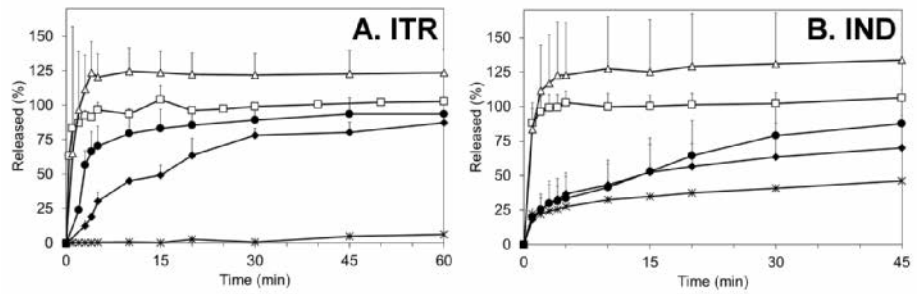

***Figure 23**. Dissolution profiles of itraconazole (ITR) (**A**) and indomethacin (IND) (**B**) powder (×), suspension (□) and printed samples on transparency film (TF) (△), rice sheet (●) and rice paper (♦). Drug release is presented as mean with standard deviation bars, n = 3.*

5.6. Combination drug delivery system with two active compounds (IV)

5.6.1. Preparation of combination drug delivery system

A combination DDS was prepared by combining electrospinning and inkjet printing technologies (**Figure 24**). This proof-of-concept formulation contained LH that was deposited on the PRX-loaded electrospun

substrates (G20-PRX) by inkjet printing. It was suggested that similar drug combinations with anti-inflammatory and anesthetic APIs could complement the prevention and treatment of oromucosal infections.

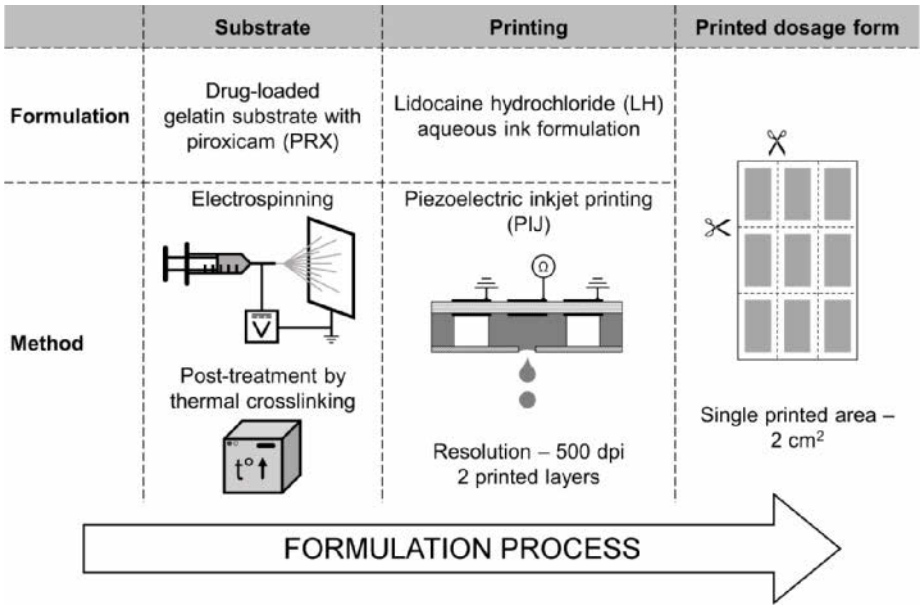

***Figure 21**. Experimental design and setup of the printed combination drug delivery system.*

5.6.2. Characterization of drug-loaded electrospun substrates

The drug-loaded G20-PRX fibrous substrates were prepared with a thickness of 0.06 ± 0.02 mm (n = 3). The electrospun G20-PRX microfibers showed a 13.3% increase in the diameter of the fibers compared to the unloaded G20 fibers (**Table 8**). The evaporation of the residual solvents during thermal crosslinking affected the size of the drug-loaded G20-PRX fibers showing a significant decrease (by 12.7%) in the average diameter of the fibers. The crosslinking improved the strength and elasticity of the G20-PRX fibers (**Table 8**). It was noted that the physical properties of the substrates were slightly affected by the incorporation of PRX into to the fibers; however, the effect was less pronounced after crosslinking.

***Table 8**. Average fiber diameter and physical properties of non-crosslinked (nonCL) and crosslinked (CL) piroxicam-loaded gelatin substrates (G20-PRX).*

	Fiber diameter[a] (nm)	Puncture test[b]		Tensile test[b]		
		Burst strength (mN/mm²)	Elongation at break (%)	Tensile strength (N/mm²)	Elongation at break (%)	Elastic modulus (kPa)
nonCL G20-PRX	1477.6 ± 217.5	37.8 ± 8.8	0.6 ± 0.1	1.6 ± 0.4	1.3 ± 0.2	16.2 ± 1.4
CL G20-PRX	1301.1 ± 216.9	71.7 ± 12.9	1.7 ± 0.1	2.5 ± 0.03	2.1 ± 0.4	9.0 ± 2.9

[a]mean ± standard deviation, n = 100. [b]mean ± standard deviation, n = 3-5.

The amorphous structure of gelatin was confirmed by XRD and ATR-FTIR spectroscopy also within the drug-loaded G20-PRX fibers (data not shown). The PRX-loaded fibrous scaffolds were stabilized by the Maillard reaction shown by the characteristic features on the DSC thermograms and the ATR-FTIR spectra similar to the unloaded G20 fibers. However, the MT-DSC thermal analysis showed that the thermal stability of the fibers was influenced by the addition of PRX, showing an approximately 20 °C decrease in the helix-coil transition temperature of gelatin.

The APIs in an amorphous state can be stabilized by the incorporation of the drug molecules into the electrospun polymer fibers (Vrbata et al., 2013; Paaver et al., 2014, 2015; Farooq et al., 2015). Therefore, thermal, X-ray diffraction and spectroscopic analyses were conducted to determine the solid state of PRX in the electrospun fibers. The characteristic thermal events for PRX were not detectable in the nonCL fibers due to the inclusion of PRX within the gelatin fibers and the overlapping with the melting endotherm of glucose at 149.5 °C (onset at 125.8 °C) (**Figure 25A**). The absence of a melting endotherm indicated that that PRX was incorporated into the fibers in an amorphous state. However, in the CL G20-PRX fibers an endotherm at 173.1 °C (onset at 150.2 °C) was detected (**Figure 25A**). It was suggested that in the thermally treated fibers the amorphous PRX crystallized into its least stable anhydrous form III with subsequent melting as shown previously for amorphous PRX and/or its solid dispersions (Vrečer, et al., 2003; Kogermann et al., 2011).

The absorbance bands at 1436, 875 and 773 cm^{-1} on the ATR-FTIR spectra were attributed to PRX in the nonCL and CL drug-loaded fibers. However, several characteristic absorbance bands for specific crystalline forms of PRX (anhydrous forms I, II, III and monohydrate) assigned by Vrečer, et al. (2003) and Taddei et al. (2001) were not present in the measured spectra. Furthermore, the changes in the spectral range from 3300 to 3400 cm^{-1} indicated the stabilization of the amorphous PRX through intermolecular interactions with gelatin. The detected disappearance of the N–H stretching vibrational mode of PRX at 3337 cm^{-1} has been assigned to hydrogen-bonding between NH group of PRX and >N– and C=O functional groups of polymers (Tantishaiyakul et al., 1999; Lust et al., 2015). The PRX in an amorphous state within the electrospun G20-PRX fibers before and after crosslinking was confirmed by the XRD analysis (**Figure 25B**).

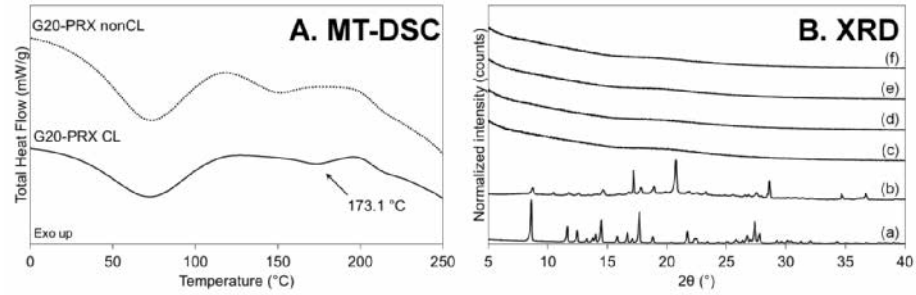

***Figure 25**. **A**: Modulated DSC (MT-DSC) (total heat flow signal) thermograms of non-crosslinked (nonCL) and crosslinked (CL) piroxicam-loaded gelatin substrates (G20-PRX). Thermograms are offset in y-axis for clarity. **B**: X-ray diffractograms of PRX anhydrous form II (c), physical mixture corresponding to the formulation of G20-PRX substrate (d), nonCL G20 (e) and G20-PRX (f) substrates and CL G20 (g) and G20-PRX (h) gelatin substrates. Diffractograms are offset in intensity for clarity.*

5.6.3. Characterization of combination drug delivery system

The drug loading of the CL G20-PRX substrate corresponded well with the theoretical content, containing 6.2 ± 0.2% (n = 3) of PRX in the fibers. The chemical stability of the API showed a non-significant loss (< 5%) after the thermal treatment at 130 °C. The PRX content of 0.35 ± 0.01 mg per a printed area of 2 cm^2 remained constant over a short-term stability study of 4 months.

The printed DDS contained 2.18 mg of LH per a printed area of 2 cm^2 (initial theoretical dose). Drug degradation of approximately 30% was detected during a short-term stability study of 4 months. The hydrolysis of LH was more distinct in the dual DDS compared to the single drug system with LH printed on unloaded G25 gelatin substrates. In the latter formulation, an approximately 8% loss of LH content was detected after 4 months.

The solid state analysis of the combination DDS showed that the printing did not affect the amorphous state of PRX. A characteristic endotherm at 175.7 °C for PRX in the drug-loaded gelatin fibers was identified also on the DSC thermograms of the printed DDS. The XRD analysis showed no crystallization of PRX or LH in the dual DDS. It was proposed that the small volume of the ink droplets and the fast evaporation rate of the solvents could not promote the crystallization of PRX. In addition, the printing provided a stabilizing barrier through the uniform deposition of the molecularly dispersed LH on the surface of the fibrous substrates.

5.6.4. *In vitro* drug release from combination drug delivery system

The results showed that the release kinetics of PRX and LH from the dual DDS were comparable to the single drug formulations (**Figure 26**). This suggested that a combination method for preparing complex DDS with multiple APIs could provide possibilities for controlling the single drug

performance in the dosage forms separately.

The electrospun G20-PRX substrate showed an immediate drug release profile with a high initial burst release that was decreased approximately 2-fold after crosslinking (**Figure 26A**). The drug release from the surface of the electrospun fibers has been reported to be the main cause for the burst effect (Agarwal et al., 2008; Hu et al., 2014; Nguyen et al., 2012). PRX monohydrate has a lower aqueous solubility compared to its crystalline counterparts (Jinno et al., 2000; Paaver et al., 2012). Thus, in the nonCL fibers, the formation of a monohydrate form was presumed due to the decreased amount of dissolved PRX after few minutes. The addition of LH by printing did not have any noticeable effect on the PRX release profile from the combination DDS compared to the CL G20-PRX substrate.

The drug release of LH was not dependent on the printing substrate, showing immediate release from the dosage forms printed on unloaded G25 and drug-loaded G20-PRX gelatin substrates (**Figure 26B**). The addition of a backing layer to such printed dosage forms could further improve the performance of oromucosal dosage forms by controlling the direction of the drug release (Preis et al., 2014, 2015).

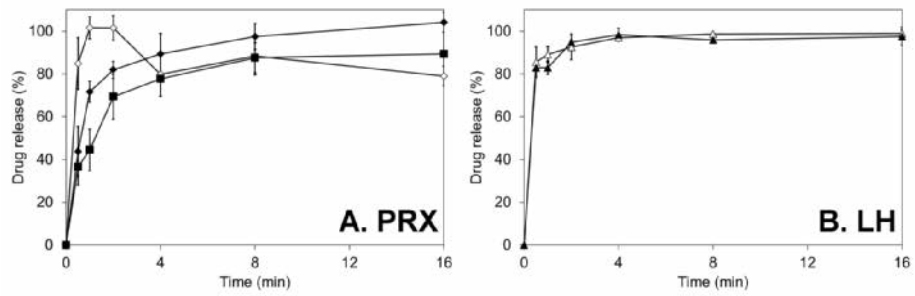

***Figure 26**. **A**. Drug release (%) of piroxicam (PRX) from non-crosslinked (nonCL) (◇) and crosslinked (CL) (♦) drug-loaded gelatin substrates (G20-PRX), and from the combination drug delivery system with lidocaine hydrochloride (LH) printed on CL G20-PRX substrate (■). **B**. Drug release (%) of LH from the printed dosage forms on CL G25 (△) and G20-PRX (▲) substrates. Drug release is presented as mean with standard deviation bars, n = 2.*

6. Conclusions and outlook

The focus of this thesis was to gain in depth knowledge about the development of drug delivery systems (DDS) by two-dimensional (2D) printing technology.

The drug-containing solutions or nanosuspensions were prepared as pharmaceutical inks for the inkjet or flexographic printing, respectively. The printability of the ink solutions was successfully estimated based on the analysis of the viscosity and the surface tension of the inks. Furthermore, the gelatin-based electrospun fibrous matrices were successfully utilized as carrier substrates in the inkjet-printed dosage forms after improving their mechanical strength by thermal crosslinking.

Solid dosage forms were obtained after the deposition of the pharmaceutical inks on biodegradable carrier matrices by means of inkjet or flexographic printing. The solid state of the printed pharmaceuticals was shown to be affected by the physicochemical properties of the drug, the ink formulation and the absorbability of the substrate. On the edible substrates, the printed pharmaceuticals penetrated at least partially into the carrier matrices. The active compounds were detected in crystalline or molecularly dispersed state in the inkjet-printed dosage forms. Whereas the solid nanoparticulate systems obtained by flexographic printing of crystalline nanosuspensions exhibited no detectable changes in the solid state of the drugs.

The estimation of the printed drug amount for individualized dose adjustment showed high dependency on the volume and the stability of the jetted droplets. The drug content analysis of the printed dosage forms confirmed that the dosing accuracy of the inkjet printing was superior to the flexography. This was attributed to the fundamental differences in the ink transfer mechanisms between those two 2D printing methods. The flexible dosing of the pharmaceuticals was obtained with high precision by adjusting the resolution of the drop-on-demand inkjet printing or the physical size of the printed dosage forms.

The non-destructive attenuated total reflectance Fourier transform infrared (ATR-FTIR) spectroscopy was found to be a good technique for the quantitative analysis of printed pharmaceuticals. The univariate analysis of the ATR-FTIR spectral data revealed a logarithmic correlation with the printed drug content. The Partial Least Squares regression models from the multivariate data analysis were obtained with an acceptable predictability regardless of the solid state of the printed drug. The results showed that spectroscopic methods have tremendous possibilities in the quality control of the printed dosage forms.

The nanoparticulate systems exhibited an enhanced *in vitro* drug release due to the spatial distribution of the nanosuspensions on the substrates

that hindered the aggregation of the solid particles. The release profiles of the drugs from the surface of the non-porous reference substrate were comparable to the initial nanosuspensions, whereas the printed formulations on the edible substrates showed a slower release rate due to the penetration of the ink into the carrier matrices.

The preparation of the combination DDS was successfully demonstrated by exploiting two different techniques for the incorporation of the active compounds. In the dual DDS, an ink solution with one drug was printed on the drug-loaded electrospun substrates containing another active compound. Both drugs exhibited an immediate drug release from the combination DDS. Thus, the use of drug-loaded fibrous substrates provided a good platform for the design of DDS with multiple active compounds.

Currently the development of printed dosage forms is being thoroughly investigated to meet the needs of individualized drug therapy, and the design of these systems seems to be limited by one's own imagination. The printed dosage forms are highly feasibile for tailored drug therapy with various active compounds at high dosing uniformity and suitable drug release behavior. The presented research work provided a comprehensive insight into the design and production of personalized dosage forms by 2D printing technology. The analysis of the printed dosage forms improved the understanding of the crucial parameters in the development process as well as the *in vitro* performance and stability of the printed pharmaceuticals.

More knowledge is continuously required on the formulation design aspects and the ink-substrate interactions that influence the solid state properties of the printed pharmaceuticals. In that context, the effect of printing parameters, for example the applied voltage and waveform in piezoelectric printing, and/or the printing temperature has not been systematically studied yet. The future prospects include the development of printed dosage forms with therapeutically relevant drug combinations and/or with controlled drug release profiles. Further perspective is aimed at the analysis of the *in vivo* performance of the printed dosage forms, since more information is needed on the behavior of these systems in physiological conditions. In addition, the optimization of specific printing units with integrated or complementary quality control tools is required for the successful implementation of this method for the on-site manufacturing of personalized dosage forms.

7. Sammanfattning (Summary in Swedish)

Design och utveckling av personifierade beredningsformer med hjälp av utskriftsteknologi

Utvecklingen av skräddarsydda beredningsformer erbjuder möjligheter till individuell läkemedelsterapi. Personifierade beredningsformer bidrar till säkrare vård och minskar risken för överdosering och biverkningar. Konventionella farmaceutiska preparat med förutbestämda dosstyrkor produceras vanligtvis i stor industriell skala. Däremot kunde beredningsformer för enskilda patienter framställas i små satser med specifika material, läkemedelsdoser och frisättningsprofiler. Därför undersöks alternativa tillverkningsmetoder, så som utskriftsteknologi, för framställning av skräddarsydda beredningsformer. Utskriftsteknologi är en flexibel framställningsmetod som även möjliggör tillverkning av farmaceutiska preparat med varierande dosstyrka vid vårdplatsen enligt patientens behov.

Syftet med denna avhandling var att undersöka ifall personifierade beredningsformer kunde tillverkas med hjälp av tvådimensionell (2D) utskriftsteknologi. Vid 2D-utskrift av läkemedel applicerades ett bläck innehållande läkemedel enligt ett fördefinierat mönster på bärarmaterialet. Den fasta beredningsformen uppnåddes efter torkning av bläcket på substratet. Doseringsnoggrannheten och reproducerbarheten av de bläckstråleutskrivna beredningsformerna möjliggjordes genom kontroll av antalet droppar och deras volym. Finjustering av beredningsformernas egenskaper och sammansättning tillät tillverkning av läkemedelsadministrationssystem (DDS) med kontrollerade frisättningsprofiler och/eller med flera olika aktiva farmaceutiska substanser.

I avhandlingen bevisades 2D-utskriftsteknologins mångsidighet genom design av utskrivna beredningsformer, med hjälp av antingen bläckstråleskrivare eller flexografisk tryckning på ätbara substrat med olika farmaceutiska bläck. De utskrivna beredningsformerna och deras komponenter analyserades för att fastställa avgörande aspekter av utvecklingsprocessen och förbättra kunskapen om utskrivna läkemedels fysikalisk-kemiska egenskaper, *in vitro* frisättningsprofil och stabilitet. Resultaten visade att utskrivbarheten av bläcket och de specifika utskrivningsparametrarna var beroende av de reologiska egenskaperna hos bläcket. Substratets förmåga att absorbera bläck, bläckets sammansättning och läkemedlens fysikalisk-kemiska egenskaper bidrog till den slutliga fasta fasen av de utskrivna läkemedlen. Analyserna visade att de slutliga fasta beredningsformerna innehöll den kristallina formen eller den molekylärt dispergerade fasen av den aktiva substansen. Den jämna distributionen av den kristallina nanosuspensionen på substraten bidrog till förbättrad *in vitro* läkemedelsfrisättning från de flexografiskt framställda fasta

nanopartikelssystemen.

Resultaten visade att en stabil bläckstråleutskrift var fördelaktigt med tanke på doseringsnoggrannheten. Den flexografiska tryckningsmetoden uppvisade mindre doseringsnoggrannhet av nanosuspensionerna främst på grund av hur bläcket överfördes till substratet. Doseringsflexibiliteten hos de utskrivna beredningsformerna uppnåddes genom bestämning av doseringsenhetens utskrivningsresolution eller den utskrivna ytan. Dämpad totalreflektion Fourierspektroskopi (ATR-FTIR) och multivariat dataanalys visade sig vara en användbar och icke-destruktiv metod för dosbestämning av de utskrivna läkemedlen.

I avhandlingen undersöktes även lämpligheten att använda elektrospunna fibrösa matriser som substrat vid framställning av de utskrivna beredningsformerna. Läkemedel inkorporerade i de elektrospunna fibrerna tillverkades med stabilisering av den amorfa fasen av det svårt vattenlösliga läkemedlet i de inre strukturerna av de elektrospunna fibrerna. Användningen av fibrösa substrat innehållande läkemedel presenterade ett nytt sätt att framställa DDS med två aktiva substanser. Detta system erhölls genom utskrift av ett läkemedel på elektrospunnet fibröst substrat innehållande ett annat läkemedel. Analyserna av de utvecklade kombinerade beredningsformerna visade att de i DDS ingående läkemedlen hade självständiga frisättningsprofiler.

I avhandlingen presenteras en omfattande översikt över de huvudsakliga aspekterna för utveckling av personifierade beredningsformer med hjälp av 2D-utskriftsteknologi. Forskningsresultaten förbättrar förståelsen av viktiga faktorer för finjustering och tillverkning av utskrivna beredningsformer, vidareutvecklar kvalitetskontrollaspekterna av utskriftsprocessen samt erbjuder insikter i väsentliga egenskaper hos de utskrivna läkemedlen.

8. Kokkuvõte (Summary in Estonian)

Personaliseeritud ravimvormide väljatöötamine printimistehnoloogia abil

Sissejuhatus

Personaliseeritud meditsiin arvestab raviskeemi koostamisel patsiendi füsioloogiliste, ealiste ja käitumuslike eripäradega, mis mõjutavad ravimite farmakokineetikat ja -dünaamikat, raviainete toimet ja kõrvaltoimete esinemist (Cohen, 1999; Breitkreutz and Boos, 2007; European Medicines Agency, 2013). Lisaks võimaldab diagnostiliste testide ühildamine patsiendile orienteeritud ravimvormidega tiheda tagasiside süsteemi loomist (Alhnan et al., 2016; Sandler and Preis, 2016). Taolise kontseptsiooni ellu viimiseks on vajalik personaliseeritud ravimvormide väiksemahuline valmistamine vastavalt patsiendi vajadustele (Hamburg and Collins, 2010). Tootmisprotsessid, mida kasutatakse tänapäeval konventsionaalsete ravimpreparaatide valmistamiseks, on tihtipeale liiga jäigad, mistõttu ei ole lihtne muuta raviplaani alusel raviaine sisaldust preparaatides. Sellepärast uuritakse alternatiivseid tootmistehnoloogiaid, mida saaks kasutada tootmaks ravimpreparaate, mille omadusi on võimalik modifitseerida vastavalt vajadusele.

Ravimprintimine tähendab ravimpreparaatide või -toodete valmistamist printimise abil. Kahe- (2D) või kolmemõõtmeline (3D) printimine pakub mitmeid tehnoloogilisi võimalusi personaliseeritud meditsiinis. Viimaste aastakümnete jooksul on loodud erinevaid prinditud ravimkandursüsteeme (Sandler et al., 2011; Kolakovic et al., 2013; Alomari et al., 2015; Preis et al., 2015; Scoutaris et al., 2016), meditsiiniseadmeid (Wu et al., 1996; Katstra et al., 2000; Tarcha et al., 2007; Shafiee and Atala, 2016) ning raviainet sisaldavaid funktsionaalseid katteid transdermaalsetele mikronõeladele (Boehm et al., 2014; Ross et al., 2015; Uddin et al., 2015) ja implantaatidele (Nganga et al., 2014).

Uurimistöös keskenduti 2D printimistehnoloogiale, sh tindiprintimisele ja fleksograafiale, mis on oma resolutsiooni ja tootlikkuse poolest sobilikud personaliseeritud ravimvormide valmistamiseks. Tindiprintimine on kontaktivaba meetod, mille puhul prinditav lahus kantakse printerist vastavalt digitaalselt kujundatud mustrile kindlale kohale kandematerjalil ehk substraadil. Fleksograafia on kõrgtrüki eriliik, kus prinditava materjali trükkimiseks kasutatakse trükivorme rullrotatsioonmasinal. Erinevalt tindiprintimisest on fleksograafiliselt prinditud ravimvormi kvaliteedi tagamiseks vajalik piisav kokkupuude prinditava materjaliga kaetud trükivormi ja substraadi vahel (Kolakovic et al., 2013).

Prinditud ravimvormide ülesehitus oleneb nende manustamisviisist.

Lisaks raviaine toime modifitseerimisel on võimalik muuta ravimvormide suurust, kuju ja organoleptilisi omadusi. Üldiselt koosneb prinditud süsteem kahest põhikomponendist: prinditav materjal ja substraat. Ravimprintimisel on prinditavaks materjaliks raviainet sisaldav lahus, (nano)suspensioon (Pardeike et al. 2011; Janßen et al., 2013) või bioloogiliselt aktiivset ainet sisaldav süsteem (Di Risio and Yan, 2007; Derby, 2008). Ravimvormides on substraatidena võimalik kasutada polümeerkilesid, söödavaid pabereid või muid bioloogiliselt ühilduvaid materjale. Üldiselt on eelistatud substraadid, mis on inertsed ja sobituvad kokku erinevate prinditavate materjalide ja raviainetega. Samas võimaldab nende funktsionaliseerimine mõjutada adhesioonivõimet, lagunemist või maitset. Lisaks saab kasutada polümeersetest nano- või mikrofiibritest koosnevate substraatide valmistamiseks elektrospinnimise meetodit (Greiner and Wendorff, 2007; Agarwal et al., 2008; Bhardwaj and Kundu, 2010). Seejuures on prinditava raviaine kogus määratletud raviaine kontsentratsiooni, prinditava pindala, kandematerjali imamisvõime ja printimiseks disainitud struktuuriga.

Prinditud ravimite kvaliteedi tagavad prinditava materjali ja substraadi omadused, nende komponentide omavaheline sobivus ja printimissätted. Lahuste prinditavust on võimalik hinnata ühikuta Z-arvu alusel (Fromm, 1984; McKinley and Renardy, 2011). Selle põhjal määravad lahuse viskoossus, pindpinevus ja tihedus ning nende muutumine printimisprotsessi jooksul tilga moodustumise ja väljutamise printerist (Barnes et al., 1989; Le, 1998; Calvert, 2001, de Gans et al., 2004). Substraadi ja lahuse omadused (substraadi poorsus ja märgumine, lahuse absorptsioon ja tahkestumine) ning nende omavaheline sobivus mõjutavad prinditud süsteemi kuivamist (Calvert, 2001; Derby, 2010; Määttänen et al., 2010). Need interaktsioonid mõjutavad ka ravimpreparaatides esineva raviaine tahket vormi (Sandler et al., 2011; Hsu et al., 2012; Raijada et al., 2013; Buanz et al., 2013).

Ravimpreparaatide kvaliteedi tagamiseks tuleb analüüsida raviainete/abiainete füsikokeemilisi omadusi kogu tootmisprotsessi erinevates etappides. Prinditud ravimvormide valmistamine vastavalt nõudlusele vähendab raviaine tahke vormi muutuste ja füsikokeemilise lagunemise esinemist (Raijada et al., 2013). Raviaine molekulaarsete omaduste ja sisalduse uurimiseks proovi kahjustamata kasutatakse eelkõige spektroskoopilisi ja röntgendifraktomeetrilisi meetodeid (Savolainen et al., 2006; Aaltonen et al., 2008). Prinditud ravimkandursüsteemide analüüsimiseks on senini kasutatud näiteks Raman ja infrapunaspektroskoopiat, röntgendifraktomeetriat ning lähi-infrapuna hüperspektraalset pildianalüüsi (Melendez et al., 2008; Buanz et al., 2013; Vakili et al., 2014).

Uurimistöö keskendus 2D printimistehnoloogia abil personaliseeritud ravimvormide valmistamisele ja iseloomustamisele. Töös hinnati prinditud ravimvormide võimalikku rakendamist personaliseeritud ravimvormide valmistamisel ja analüüsiti prinditud raviainete füsikokeemilisi omadusi.

Uurimistöö põhieesmärgid

Uurimistöö põhieesmärk oli välja selgitada 2D printimistehnoloogia rakendamisvõimalused personaliseeritud ravimvormide valmistamisel. Uurimistöö oli suunatud prinditud ravimvormide valmistamisele ja analüüsimisele ning arendusprotsessi eripärasuste kindlaks määramisele.

Uurimistöö spetsiifilised eesmärgid olid:

- valmistada tindi- ja fleksograafilises printimises kasutatavad farmatseutilised lahused, nanosuspensioonid ja kandesubstraadid;
- analüüsida prinditud ravimvormide füsikokeemilisi omadusi;
- hinnata tindiprintimise täpsust ja paindlikkust raviainete annustamisel;
- kasutada infrapunaspektroskoopiat prinditud raviainete kvantifitseerimiseks;
- analüüsida raviainete *in vitro* vabanemist fleksograafiliselt prinditud nano-osakestega süsteemidest;
- kujundada ja analüüsida kahte raviainet sisaldavat prinditud ravimkandursüsteemi.

Materjalid ja meetodid

Printimislahustes kasutatud mudelraviained olid veevaba kofeiin (CAF), loperamiidvesinikkloriid (LOP) ja lidokaiinvesinikkloriidi (LH) monohüdraat. Printimise baaslahus sisaldas lahustina puhastatud vett või etanooli (≥99,7%) ning solubiliseeriva ainena propüleenglükooli (PG). Vesi-nanosuspensioonid fleksograafiliseks printimiseks valmistati vees halvasti lahustuva itrakonasooli (ITR) ja indometasiiniga (IND).

Raviained prinditi kommertsiaalsetele kandesubstraatidele, laboratoorselt valmistatud hüdroksüpropüültselluloosi polümeerkiledele ja elektrospinnitud želatiinipõhistele fiibermattidele. Lisaks valmistati printimiseks piroksikaami (PRX) sisaldavad fiibermatid. Elektrospinnitud fiibermaatriksid ristseoti termilisel töötlemisel glükoosi juuresolekul.

Prinditud ravimvormid valmistati piesoelektrilise tindiprintimise või fleksograafilise trükkimise abil. CAF ja LOP sisaldust prinditud ravimvormides varieeriti muutes printimisresolutsiooni või prinditavat pindala. Piesoelektriliselt prinditud LH sisaldavate ravimvormide stabiilsust uuriti 4 või 8 kuu vältel.

CAF ja LOP sisaldavate printimislahuste prinditavust hinnati lahuste viskoossust ja pindpinevust mõõtes. Nanosuspensioonides määrati dünaamilise valguse hajuvuse meetodil tahkete osakeste suurus ja suurusjaotus. Elektrospinnitud fiibermattide mehhaanilise tugevuse hindamiseks viidi läbi läbistus- ja tõmbekatsed tekstuurianalüsaatoriga.

Uurimistöös kasutati prinditud ravimvormide analüüsimiseks järgmisi meetodeid: skaneeriv elektronmikroskoopia, diferentsiaalne skaneeriv kalorimeetria, röntgendifraktomeetria ja nõrgendatud täieliku sisepeegelduse Fourier' teisendusega infrapunaspektroskoopia. Raviainete kvantitatiivses analüüsis rakendati ultraviolett-nähtav spektrofotomeetriat või kõrgefektiivset

vedelikkromatograafiat. Lisaks kasutati ühe- ja mitmemõõtmelist andmeanalüüsi määramaks CAF ja LOP sisaldust prinditud süsteemides infrapunaspektrite põhjal.

ITR ja IND vabanemist prinditud ravimvormidest uuriti kohandatud *in vitro* dissolutsioonitestiga vastavalt fosfaatpuhvris (pH 5,0) või 0,1 M vesinikkloriidi lahuses (pH 1,2). LH ja PRX sisaldavatest ravimvormidest raviaine vabanemiskiiruse määramiseks simuleeritud süljelahuses (pH 6,8) (Marques et al., 2011) kasutati samuti modifitseeritud *in vitro* dissolutsioonitesti katsesüsteemi.

Tulemused ja arutelu

Mõõdetud viskoossuse, pindpinevuse ja tiheduse põhjal arvutatud Z-arv jäi CAF ja LOP sisaldavate printimislahuste puhul vahemikku 1–14, mis sobib piesoelektrilisel tindiprintimisel ühtlase tulemuse saavutamiseks. Sellele vaatamata erines nende lahuste pindpinevus märgatavalt, mis põhjustas tilga väljutamisel satelliit-tilkade (CAF lahus) või väljavenitatud tilkade (LOP lahus) moodustumist. Samas oli LH lahuse korral võimalik printimissätete muutmisega tagada pidev sfääriliste tilkade moodustumine. ITR ja IND nanosuspensioonides oli osakeste keskmine suurus vastavalt ~420 ja ~700 nm. Kuulveskis valmistatud vesi-nanosuspensioonid sisaldasid stabilisaatorina mitteioonset surfaktanti Poloxamer 407 ja raviainet selle kristallilises vormis. Elektrospinnitud želatiinipõhised substraadid sisaldasid nanofiibreid, mille keskmine diameeter oli ~600 nm. Nende fiibermattide mehaaniline tugevus paranes kuni 5-kordselt termilise töötlemise järel. Fiibrite ristsidumine põhines mitte-ensümaatilisel Maillardi reaktsioonil glükoosi karbonüülrühma ja želatiini aminorühma vahel (Siimon et al., 2014, 2015; Etxabide et al., 2015).

Printimislahuse ja substraadi vahelist füüsikalist koosmõju hinnati märgumisnurga mõõtmisega. Tulemused näitasid, et lahuste sorptsioon oli mõjutatud eelkõige pindpinevusest ning substraatide paksusest. Elektrospinnitud fiibrite lühiajaline hoiustamine ~70% õhuniiskuse juures muutis fiibermattide struktuuri kõvaks ja rabedaks, erinevalt termiliselt töödeldud fiibermattidest, mis säilitasid oma algse väljanägemise.

Prinditud ravimvormide pinnamorfoloogia näitas, et veevaba CAF II vormi kristalliseerumise ulatus substraatidel olenes nende vedeliku imamisvõimest. Samas tahkestus LOP lahus uuritud substraatidel tilkadena, tagades raviaine molekulaarselt dispersse jaotumise. Printimisresolutsiooni suurendamisel oli näha LOP lahuse tahkestumist suuremate omavahel liitunud tilkadena. Glasuurlehtedel imendusid mõlemad lahused laias ulatuses materjali sisse, mistõttu substraadi pinnal oli tuvastatud raviaine kogus märgatavalt väiksem. Nanosuspensioonide fleksograafilisel trükkimisel oli prinditud pinna topograafia ebaühtlane, kuid sellele vaatamata ei täheldatud nano-osakeste ulatuslikku agregatsiooni. Nii ITR kui ka IND säilitasid printimise teel saadud tahketes nano-osakestega süsteemides

oma stabiilse kristallise vormi. Töödeldud fiibermatid ei lahustunud LH lahuse printimisel, kuid üksikud fiibrid pundusid ja kleepusid üksteise külge ning tasandasid ravimvormide prinditud ala. Sarnaselt LOP-ile oli ka LH prinditud ravimvormides molekulaarselt dispergeeritud. Tulemused viitasid, et viskoossuse tõstmiseks lisatud abiaine PG takistas prinditud raviainete kristalliseerumist.

Tindiprinditud raviainete teoreetiline annus arvutati tilgamahu (pL), printimisresolutsiooni (dpi), printava pindala (cm^2), prinditavate kihtide arvu ja lahuse kontsentratsiooni (mg/mL) põhjal. Raviainete annustamine tindiprintimisel valmistatud ravimvormides andis kvantitatiivses analüüsis tulemusi all 4%-lise suhtelise standardhälbega, mis oli märgatavalt täpsem võrreldes fleksograafiliselt trükitud ravimvormidega. Seejuures täheldati, et 8 kuu jooksul lagunes hüdrolüüsi tõttu ligikaudu 18% prinditud LH-st. Printimisresolutsiooni või prinditava pindala muutmisega sai reguleerida raviaine annust manustatavas ühikus. Prinditud pindala oli lineaarses korrelatsioonis prinditud raviaine kogusega. Seos raviaine koguse ja printimisresolutsiooni vahel oli määratud astmefunktsiooniga.

Lisaks traditsioonilistele mõõtmismeetoditele analüüsiti CAF ja LOP kvantifitseerimiseks valmistatud prnditud ravimvormide infrapunaspektreid. Spektrite ühemõõtmeline analüüs, kus kasutati raviaine-spetsiifiliste neeldumismaksimumide intensiivsust või pindala, näitas lineaarset korrelatsiooni printimisresolutsiooniga ning logaritmilist seost raviaine kogusega. Selleks, et vähendada raviaine tahkest vormist, abiainetest ja/või substraadist tingitud varieeruvust, kasutati spektrite mitmemõõtmelist analüüsi. Kvantifitseerimiseks koostati korrelatsioonikogumi põhjal osalise vähimruudu (PLS) regressiooni mudelid. Tänu madala hindamisvea ja hea ennustusvõimega mudelitele sai infrapunaspektrite põhjal määrata raviaine sisaldust katsekogumis olevates prinditud ravimvormides.

Nanosuspensioonide valmistamine parandas raviainete *in vitro* lahustumiskiirust vesikeskkonnas. Fleksograafiliselt prinditud nano-osakestega süsteemides sõltus raviaine vabanemine substraadist. Nanosuspensioonide inkorporeerumine poorsete riisipaberite struktuuri aeglustas raviaine vabanemist võrreldes plastkiledele prinditud ravimvormidega. Prinditud raviaine osakeste ruumiliselt ühtlane jaotumine substraadil takistas agregatsiooni ja soodustas raviaine lahustumiskiiruse paranemist.

Kahte raviainet sisaldava ravimkandursüsteemi valmistamiseks kombineeriti raviainete lisamiseks kaks erinevat meetodit. Esmalt valmistati elektrospinnimise teel 6,5% (m/m) PRX sisaldavad mikrofiibrid, mis sarnaselt raviaineta fiibermattidele ristseoti termilisel töötlemisel. Erinevate analüüsimeetoditega tuvastati, et elektrospinnitud mikrofiibrites oli PRX stabiliseeritud amorfses vormis, mis oli eelkõige tänu fiibrite struktuurilisele eripärale. PRX sisaldavaid fiibermatte kasutati substraatidena LH

vesilahuse printimisel. Lõpptulemusena saadi kahe raviainega prinditud ravimkandursüsteem, kus amorfset PRX sisaldava fiibersubstraadi pinnal oli LH molekulaarselt dispersses vormis. *In vitro* dissolutsioonitesti tingimustes vabanesid ravimkandursüsteemist mõlemad raviained koheselt üksteisest sõltumata.

Järeldused

Uurimistöö tulemused andsid põhjaliku ülevaate ravimvormide valmistamisest 2D printimistehnoloogia abil. Prinditud ravimkandursüsteemide analüüs parandas arusaamist tootmisprotsessi olulistest parameetritest, prinditud raviainete stabiilsusest ja *in vitro* käitumisest.

Tindi- või fleksograafilise printimise jaoks valmistati vastavalt raviainet sisaldavad lahused või nanosuspensioonid. Selgitati, et valmistatud raviainelahuste viskoossus ja pindpinevus olid olulised parameetrid prinditavuse hindamisel. Prinditud ravimvormides kasutati kandesubstraatidena esmakordselt ka elektrospinnimise teel valmistatud želatiinipõhiseid fiibermatte.

Tahkete ravimvormide valmistamisel prinditi erinevad raviained biolagunevatele kandesubstraatidele. Raviainete füsikokeemilised omadused, printimislahuste koostis ja substraatide imamisvõime mõjutasid prinditud raviainete tahke aine vormi. Samas ei täheldatud fleksograafiliselt valmistatud nano-osakestega süsteemides raviainete tahke vormi muutusi.

Kontaktivaba tindiprintimine oli võrreldes fleksograafilise trükimeetodiga raviaine annustamisel täpsem. Tindiprintimisel võimaldas printimisresolutsiooni ja prinditava pindala süstemaatiline kohandamine reguleerida raviaine annust.

Nõrgendatud täieliku sisepeegelduse Fourier' teisendusega infrapunaspektroskoopia ja mitmemõõtmise andmeanalüüsi abil sai hinnata prinditud raviainete kvantitatiivset sisaldust proovi kahjustamata. Tulemused viitasid spektroskoopiliste meetodite mitmetele kasutamisvõimalustele prinditud ravimvormide kvaliteedikontrollis.

Raviaine *in vitro* vabanemiskiirus tahkest nano-osakestega süsteemist paranes tänu osakeste ruumilisele jaotumisele, mis takistas nano-osakeste kuhjumist substraadi pinnal. Raviaine vabanemisprofiil mittepoorsele pinnale prinditud süsteemist oli võrdväärne algse nanosuspensiooniga. Samas raviaine inkorporeerumine biolaguneva kandematerjali maatriksisse aeglustas raviaine vabanemist.

Kahe erineva tehnoloogia kasutamise abil oli võimalik valmistada kombinatsioon-ravimkandursüsteem, kus raviainete vabanemine oli üksteisest sõltumatu. Valmistatud mudelsüsteem sisaldas LH, mis oli prinditud amorfset PRX sisaldavatele elektrospinnitud fiibermattidele. Seega saab luua kombinatsioon-ravimkandursüsteeme, kasutades raviainet sisaldavaid substraate.

9. Acknowledgments

The research work presented in this thesis was carried out at the Pharmaceutical Sciences Laboratory, Faculty of Science and Engineering, Åbo Akademi University and at the Institute of Pharmacy, Faculty of Medicine, the University of Tartu, during the years 2012–2017.

The research was supported by Tekes, the Academy of Finland, NordForsk, the institutional research funding IUT-34-18 of the Estonian Ministry of Education and Research, the Estonian Research Council grant PUT1088 and the Estonian Science Foundation grant ETF7980. My work was also financed by Andreas ja Elmerice Traks scholarship (the University of Tartu Foundation) and personal grants from the national scholarship program Kristjan Jaak (the Archimedes Foundation and the Estonian Ministry of Education and Research), the Finnish Cultural Foundation's Central Fund and Åbo Akademi University.

I would like to express my deepest gratitude and respect to my supervisors. First and foremost, I am very thankful to PhD Karin Kogermann, Professor Jyrki Heinämäki and Professor Niklas Sandler for their endless guidance and scientific advice throughout the years. I am especially grateful to PhD Karin Kogermann for her positive attitude and constant motivational support that has always accompanied my research work, already from the time of my Master's studies. I am also sincerely thankful to PhD Natalja Genina for her support and guidance when I started working in Åbo in 2012, and to PhD Ruzica Kolakovic for her enthusiasm and help during her post-doctoral research work in 2013.

I am honored to have Professor Julijana Kristl from the University of Ljubljana, Slovenia and Professor Bente Steffansen from the University of Southern Denmark, Denmark as reviewers of this thesis.

I would like to acknowledge all the co-authors and co-workers from Åbo Akademi University, the University of Tartu, the University of Turku and the University of Helsinki for their substantial help and contribution in the presented research work.

I am thankful to all my friends, colleagues, and personnel at the Pharmaceutical Sciences Laboratory, Åbo Akademi University and at the Institute of Pharmacy, the University of Tartu for creating a positive work atmosphere and for their helpful advice and encouragement over the years.

Last but not least, I am grateful to my family and friends for their patience and unconditional support throughout my studies.

Åbo, 2017
Mirja Palo

10. References

Aaltonen, J., Heinänen, P., Peltonen, L., Korterjärvi, H., Tanninen, V. P., Christiansen, L., Hirvonen, J., Yliruusi, J. and Rantanen, J. (2006). In Situ measurement of solvent-mediated phase transformations during dissolution testing. *Journal of Pharmaceutical Sciences*, *95* (12), 2730–2737.

Aaltonen, J., Gordon, K. C., Strachan, C. J. and Rades, T. (2008). Perspectives in the use of spectroscopy to characterise pharmaceutical solids. *International Journal of Pharmaceutics*, *364*, 59–169.

Aaltonen, J., Allesø, M., Mirza, S., Koradia, V., Gordon, K. C. and Rantanen, J. (2009). Solid form screening – A review. *European Journal of Pharmaceutics and Biopharmaceutics*, *71*, 23–37.

Adamo, A., Beingessner, R. L., Behnam, M., Chen, J., Jamison, T. F., Jensen, K. F., Monbaliu, J.-C. M., Myerson, A. S., Revalor, E. M., Snead, D. R., Stelzer, T., Weeranoppanant, N., Wong, S. Y. and Zhang, P. (2016). On-demand continuous-flow production of pharmaceuticals in a compact, reconfigurable system. *Science*, *352* (6281), 61–67.

Airaksinen, S., Karjalainen, M., Kivikero, N., Westermarck, S., Shevchenko, A., Rantanen, J. and Yliruusi, J. (2005). Excipient selection can significantly affect solid-state phase transformation in formulation during wet granulation. *AAPS PharmSciTech*, *6* (2), 311–322.

Agarwal, S., Wendorff, J. H. and Greiner, A. (2008). Use of electrospinning technique for biomedical applications. *Polymer*, *49* (26), 5603–5621.

Aguiar, A., Krc, J., Jr., Kinkel, A. W. and Samyn, J. C. (1967). Effect of polymorphism on the absorption of chloramphenicol from chloramphenicol palmitate. *Journal of Pharmaceutical Sciences*, *56* (7), 847–853.

Alhnan, M. A., Okwuosa, T. C., Sadia, M., Wan, K.-W., Ahmed, W. and Arafat, B. (2016). Emergence of 3D printed dosage forms: opportunities and challenges. *Pharmaceutical Research*, *33*, 1817–1832.

Ali, H. S. M., York, P., Ali, A. M. A. and Blagden, N. (2011). Hydrocortisone nanosuspensions for ophthalmic delivery: A comparative study between microfluidic nanoprecipitation and wet milling. *Journal of Controlled Release*, *149*, 175–181.

Alomari, M., Mohamed, F. H., Basit, A. W. and Gaisford, S. (2015). Personalised dosing: Printing a dose of one's own medicine. *International Journal of Pharmaceutics*, *494* (2), 568–577.

Amidon, G. L., Lennernäs, H., Shah, V. P. and Crison, J.R. (1995). A theoretical basis for a biopharmaceutic drug classification: the correlation of *in vitro* drug product dissolution and in vivo bioavailability. *Pharmaceutical Research*, *12* (3), 413–420.

Anaya, J.-M., Duarte-Rey, C., Sarmiento-Monroy, J. C., Bardey, D., Castiblanco, J. and Rojas-Villarraga, A. (2016). Personalized medicine. Closing the gap between knowledge and clinical practice. *Autoimmunity Reviews*, *15*, 833–842.

Aprecia (2014). Zipdose® technology. Available from: https://aprecia.com/zipdose-platform/zipdose-technology.php (28.03.2017)

Arrabito, G. and Pignataro, B. (2010). Inkjet printing methodologies for drug screening. *Analytical Chemistry, 82*, 3104–3107.

Auer, M. E., Griesser, U. J. and Sawatzki, J. (2003). Qualitative and quantitative study of polymorphic forms in drug formulations by near infrared FT-Raman spectroscopy. *Journal of Molecular Structure*, *661–662*, 307–317.

Bagmar Ujwala, R., Redasani, V. K. and Kothawade Sachin, N. (2013). Preparation and in-vitro evaluation of loperamide hydrochloride spherical crystals by emulsion solvent diffusion technique. *International Journal of Pharmacy and Pharmaceutical Sciences*, *5* (2), 409–413.

Barnes, H. A., Hutton, J. F. and Walters FRS, K. (Eds.) (1989). *An introduction to rheology*. Amsterdam, the Neatherlands; Elsevier Science Publishers B.V.

Beaver, N., Koch, G., Konski, A. and Waltz, J. (2016). Personalized medicine: A new paradigm. *Association of Corporate Counsel*. Available from: http://www.acc.com/legalresources/quickcounsel/personalized-medicine-a-new-paradigm.cfm (28.03.2017)

Bhardwaj, N. and Kundu, S. C. (2010). Electrospinning: A fascinating fiber fabrication technique. *Biotechnology Advances*, *28*, 325–347.

Boehm, R. D., Miller, P. R., Daniels, J., Stafslien, S. and Narayan, R. J. (2014). Inkjet printing for pharmaceutical applications. *Materials Today*, *17* (5), 247–252.

Boateng, J. S., Stevens, H. N. E., Eccleston, G. M., Auffret, A. D., Humphrey M. J. and Matthews, K. H. (2009). Development and mechanical characterization of solvent-cast polymeric films as potential drug delivery systems to mucosal surfaces. *Drug Development and Industrial Pharmacy*, *35* (8), 986–996.

Borchers, K., Schönhaar, V., Hirth, T., Tovar, G. E. M. and Weber, A. (2011). Ink formulation for inkjet printing of streptavidin and streptavidin functionalized nanoparticles. *Journal of Dispersion Science and Technology, 32* (12), 1759–1764.

Boyer, C., Bregere, B., Crouchet, S., Gaudin, K. and Dubost, J. P. (2006). Direct determination of niflumic acid in a pharmaceutical gel by ATR/FTIR spectroscopy and PLS calibration. *Journal of Pharmaceutical and Biomedical Analysis*, *40* (2), 433–437.

Breitkreutz, J. and Boos, J. (2007). Paediatric and geriatric drug delivery. *Expert Opinion on Drug Delivery*, *4* (1), 37–45.

Bruni, G., Maietta, M., Maggi, L., Mustarelli, P., Ferrara, C., Berbenni, V., Freccero, M., Scotti, F., Milanese, C., Girella, A. and Marini, A. (2013). An experimental and theoretical investigation of loperamide hydrochloride-glutaric acid cocrystals. *The Journal of Physical Chemistry B*, *117* (27), 8113–8121.

Buanz, A. B. M., Saunders, M. H., Basit, A. W., and Gaisford, S. (2011). Preparation of personalized-dose salbutamol sulphate oral films with thermal ink-jet printing. *Pharmaceutical Research*, *28*, 2386–2392.

Buanz, A. B. M.; Telford, R., Scowen, I. J. and Gaisford, S. (2013). Rapid preparation of pharmaceutical co-crystals with thermal ink-jet printing. *CrystEngComm*, *15,* 1031–1035.

Buanz, A. B. M., Belaunde, C. C., Soutari, N., Tuleu, C. Gul, M. O. and Gaisford, S. (2015). Ink-jet printing versus solvent casting to prepare oral films: Effect on mechanical properties and physical stability. *International Journal of Pharmaceutics*, *494*, 611–618.

Byrn, S. R., Pfeiffer, R. R., Stephenson, G., Grant, D. J. W. and Gleason, W. B. (1994). Solid-state Pharmaceutical Chemistry. *Chemistry of Materials*, *6* (8), 1148–1158.

Calvert, P. (2001). Inkjet printing for materials and devices. *Chemistry of Materials*, *13*, 3299–3305.

Campbell Roberts, S. N., Williams, A. C., Grimsey, I. M. and Booth, S. W. (2002). Quantitative analysis of mannitol polymorphs. FT-Raman spectroscopy. *Journal of Pharmaceutical and Biomedical Analysis*, *28*, 1135–1147.

Chan, K. L. A. and Kazarian, S. G. (2005). Fourier transform infrared imaging for high-throughput analysis of pharmaceutical formulations. *Journal of Combinatorial Science*, *7* (2), 185–189.

Chen, X., Bates, S. and Morris, K. R. (2001). Quantifying amorphous content of lactose using parallel beam X-ray powder diffraction and whole pattern fitting. *Journal of Pharmaceutical and Biomedical Analysis*, *26*, 63–72.

Cheow, W. S., Kiew, T. Y. and Hadinoto, K. (2015). Combining inkjet printing and amorphous nanonization to prepare personalized dosage forms of poorly-soluble drugs. *European Journal of Pharmaceutics and Biopharmaceutics*, *96*, 314–321.

Chieng, N., Rades, T. and Aaltonen, J. (2011). An overview of recent studies on the analysis of pharmaceutical polymorphs. *Journal of Pharmaceutical and Biomedical Analysis*, *55*, 618–644.

Christy, A. A. and Egeberg, P. K. (2006). Quantitative determination of saturated and unsaturated fatty acids in edible oils by infrared spectroscopy and chemometrics. *Chemometrics and Intelligent Laboratory Systems*, *82*, 130–136.

Chung, N., Lee, M. K. and Lee, J. (2012). Mechanism of freeze-drying drug nanosuspensions. *International Journal of Pharmaceutics*, *437* (1–2), 42–50.

Cilurzo, F., Minghetti, P., Casiraghi, A., Tosi, L., Pagani, S. and Montanari, L. (2005). Polymethacrylates as crystallization inhibitors in monolayer transdermal patches containing ibuprofen. *European Journal of Pharmaceutics and Biopharmaceutics*, *60*, 61–66.

Cohen, J. S. (1999). Ways to minimize adverse drug reactions. *Postgraduate Medicine*, *106* (3), 163–172.

Collins, F. S. and Varmus, H. (2015). A new initiative on precision medicine. *The New England Journal of Medicine*, *372*, 793–795.

Derby, B. (2008). Bioprinting: Inkjet printing proteins and hybrid cell-containing materials and structures. *Journal of Materials Chemistry*, *18*, 5717–5721.

Derby, B. (2010). Inkjet printing of functional and structural materials: Fluid property requirements, feature stability, and resolution. *Annual Review of Materials Research*, *40*, 395–414.

Daly, R., Harrington, T. S., Martin, G. D. and Hutchings, I. M. (2015). Inkjet printing for pharmaceutics – A review of research and manufacturing. *International Journal of Pharmaceutics*, *494* (2), 554–567.

Davies, C., Baird, L., Jacobson, M. and Tabibkhoei, F. (Eds.) (2015). *3D printing of medical devices: when a novel technology meets traditional legal principles*. Reedsmith. Available from: https://www.reedsmith.com/3D-Printing-of-Medical-Devices--When-a-Novel-Technology-Meets-Traditional-Legal-Principles-09-09-2015/ (28.03.2017)

De Gans, B.-J., Duineveld, P. C. and Schubert, U. S. (2004). Inkjet printing of polymers: State of the art and future developments. *Advanced Materials*, *16* (3), 203–213.

Di Prima, M., Coburn, J., Hwang, D., Kelly, J., Khairuzzaman, A. and Ricles, L. (2016). Additively manufactured medical products – the FDA perspective. *3D Printing in Medicine*, *2*, 1–6.

Di Risio, S. and Yan, N. (2007). Piezoelectric ink-jet printing of horseradish peroxidase: Effect of ink viscosity modifiers on activity. *Macromolecular Rapid Communications*, *28*, 1934–1940.

Dixit, R. P. and Puthli, S.P. (2009). Oral strip technology: Overview and future potential. Journal of Controlled Release, 139, 94–107.

Dong, H., Carr, W. W. and Morris, J. F. (2006). Visualization of drop-on-demand inkjet: Drop formation and deposition. *Review of Scientific Instruments*, *77*, 085101.

Drues, M. (2013). The case of the New England Compounding Center. *Healthcare packaging*. Available from: https://www.healthcarepackaging.com/case-new-england-compounding-center (28.03.2017)

Elele, E., Shen, Y., Susarla, R. Khusid, B., Keyvan, G. and Michniak-Kohn, B. (2012). Electrodeless electrohydrodynamic drop-on-demand encapsulation of drugs into porous polymer films for fabrication of personalized dosage units. *Journal of Pharmaceutical Sciences*, *101* (7), 2523–2533.

Elliott, D. E., Davis, F. J., Mitchell, G. R. and Olley, R. H. (2009). Structure development in electrospun fibres of gelatin. *Journal of Physics: Conference Series*, *183* (1), 012021.

Essel, J. T., Ihnen, A. C. and Carter, J. D. (2014). Production of naproxen nanoparticle colloidal suspensions for inkjet printing applications. *Industrial & Engineering Chemistry Research*, *53*, 2726–2731.

Eriksson, L., Johansson, E., Kettaneh-Wold, N. and S. Wold (2001). *Multi- and megavariate data analysis. Principles and Applications*. Umeå, Sweden: Umetrics AB.

Etxabide, A., Uranga, J., Guerrero, P. and de la Caba, K. (2015). Improvement of barrier properties of fish gelatin films promoted by gelatin glycation with lactose at high temperatures. *LWT – Food Science and Technology*, *63*, 315–321.

European Medicines Agency (2013). Guideline on pharmaceutical development of medicines for paediatric use. *EMA/CHMP/QWP/805880/2012 Rev. 2*, 1–24.

European Medicines Agency (2016). ICH guideline Q3C (R6) on impurities: guideline for residual solvents. *EMA/CHMP/ICH/82260/2006*, 1–35.

European Pharmacopoeia (2016a). Oromucosal preparations. In *European Pharmacopoeia Online 8.0*, 793–796. Strasbourg: Council of Europe.

European Pharmacopoeia (2016b). Caffeine. In *European Pharmacopoeia Online 8.0*, 1718–1719. Strasbourg: Council of Europe.

European Pharmacopoeia (2016c). Lidocaine hydrochloride. In *European Pharmacopoeia Online 8.0,* 2621–2622. Strasbourg: Council of Europe.

European Pharmacopoeia (2016d). Loperamide hydrochloride. In *European Pharmacopoeia Online 8.0*, 2631–2633. Strasbourg: Council of Europe.

European Pharmacopoeia (2016e). Piroxicam. In *European Pharmacopoeia Online 8.0*, 3048–3049. Strasbourg: Council of Europe.

Fahrenfort, J. (1961). Attenuated total reflection: a new principle for the production of useful infra-red reflection spectra of organic compounds. *Spectrochimica Acta*, *17* (7), 698–709.

Farooq, A., Yar, M., Khan, A. S., Shahzadi, L., Siddiqi, S. A., Mahmood, N., Rauf, A., Qureshi, Z.-A., Manzoor, F., Chaudhry, A. A. and ur Rehman, I. (2015). Synthesis of piroxicam loaded novel electrospun biodegradable nanocomposite scaffolds for periodontal regeneration. *Materials Science and Engineering: C*, *56*, 104–113.

Figueroa, I. D. and Ruiz, O. (2005). System and a method for producing layered oral dosage forms. US patent 7727576.

Figueroa, C. E. and Bose, S. (2013). Spray granulation: Importance of process parameters on *in vitro* and in vivo behavior of dried nanosuspensions. *European Journal of Pharmaceutics and Biopharmaceutics*, *85* (3, Part B), 1046–1055.

Food and Drug Administration (2014). Transcript of FDA Public Workshop: Additive Manufacturing of Medical Devices: An interactive discussion on medical considerations of 3D printing. Available from: http://www.fda.gov/downloads/MedicalDevices/NewsEvents/WorkshopsConferences/UCM425399.pdf (28.03.2017)

Fromm, J. E. (1984). Numerical calculation of the fluid dynamics of drop-on-demand jets. *IBM Journal of Research and Development*, 28 (3), 322–333.

Genina, N., Fors, D., Vakili, H., Ihalainen, P., Pohjala, L., Ehlers, H., Kassamakov, I., Haeggström, E., Vuorela, P., Peltonen, L. and Sandler, N. (2012). Tailoring controlled-release oral dosage forms by combining inkjet and flexographic printing techniques. *European Journal of Pharmaceutical Sciences*, *47* (3), 615–623.

Genina, N., Janßen, E. M., Breitenbach, A., Breitkreutz, J. and Sandler, N. (2013). Evaluation of different substrates for inkjet printing of rasagiline mesylate. *European Journal of Pharmaceutics and Biopharmaceutics*, *85*, 1075–1083.

GlaxoSmithKline. (n.d.). Liquid Dispensing Technology (LDT) [Leaflet]. Available from: https://www.gsk.com/media/2758/liquid-dispensing-technology-leaflet.pdf (15.05.2017)

Goodall, S., Chew, N., Chan, K., Auriac, D. and Waters, M. J. (2002). Aerosolization of protein solutions using thermal inkjet technology. *Journal of Aerosol Medicine*, *15* (3), 351–357.

Goole, J. and Amighi, K. (2016). 3D printing in pharmaceutics: A new tool for designing customized drug delivery systems. *International Journal of Pharmaceutics*, *499* (1–2), 376–394.

Greiner, A. and Wendorff, J. H. (2007). Electrospinning: A fascinating method for the preparation of ultrathin fibers. *Angewandte Chemie International Edition*, *46*, 5670–5703.

Hajjou, M., Qi, Y., Bradby, S., Bempong, D. and Lukulay, P. (2013). Assessment of the performance of a handheld Raman device for potential use as a screening tool in evaluating medicines quality. *Journal of Pharmaceutical and Biomedical Analysis*, *74*, 47–55.

Haleblian, J. and McCrone, W. (1969). Pharmaceutical applications of polymorphism. *Journal of*

Pharmaceutical Sciences, *58* (8), 911–929.

Hamburg, M. A. and Collins, F. S. (2010). The path to personalized medicine. *The New England Journal of Medicine, 363* (4), 301–304.

Hammes, F., Hille, T. and Kissel, T. (2014). Reflectance infrared spectroscopy for in-line monitoring of nicotine during a coating process for an oral thin film. *Journal of Pharmaceutical and Biomedical Analysis*, *89*, 176–182.

Hancock, B. C. and Zografi, G. (1997). Characteristics and significance of the amorphous state in pharmaceutical systems. *Journal of Pharmceutical Sciences*, *86* (1), 1–12.

Hancock, B. C. and Parks, M. (2000). What is the true solubility advantage for amorphous pharmaceuticals? *Pharmaceutical Research*, *17* (4), 397–404.

Heinz, A., Savolainen, M., Rades, T. and Strachan, C. J. (2007). Quantifying ternary mixtures of different solid-state forms of indomethacin by Raman and near-infrared spectroscopy. *European Journal of Pharmaceutical Sciences*, *32*, 182–192.

Helmy, R., Zhou, G. X., Chen, Y. W., Crocker, L., Wang, T., Wenslow, R. M. and Vailaya, A. (2003). Characterization and quantitation of aprepitant drug substance polymorphs by attenuated total reflectance Fourier transform infrared spectroscopy. *Analyical Chemistry*, *75* (3), 605–611.

Hirshfield, L., Giridhar, A., Taylor, L. S., Harris, M. T. and Reklaitis, G. V. (2014). Dropwise additive manufacturing of pharmaceutical products for solvent-based dosage forms. *Journal of Pharmaceutical Sciences*, *103*, 496–506.

Hoffmann, E. M, Breitenbach, A. and Breitkreutz, J. (2011). Advances in orodispersible films for drug delivery. *Expert Opinion on Drug Delivery*, *8* (3), 299–316.

Holman, R. K., Uhland, S. A., Cima, M. J. and Sachs, E. (2002). Surface adsorption effects in the inkjet printing of an aqueous polymer solution on a porous oxide ceramic substrate. *Journal of Colloid and Interface Science*, *247*, 266–274.

Horsnell, D. A., Tomlin, M. B., Lecheheb, A. Prime, O. J., Fox, M. J. and Bates, C. M. (2009). Solenoid valve for a drop on demand ink jet printer. US Patent 7571986.

Hsu, H.-Y., Toth, S., Simpson, G. J. Taylor, L. S. and Harris, M. T. (2012). Effect of substrates on naproxen-polyvinylpyrrolidone solid dispersions formed via the drop printing technique. *Journal of Pharmaceutical Sciences*, *102* (2), 638–648.

Hu, X., Liu, S., Zhou, G., Huang, Y., Xie, Z. and Jing, X. (2014). Electrospinning of polymeric nanofibers for drug delivery applications. *Journal of Controlled Release*, *185*, 12–21.

Ihalainen, P., Majumdar, H., Viitala, T., Törngren, B., Närjeoja, T., Määttänen, A., Sarfraz, J., Härmä, H., Yliperttula, M., Österbacka, R. and Peltonen, J. (2013). Application of paper-supported printed gold electrodes for impedimetric immunosensor development. *Biosensors*, *3*, 1–17.

Ihalainen, P., Määttänen, A. and Sandler, N. (2015). Printing technologies for biomolecule and cell-based applications. *International Journal of Pharmaceutics*, *494* (2), 585–592.

International Conference on Harmonisation (1999a). ICH harmonised tripartite guideline. Q6A specifications: test procedures and acceptance criteria for new drug substances and new drug products: chemical substances. Available from: https://www.ich.org/fileadmin/Public_Web_Site/ICH_Products/Guidelines/Quality/Q6A/Step4/Q6Astep4.pdf (28.03.2017)

International Conference on Harmonisation (1999b). Decision tree #4: Investigating the need to set acceptance criteria for polymorphism in drug substances and drug products. Available from: https://www.ich.org/fileadmin/Public_Web_Site/ICH_Products/Guidelines/Quality/Q6A/Step4/Decision_Trees.pdf (28.03.2017)

International Conference on Harmonisation (2008). ICH harmonised tripartite guideline. Q10 Pharmaceutical Quality System. Available from: https://www.ich.org/fileadmin/Public_Web_Site/ICH_Products/Guidelines/Quality/Q10/Step4/Q10_Guideline.pdf (28.03.2017)

Jacobson, M. (2015). The regulatory and legal implications of 3D printing. *Medical design technology*. Available from: https://www.mdtmag.com/blog/2015/09/regulatory-and-legal-implications-3d-printing (28.03.2017)

Jang, D., Kim, D. and Moon, J. (2009). Influence of fluid physical properties on ink-jet printability. *Langmuir*, *25* (5), 2629–2635.

Janßen, E. M., Schliephacke, R., Breitenbach, A. and Breitkreutz, J. (2013). Drug-printing by flexographic printing technology – A new manufacturing process for orodispersible films. *International Journal of Pharmaceutics*, *441* (1–2), 818–825.

Jenkins, R. and Snyder, R. L. (1996). *Introduction to X-ray Powder Diffractometry*. New York, USA: Wiley.

Jinno, J., Oh, D.-M., Crison, J. R. and Amidon, G. L. (2000). Dissolution of ionizable water-insoluble drugs: The combined effect of pH and surfactant. *Journal of Pharmaceutical Sciences*, *89*, 268-274.

Jørgensen, A., Rantanen, J., Karjalainen, M., Khriachtchev, L., Räsänen, E. and Yliruusi, J. (2002). Hydrate formation during wet granulation studied by spectroscopic methods and multivariate analysis. *Pharmaceutical Research*, *19* (9), 1285–1291.

Kalinkova, G.N. (1999). Infrared spectroscopy in pharmacy. *Vibrational Spectroscopy*, *19* (2), 307–320.

Kaneniwa, N., Otsuka, M. and Hayashi, T. (1984). Physicochemical characterization of indomethacin polymorphs and the transformation Kinetics in ethanol. *Chemical and Pharmaceutical Bulletin*, *33* (8), 3447–3455.

Katstra, W. E., Palazzolo, R. D., Rowe, C. W., Giritlioglu, B., Teunga, P. and Cima, M. J. (2000). Oral dosage forms fabricated by Three Dimensional Printing ™. *Journal of Controlled Release*, *66*, 1–9.

Kayaert, P. and Van den Mooter, G. (2012). Is the amorphous fraction of a dried nanosuspension caused by milling or by drying? A case study with naproxen and cinnarizine. *European Journal of Pharmaceutics and Biopharmaceutics*, *81* (3), 650–656.

Kesimli, B., Topacli, A. and Topacli, C. (2003). An interaction of caffeine and sulfamethoxazole: studied by IR spectroscopy and PM3 method. *Journal of Molecular Structure*, *645* (2), 199–204.

Koehler, H. M. and Hefferren, J. J. (1964). Mineral acid salts of lidocaine. *Journal of Pharmaceutical Sciences*, *53* (9), 1126–1127.

Kogermann, K., Aaltonen, J., Strachan, C. J., Pöllänen, K., Heinämäki, J., Yliruusi, J. and Rantanen, J. (2008). Establishing quantitative in-line analysis of multiple solid-state transformations during dehydration. *Journal of Pharmaceutical Sciences*, *97* (11), 4983–4999.

Kogermann, K., Veski, P., Rantanen, J. and Naelapää, K. (2011). X-ray powder diffractometry in combination with principal component analysis – A tool for monitoring solid state changes. *European Journal of Pharmaceutical Sciences*, *43*, 278–289.

Kolakovic, R., Viitala, T., Ihalainen, P., Genina, N., Peltonen, J. and Sandler, N. (2013). Printing Technologies in Fabrication of Drug Delivery Systems. *Expert Opinion on Drug Delivery*, *10* (12), 1711–1723.

Kozlov, P. V. and Burdygina, G. I. (1983). The structure and properties of solid gelatin and the principles of their modification. *Polymer*, *24*, 651–666.

Krampe, R., Visser, J. C., Frijlink, H. W., Breitkreutz, J., Woerdenbag H. J. and Preis, M. (2015). Oromucosal film preparations: Points to consider for patient centricity and manufacturing processes. *Expert Opinion on Drug Delivery*, *13* (4), 493–506.

Le, H. P. (1998). Progress and trends in ink-jet printing technology. *Journal of Imaging Science and Technology*, *42* (1), 49–62.

Lee, J. (2003). Drug nano- and microparticles processed into solid dosage forms: Physical properties. *Journal of Pharmaceutical Sciences*, *92* (10), 2057–2068.

Lee, B. K., Yun, Y. He., Choi, J. S., Choi, Y. C., Kim, J. D. and Cho, Y. W. (2012). Fabrication of drug-loaded polymer microparticles with arbitrary geometries using a piezoelectric inkjet printing system. *International Journal of Pharmaceutics*, *427*, 305–310.

Lemmo, A. V., Rose, D. J. and Tisone, T. C. (1998). Inkjet dispensing technology: Applications in drug discovery. *Current Opinion in Biotechnology*, *9*, 615–617.

Lesko, L. J. and Woodcock, J. (2002). Pharmacogenomic-guided drug development: Regulatory perspective. *The Pharmacogenomics Journal*, *2*, 20–24.

Leuner, C. and Dressman, J. (2000). Improving drug solubility for oral delivery using solid dispersions. *European Journal of Pharmaceutics and Biopharmaceutics*, *50* (1), 47–60.

Liang, D., Hsiao, B. S. and Chu, B. (2007). Functional Electrospun Nanofibrous Scaffolds for Biomedical Applications. *Advanced Drug Delivery Reviews*, *59* (14), 1392–1412.

Lim, T. Y., Poole, R. L. and Pageler, N. M. (2014). Propylene glycol toxicity in children. *Journal of Pediatric Pharmacology and Therapeutics*, *19* (4), 277–282.

Liu, P., Rong, X., Laru, J., van Veen, B., Kiesvaara, J., Hirvonen, J., Laaksonen, T. and Peltonen, L. (2011). Nanosuspensions of poorly soluble drugs: Preparation and development by wet milling. *International Journal of Pharmaceutics*, *411*, 215–222.

Liu, Y.-F., Tsai, M.-H., Pai, Y.-F. and Hwang, W.-S. (2013). Control of droplet formation by operating waveform for inks with various viscosities in piezoelectric inkjet printing. *Applied Physics A: Materials Science & Processing*, *111* (2), 509–516.

Lust, A., Strachan, C. J., Veski, P., Aaltonen, J., Heinämäki, J., Yliruusi, J. and Kogermann, K. (2015). Amorphous solid dispersions of piroxicam and Soluplus®: Qualitative and quantitative analysis of piroxicam recrystallization during storage. *International Journal of Pharmaceutics*, *486*, 306–314.

Malamatari, M., Somavarapu, S., Taylor, K. M. G. and Buckton, G. (2016). Solidification of nanosuspensions for the production of solid oral dosage forms and inhalable dry powders. *Expert Opinion on Drug Delivery*, *13* (3), 435–450.

March, R., Cheeseman, K. and Doherty, M. (2001). Pharmacogenetics – legal, ethical and regulatory considerations. *Pharmacogenomics*, *2* (4), 317–327.

Marques, M. R. C., Loebenberg, R. and Almukainzi, M. (2011). Simulated biological fluids with possible application in dissolution testing. *Dissolution Technologies*, 15–28.

Mazurek, S. and Szostak, R. (2011). Comparison of infrared attenuated total reflection and Raman spectroscopy in the quantitative analysis of diclofenac sodium in tablets, *Vibrational Spectroscopy*, *57* (1), 157–162.

Mazurek, S. and Szostak, R. (2012). Quantitative analysis of thiamine hydrochloride in tablets e comparison of infrared attenuated total reflection, diffuse reflectance infrared and Raman spectroscopy. *Vibrational Spectroscopy*, *62*, 10–16.

McKinley, G. H. and Renardy, M. (2011). Wolfgang von Ohnesorge. *Physics of Fluids*, *23*, 127101.

Melendez, P.A., Kane, K. M., Ashvar, C. S., Albrecht, M. and Smith, P. A. (2008). Thermal inkjet application in the preparation of oral dosage forms: Dispensing of prednisolone solutions and polymorphic characterization by solid-state spectroscopic techniques. *Journal of Pharmaceutical Sciences*, *97* (7), 2619–2636.

Merisko-Liversidge, E. M. and Liversidge, G. G. (2008). Drug nanoparticles: Formulating poorly water-soluble compounds. *Toxicologic Pathology*, *36* (1), 43–48.

Mindru, T. B., Mindru, I. B., Malutan, T. and Tura, V. (2007). Electrospinning of high concentration gelatin solutions. *Journal of Optoelectronics and Advanced Materials*, *9* (11), 3633–3638.

Montenegro-Nicolini, M. and Morales, J. O. (2016a). Overview and future potential of buccal mucoadhesive films as drug delivery systems for biologics. *AAPS PharmSciTech*, *18*(1), 3–14.

Montenegro-Nicolini, M., Miranda, V. and Morales, J. O. (2016b). Inkjet printing of proteins: An experimental approach. *The AAPS Journal*, *19* (1), 234–243.

Morales, J. O. and McConville, J. T. (2011). Manufacture and characterization of mucoadhesive buccal films. *European Journal of Pharmaceutics and Biopharmaceutics*, *77*, 187–199.

Määttänen, A., Ihalainen, P., Bollström, R., Toivakka, M. and Peltonen, J. (2010). Wetting and print quality study of an inkjet-printed poly(3-hexylthiophene) on pigment coated papers. *Colloids and Surfaces A: Physicochemical and Engineering Aspects*, *367*, 76–84.

Müller, R.H. and Peters, K. (1998). Nanosuspensions for the formulation of poorly soluble drugs: I. preparation by a size-reduction technique. *International Journal of Pharmaceutics*, *160* (2), 229–237.

Naelapää, K., Boetker, J. P., Veski, P., Rantanen, J., Rades, T. and Kogermann, K. (2012). Polymorphic form of piroxicam influences the performance of amorphous material prepared by ball-milling. *International Journal of Pharmaceutics*, *429*, 69–77.

Neves, L. S., Rodrigues, M. T., Reis, R. L. and Gomes, M. E. (2016). Current approaches and future perspectives on strategies for the development of personalized tissue engineering therapies. *Expert Review of Precision Medicine and Drug Development*, *1* (1), 93–108.

Neville, G. A. and Regnier, Z. R. (1969). Hydrogen bonding in lidocaine salts. I. The NH stretching band and its dependence on the associated anion. *Canadian Journal of Chemistry*, *47*, 4229–4235.

Newman, A. W. and Byrn, S. R. (2003). Solid-state analysis of the active pharmaceutical ingredient in drug products. *Drug Discovery Today*, *8* (19), 898–905.

Nganga, S., Moritz, N., Kolakovic, R., Jakobsson, K., Nyman, J. O., Borgogna, M., Travan, A., Crosera, M., Donati, I., Vallittu, P. K. and Sandler, N. (2014). Inkjet printing of Chitlac-nanosilver – A method to create functional coatings for non-metallic bone implants. *Biofabrication*, *6* (4), 041001.

Nguyen, T. H. and Lee, B.-T. (2010). Fabrication and characterization of cross-linked gelatin electro-spun nano-fibers. *Journal of Biomedical Science and Engineering*, *3*, 1117–1124.

Nolasco, M. M., Amado, A. M. and Ribeiro-Claro, P. J. (2006). Computationally-assisted approach to the vibrational spectra of molecular crystals: study of hydrogenbonding and pseudo-polymorphism. *ChemPhysChem*, *7* (10), 2150–2161.

Noyes, A. A. and Whitney, W. R. (1897). The rate of solution of solid substances in their own solutions. *Journal of the American Chemical Society*, *19* (12), 930–934.

Offermann, V., Grosse, P., Feuerbacher, M. and Dittmar, G. (1995). Experimental aspects of attenuated total reflectance spectroscopy in the infrared. *Vibrational Spectroscopy*, *8* (2), 135–140.

Okamoto, T., Suzuki, T. and Yamamoto, N. (2000). Microarray fabrication with covalent attachment of DNA using Bubble Jet technology. *Nature Biotechnology*, *18*, 438–441.

Paaver, U., Lust, A., Mirza, S., Rantanen, J., Veski, P., Heinämäki, J. and Kogermann, K. (2012). Insight into the solubility and dissolution behavior of piroxicam anhydrate and monohydrate forms. *International Journal of Pharmaceutics*, *431*, 111–119.

Paaver, U., Tamm, I., Laidmäe, I., Lust, A., Kirsimäe, K., Veski, P., Kogermann, K. and Heinämäki, J. (2014). Soluplus graft copolymer: Potential novel carrier polymer in electrospinning of nanofibrous drug delivery systems for wound therapy. *BioMed Research International*, *2014*, 789765.

Paaver, U., Heinämäki, J., Laidmäe, I., Lust, A., Kozlova, J., Sillaste, E., Kirsimäe, K., Veski, P. and Kogermann, K. (2015). Electrospun nanofibers as a potential controlled-release solid dispersion system for poorly water-soluble drugs. *International Journal of Pharmaceutics*, *479*, 252–260.

Pardeike, J., Strohmeier, D. M., Schrödl, N., Voura, C., Gruber, M., Khinast, J. G. and Zimmer, A. (2011). Nanosuspensions as advanced printing ink for accurate dosing of poorly soluble drugs in personalized medicines. *International Journal of Pharmaceutics*, *420*, 93–100.

Park, S.-N., Park, J.-C., Kim, H. O., Song, M. J. and Suh, H. (2002). Characterization of porous collagen/hyaluronic acid scaffold modified by 1-ethyl-3-(3-dimethylaminopropyl)carbodiimide crosslinking. *Biomaterials*, *23*, 1205–1212.

Park, J. and Moon, J. (2006). Control of colloidal particle deposit patterns within picoliter droplets ejected by ink-jet printing. *Langmuir*, *22* (8), 3506–3513.

Phadnis, N. V., Cavatur, R. K. and Suryanarayanan, R. (1997). Identification of drugs in pharmaceutical dosage forms by X-ray powder diffractometry. *Journal of Pharmaceutical and Biomedical Analysis*, *15* (7), 929–943.

Pickup, R. L., Lo, C. C. and Noonan, W. D. (2003). Cutaneous administration system. US patent 6723077.

Planchette, C., Pichler, H., Wimmer-Teubenbacher, M., Gruber, M., Gruber-Woelfler, H., Mohr, S., Tetyczka, C., Hsiao, W.-K., Paudel, A., Roblegg, E. and Khinast, J. (2016). Printing medicines as orodispersible dosage forms: Effect of substrate on the printed micro-structure. *International Journal of Pharmaceutics*, *509* (1–2), 518–527.

Pollack, S. and Coburn, J. (2015). FDA goes 3-D. *FDA Voice blog*. Available from: https://blogs.fda.gov/fdavoice/index.php/tag/osel/ (28.03.2017)

Preis, M., Knop, K. and Breitkreutz, J. (2014). Mechanical strength test for orodispersible and buccal films. *International Journal of Pharmaceutics*, *461*, 22–29.

Preis, M., Breitkreutz, J. and Sandler, N. (2015). Perspective: Concepts of printing technologies for oral film formulations. *International Journal of Pharmaceutics*, *494* (2), 578–584.

Pöllänen, K., Hakkinen, A., Reinikainen, S.-P., Rantanen, J., Karjalainen, M., Louhi-Kultanen, M. and Nyström, L. (2005). IR spectroscopy together with multivariate data analysis as a process analytical tool for in-line monitoring of crystallization process and solid-state analysis of crystalline product. *Journal of Pharmaceutical and Biomedical Analysis*, *38* (2), 275–284.

Rajalahti, T. and Kvalheim, O. M. (2011). Multivariate data analysis in pharmaceutics: a tutorial review. *International Journal of Pharmaceutical Sciences*, *417* (1–2), 280–290.

Raje, P. V. and Murmu, N. C. (2014). A review on electrohydrodynamic-inkjet printing technology. *International Journal of Emerging Technology and Advanced Engineering*, *4* (5), 174–183.

Raijada, D., Genina, N., Fors, D., Wisaeus, E., Peltonen, J., Rantanen, J. and Sandler, N. (2013). A step toward development of printable dosage forms for poorly soluble drugs. *Journal of Pharmaceutical Sciences*, *102*, 3694–3704.

Raijada, D., Genina, N., Fors, D., Wisaeus, E., Peltonen, J., Rantanen, J. and Sandler, N. (2014). Designing printable medicinal products: Solvent system and carrier-substrate screening. *Chemical Engineering & Technology*, *37*, 1291–1296.

Reidenberg, M. M. (2003). Evolving ways that drug therapy is individualized. *Clinical Pharmacology & Therapeutics*, *74* (3), 197–202.

Rodríguez-Spong, B., Price, C. P., Jayasankar, A., Matzger, A. J. and Rodríguez-Hornedo, N. (2004). General principles of pharmaceutical solid polymorphism: A supramolecular perspective. *Advanced Drug Delivery Reviews*, *56*, 241–274.

Ross, S., Scoutaris, N., Lamprou, D., Mallinson, D. and Douroumis, D. (2015). Inkjet printing of insulin microneedles for transdermal delivery. *Drug Delivery and Translational Research*, *5*, 451–461.

Sandler, N., Määttänen, A., Ihalainen, P., Kronberg, L., Meierjohann, A., Viitala, T. and Peltonen, J. (2011). Inkjet printing of drug substances and use of porous substrates – towards individualized dosing. *Journal of Pharmaceutical Sciences*, *100* (8), 3386–3395.

Sandler, N. and Preis, M. (2016). Printed drug-delivery systems for improved patient treatment. *Trends in Pharmacological Sciences*, *37* (12), 1070–1080.

Sarnes, A., Kovalainen, M., Häkkinen, M.R., Laaksonen, T., Laru, J., Kiesvaara, J., Ilkka, J., Oksala, O., Rönkkö, S., Järvinen, K., Hirvonen, J. and Peltonen, L. (2014). Nanocrystal-based per-oral itraconazole delivery: superior *in vitro* dissolution enhancement versus Sporanox® is not realized in in vivo drug absorption. *Journal of Controlled Release*, *180* (0), 109–116.

Savolainen, M., Heinz, A., Strachan, C., Gordon, K. C., Yliruusi, J., Rades, T. and Sandler, N. (2006). Screening for differences in the amorphous state of indomethacin using multivariate visualization. *European Journal of Pharmaceutical Sciences*, *30*, 113–123.

Schiffmann, J. D. and Schauer, C. L. (2008). A review: Electrospinning of biopolymer nanofibers and their applications. *Polymer Reviews*, *48* (2), 317–352.

Scoutaris, N., Alexander M. R., Gellert, P. R. and Roberts, C. J. (2011). Inkjet printing as a novel medicine formulation technique. *Journal of Controlled Release*, *156*, 179–185.

Scoutaris, N., Hook, A. L., Gellert, P. R., Roberts, C. J., Alexander, M. R. and Scurr, D. J. (2012). ToF-SIMS analysis of chemical heterogeneities in inkjet micro-array printed drug/polymer formulations. *Journal of Materials Science: Materials in Medicine*, *23* (2), 385–391.

Scoutaris, N., Ross, S. and Douroumis, D. (2016). Current trends on medical and pharmaceutical applications of inkjet printing technology. *Pharmaceutical Research*, *33* (8), 1799–1816.

Serajuddin, A. T. M. (1999). Solid dispersion of poorly water-soluble drugs: Early promises, subsequent problems, and recent breakthroughs. *Journal of Pharmaceutical Sciences*, *88* (10), 1058–1066.

Shafiee, A. and Atala, A. (2016). Printing technologies for medical applications. *Trends in Molecular Medicine*, *22* (3), 254–265.

Siemann, U. (2005). Solvent cast technology – a versatile tool for thin film production. *Progress in Colloid and Polymer Science*, 130, 1–14.

Siimon, K. Reemann, P., Põder, A., Pook, M., Kangur, T., Kingo, K., Jaks, V., Mäeorg, U. and Järvekülg, M. (2014). Effect of glucose content on thermally cross-linked fibrous gelatin scaffolds for tissue engineering. *Materials Science and Engineering C*, *42*, 538–545.

Siimon, K., Siimon, H. and Järvekülg, M. (2015). Mechanical characterization of electrospun gelatin scaffolds cross-linked by glucose. *Journal of Materials Science: Materials in Medicine*, *26* (1), 37.

Silva, F. E., Ferrao, M. F., Parisotto, G., Muller, E. I. and Flores, E. M. (2009). Simultaneous determination of sulphamethoxazole and trimethoprim in powder mixtures by attenuated total reflection-Fourier transform infrared and multivariate calibration. *Journal of Pharmaceutical and Biomedical Analysis*, *49* (3), 800–805.

Slavkova, M. and Breitkreutz, J. (2015). Orodispersible drug formulations for children and elderly. *European Journal of Pharmaceutical Sciences*, *75*, 2–9.

Sorak, D., Herberholz, L., Iwascek, S., Altinpinar, S., Pfeifer, F. and Siesler, H. W. (2012). New developments and applications of handheld Raman, mid-infrared, and near-infrared spectrometers. *Applied Spectroscopy Reviews*, *47* (2), 83–115.

Sparrow, N. (2014). FDA tackles opportunities, challenges of 3D-printed medical devices. *Plastics today*. Available from: https://www.plasticstoday.com/content/fda-tackles-opportunities-challenges-3d-printed-medical-devices/13081585320639 (28.03.2017)

Spritam (2016). Spritam® – full prescribing information. Available from: https://www.spritam.com/pdfs/spritam-full-prescribing-information.pdf (28.03.2017)

Sridhar, R., Venugopal, J. R., Sundarrajan, S., Ravichandran, R., Ramalingam, B. and Ramakrishna, S. (2011). Electrospun nanofibers for pharmaceutical and medical applications *Journal of Drug Delivery Science and Technology*, 21 (6), 451–468.

Srivastava, S. K. and Singh, V. B. (2013). Ab initio and DFT studies of the structure and vibrational spectra of anhydrous caffeine. *Spectrochimica Acta Part A: Molecular and Biomolecular Spectroscopy*, *115*, 4–50.

Taddei, P., Torreggiani, A. and Simoni, R. (2001). Influence of environment on piroxicam polymorphism: Vibrational spectroscopic study. *Biopolymers*, *62*, 68–78.

Tantishaiyakul, V., Kaewnopparat, N. and Ingkatawornwong, S. (1999). Properties of solid dispersions of piroxicam in polyvinylpyrrolidone. *International Journal of Pharmaceutics*, *181*, 143–151.

Tarcha, P. J., Verlee, D. Hui, H. W., Setesak, J., Antohe, B. Radulescu, D. and Wallace, D. (2007). The application of ink-jet technology for the coating and loading of drug-eluting stents. *Annals of Biomedical Engineering*, *35* (10), 1791–1799.

Taylor, G. (1964). Disintegration of water drops in an electric field. *Proceedings of the Royal Society of London, Series A: Mathematical, Physical and Engineering Sciences*, *280*, 383–397.

Tumuluri, S. V., Prodduturi, S., Crowley, M. M., Stodghill, S. P., McGinity, J. W. Repka, M. A. and Avery, B. A. (2004). The use of near-infrared spectroscopy for the quantitation of a drug in hot-melt extruded films. *Drug Development and Industrial Pharmacy*, *30* (5), 505–511.

Tumuluri, S. V., Kemper, M. S., Lewis, I. R., Prodduturi, S., Majumdara, S., Avery, B. A. and Repka, M. A. (2008). Off-line and on-line measurements of drug-loaded hot-melt extruded films using Raman spectroscopy. *International Journal of Pharmaceutics*, *357*, 77–84.

Uddin, M. J., Scoutaris, N., Klepetsanis, P., Chowdhry B., Prausnitz, M. R. and Douroumis, D. (2015). Inkjet printing of transdermal microneedles for the delivery of anticancer agents. *International Journal of Pharmaceutics*, *494*, 593–602.

Vakili, H., Kolakovic, R., Genina, N., Marmion, M., Salo, H., Ihalainen, P., Peltonen, J. and Sandler, N. (2015). Hyperspectral imaging in quality control of inkjet printed personalised dosage forms. *International Journal of Pharmaceutics*, *483*, 244–249.

Vakili, H., Nyman, J. O., Genina, N., Preis, M. and Sandler, N. (2016). Application of a colorimetric technique in quality control for printed pediatric orodispersible drug delivery systems containing propranolol hydrochloride. *International Journal of Pharmaceutics*, *511*, 606–618.

Van Eerdenbrugh, B., Froyen, L., Van Humbeeck, J., Martens, J. A., Augustijns, P. and Van den Mooter, G. (2008a). Drying of crystalline drug nanosuspensions – The importance of surface hydrophobicity on dissolution behavior upon redispersion. *European Journal of Pharmaceutical Sciences*, *35* (1–2), 127–135.

Van Eerdenbrugh, B., Van den Mooter, G. and Augustijns, P. (2008b). Top-down production of drug nanocrystals: Nanosuspension stabilization, miniaturization and transformation into solid products. *International Journal of Pharmaceutics*, *364* (1), 64–75.

Van Rompay, J. and Carter, J. E. (1990). Loperamide hydrochloride. In K. Florey (Ed.), *Analytical profiles of drug substances, volume 19* (pp. 341–365). San Diego, CA: Academic Press Inc..

Vippagunta, S. R., Brittain, H. G. and Grant, D. J. W. (2001). Crystalline solids. *Advanced Drug Delivery Reviews*, *48*, 3–26.

Voura, C., Schroedl, N., Gruber, M. M., Strohmeier, D., Eitzinger, B., Bauer, W., Brenn, G., Khinast, J. G.

and Zimmer, A. (2011). Printable medicines: A microdosing device for producing personalised medicines. *Pharmaceutical Technology Europe*, *23* (1), 32–36.

Vrbata, P., Berka, P., Stránská, D., Doležal, P., Musilová, M. and Cížinská, L. (2013). Electrospun drug loaded membranes for sublingual administration of sumatriptan and naproxen. *International Journal of Pharmaceutics*, *457*, 168–176.

Vrečer, F., Vrbinc, M. and Meden, A. (2003). Characterization of piroxicam crystal modifications. *International Journal of Pharmaceutics*, *256*, 3–15.

Wening, K. and Breitkreutz, J. (2011). Oral drug delivery in personalized medicine: Unmet needs and novel approaches. *International Journal of Pharmaceutics*, *404*, 1–9.

Weuts, I., Kempen, D., Decorte, A., Verreck, G., Peeters, J., Brewster, M. and Van den Mooter, G. (2004). Phase behaviour analysis of solid dispersions of loperamide and two structurally related compounds with the polymers PVP-K30 and PVP-VA64. *European Journal of Pharmaceutical Sciences*, *22* (5), 375–385.

Weuts, I., Kempen, D., Decorte, A., Verreck, G., Peeters, J., Brewster, M. and Van den Mooter, G. (2005). Physical stability of the amorphous state of loperamide and two fragment molecules in solid dispersions with the polymers PVP-K30 and PVP-VA64. *European Journal of Pharmaceutical Sciences*, *25*, 313–320.

Wickström, H., Palo, P., Rijckaert, K., Kolakovic, R., Nyman, J. O., Määttänen, A., Ihalainen, P., Peltonen, J., Genina, N., de Beer, T., Löbmann, K., Rades, T. and Sandler, N. (2015). Improvement of dissolution rate of indomethacin by inkjet printing. *European Journal of Pharmaceutical Sciences*, *75*, 91–100.

Wickström, H., Nyman, J. O., Indola, M., Sundelin, H., Kronberg, L., Preis, M., Rantanen, J. and Sandler, N. (2016). Colorimetry as quality control tool for individual inkjet-printed pediatric formulations. *AAPS PharmSciTech*, *18* (2), 293–302.

Wilson, W. C, Jr. and Boland, T. (2003). Cell and organ printing 1: Protein and cell printers. *The Anatomical Record Part A*, *272A*, 491–496.

Wold, S., Sjöström, M. and Eriksson, L. (2001). PLS-regression: A basic tool of chemometrics. *Chemometrics and Intelligent Laboratory Systems*, *58* (2), 109–130.

Woodcock, J. (2007). The prospects for "personalized medicine" in drug development and drug therapy. *Clinical Pharmacology & Therapeutics*, *81* (2), 164–169.

Wu, B. M., Borland, S. W., Giordano, R. A., Cima, L. G., Sachs, E. M. and Cima, M. J. (1996). Solid free-form fabrication of drug delivery devices. *Journal of Controlled Release*, *40*, 77–87.

Wyttenbach, N., Alsenz, J. and Grassmann, O. (2007). Miniaturized assay for solubility and residual solid screening (SORESOS) in early drug development. *Pharmaceutical Research*, *24* (5), 888–898.

Yeo, Y., Basaran, O. A. and Park, K. (2003). A new process for making reservoir-type microcapsules using inkjet technology and interfacial phase separation. *Journal of Controlled Release*, *93*, 161–173.

Yu, L. (2001). Amorphous pharmaceutical solids: Preparation, characterization and stabilization. *Advanced Drug Delivery Reviews*, *48*, 27–42.

Yun, Y. H., Kim, J. D., Lee, B. K., Yoo, B., Lee, J.-H. and Cho, Y. W. (2009). Construction of micro-patterned polymer structures by piezoelectric inkjet printing. *Polymer-Plastics Technology and Engineering*, *48* (12), 1318–1323.

Zha, Z., Teng, W., Markle, V., Dai, Z. and Wu, X. (2012). Fabrication of gelatin nanofibrous scaffolds using ethanol/phosphate buffer saline as a benign solvent. *Biopolymers*, *97* (12), 1026–1036.

Zhang, G. G. Z., Law, D., Schmitt, E. A. and Qiu, Y. (2004). Phase transformation considerations during process development and manufacture of solid oral dosage forms. *Advanced Drug Delivery Reviews*, *56*, 371–390.

Zhang, Y. Z., Venugopal, J., Huang, Z.-M., Lim, C. T. and Ramakrishna, S. (2006). Crosslinking of the electrospun gelatin nanofibers. *Polymer*, *47*, 2911–2917.

Zhang, J., Ying, Y., Pielecha-Safira, B., Bilgili, E., Ramachandran, R., Romañach, R., Davé, R. N. and Iqbal, Z. (2014). Raman spectroscopy for in-line and off-line quantification of poorly soluble drugs in strip films. *International Journal of Pharmaceutics*, *475*, 428–437.

Zhu, X., Zheng, Q., Yang, H., Cai, J., Huang, L., Duan, Y., Xu, Z. and Cen, P. (2012). Recent advances in inkjet dispensing technologies: Applications in drug discovery. *Expert Opinion on Drug Delivery*, *7* (9), 761–770.

ORIGINAL PUBLICATIONS

I

Genina, N., Fors, D., **Palo, M.**, Peltonen, J. and Sandler, N. (2013). Behavior of printable formulations of loperamide and caffeine on different substrates – Effect of print density in inkjet printing. *International Journal of Pharmaceutics*, *453* (2), 488–497.

doi: 10.1016/j.ijpharm.2013.06.003

II

Palo, M., Kogermann, K., Genina, N., Fors, D., Peltonen, J., Heinämäki, J. and Sandler, N. (2016). Quantification of caffeine and loperamide in printed formulations by infrared spectroscopy. *Journal of Drug Delivery Science and Technology*, *34*, 60–70.

doi: 10.1016/j.jddst.2016.02.007

III

Palo, M., Kolakovic, R., Laaksonen, T., Määttänen, A., Genina, N., Salonen, J., Peltonen, J. and Sandler, N. (2015). Fabrication of drug-loaded edible carrier substrates from nanosuspensions by flexographic printing. *International Journal of Pharmaceutics*, *494* (2), 603–610.

doi: 10.1016/j.ijpharm.2015.01.027

IV

Palo, M., Kogermann, K., Laidmäe, I., Meos, A., Preis, M., Heinämäki, J. and Sandler, N. (2017). Development of oromucosal dosage forms by combining electrospinning and inkjet printing. *Molecular Pharmaceutics*, *14* (3), 808–820.

doi: 10.1021/acs.molpharmaceut.6b01054

ISBN 978-952-12-3558-0